OPTIMIZATION ANALYSIS OF CLASSICAL, MESOSCOPIC AND QUANTUM HEAT ENGINES IN FINITE-TIME THERMODYNAMICS

Varinder Singh

A thesis submitted for the partial fulfillment of

the degree of Doctor of Philosophy

Department of Physical Sciences

Indian Institute of Science Education and Research Mohali

Knowledge city, Sector 81, SAS Nagar, Manauli PO, Mohali 140306, Punjab, India.

October, 2019

Declaration

The work presented in this thesis has been carried out by me under the guidance of Prof. Ramandeep Singh Johal at the Indian Institute of Science Education and Research Mohali. This work has not been submitted in part or in full for a degree, a diploma, or a fellowship to any other university or institute. Whenever contributions of others are involved, every effort is made to indicate this clearly, with due acknowledgement of collaborative research and discussions. This thesis is a bona fide record of original work done by me and all sources listed within have been detailed in the bibliography.

Varinder Singh

In my capacity as the supervisor of the candidate's thesis work, I certify that the above statements by the candidate are true to the best of my knowledge.

Prof. Ramandeep Singh Johal

Acknowledgements

I would like to thank my supervisor Prof. Ramandeep S. Johal for his immense support and guidance. This thesis would not have been possible without his support and active involvement.

I am thankful to Dr. Sanjeev Kumar, Head of the Department of Physical Sciences, for support and encouragement. I am grateful to my internal monitoring committee members Dr. Sanjeev Kumar and Dr. Satyajit Jena for insightful suggestions and motivation. I owe special thanks to Dr. Abhishek Chaudhuri and Dr. Sanjeev Kumar for teaching and inspiring me.

I am grateful to IISER Mohali for providing advanced infrastructure and excellent research environment. I also thank IISER Mohali for financial support and hostel facility. My gratitude to the Library facility of IISER Mohali for providing subscription to various journals, which plays an essential role in research.

I thank my group members: Jasleen Kaur, Venu Mehta, I. Iyyappan, Tanmoy Pandit, Shashank and Keshav for encouragement and discussions in the group meetings. I deeply appreciate the help and concern from my friends Jaskaran Singh and Satnam Singh during these years. I also thank my friends Shishram, Gopal, Jaskaran Singh Nirankari and Preetinder Singh for various memorable moments.

I owe special thanks to my wife Kirandeep Kaur for unconditional support, constant care and useful discussions, which allowed me to preserve and accomplish my aim despite many difficulties and challenges.

My deepest gratitude to my parents and family members for their unflagging love and kindness.

I also thank the Director IISER Mohali, Deans, faculty members, non-teaching staff, research scholars and BS-MS students of IISER Mohali for making the campus an excellent place to pursue research.

Varinder Singh

List of Publications

1. **V. Singh** and R. S. Johal, *Feynman's ratchet and pawl with ecological criterion: Optimal performance versus estimation with prior information*, Entropy **19**, 576 (2017).

2. **V. Singh** and R. S. Johal, *Feynman-Smoluchowski engine at high temperatures and the role of constraints*, J. Stat. Mech. (2018), 073205.

3. **V. Singh** and R. S. Johal, *Low-dissipation Carnot-like heat engines at maximum efficient power*, Phys. Rev. E **98**, 062132 (2018).

4. **V. Singh** and R. S. Johal, *Three level-laser heat engine at optimal performance with ecological function*, Phys. Rev. E **100**, 012138 (2019).

5. **V. Singh** and R. S. Johal, *Performance of Feynman's ratchet under a trade-off figure of merit: Exact analysis versus estimation from prior information*, J. Stat. Mech. (2019), 093208.

List of Figures

List of Symbols

Symbol	Description
T_h (T_1), T_c (T_2)	Temperature of the hot reservoir and cold reservoir
Q_h (Q_1), Q_c (Q_2)	The amount of heat absorbed from hot reservoir, rejected to cold reservoir
W, P	Work output, power output
$\eta, \eta_C, \eta_{\max}$	The efficiency, the Carnot efficiency, maximum efficiency
η_{CA}, η_{SS}	Curzon and Ahlborn efficiency, Schmiedl-Seifert efficiency,
η_{FS}	Efficiency at maximum power of Feynman-Smoluchowski engine
η_-, η_+	Lower and upper bounds on efficiency at the optimal of the chosen objective function
$\zeta, \zeta_C, \zeta_{\mathrm{CA}}$	The coefficient of performance (COP), Carnot COP, Curzon-Ahlborn COP
T_{hW}, T_{cW}	Temperatures of the working fluid during the hot and cold isotherms
α_h, α_c	Heat transfer coefficients for the hot and cold contacts
t_h, t_c	Contact times of the system with the hot and cold baths
$\dot{Q}_h$ ($\dot{Q}_1$), $\dot{Q}_c$ ($\dot{Q}_2$)	The input flux, output heat flux
χ, P_η, Ω	Chi function, efficient power function and Omega function
$E, \mathcal{E}$	Ecological function for heat engine and refrigerator
η_P, η_Ω	efficiency at maximum power, efficiency at maximum Ω function
$\eta_{P\eta}$	Efficiency at maximum efficient power
X_k, J_k	Generalized forces, generalized fluxes
L_{kj}	Onsager coefficients
q	Coupling strength between heat and work fluxes
S, $\dot{S}_{\mathrm{tot}}$	Entropy, entropy production rate
ξ	Extensive variable
$\bar{E}(\bar{\mathcal{E}})$, $\bar{P}_\eta$	Average ecological function for engine (refrigerator), average efficient power
ϵ_1, ϵ_2	Energy scales of Feynman's ratchet and pawl model

Symbol	Description
R_F, F_B	Rate of forward and backward jumps
r_0	Rate constant for forward or backward jumps in Feynman's model
$k_B, \hbar$	Boltzmann's constant, Planck's constant divided by 2π
ϕ, Z	Angle of rotation, torque
$\sigma, \alpha, \beta, \delta; \dot{Q}_L$	Coefficients of thermal conductance; heat leaks between the reservoirs
$\bar{T}, \tilde{T}$	Effective temperatures
$\Pi(\epsilon_1), \Pi(\epsilon_2)$	Prior probability distribution over ϵ_1 and ϵ_2
$\bar{\eta}, \bar{\zeta}$	Efficiency and COP obtained from prior information approach
Σ_h, Σ_h	Dissipation coefficients at the hot and cold contacts
Γ_h, Γ_c	Wigner-Weisskopf constants at the hot and cold contacts
γ	Ratio of Σ_c and Σ_h in Chapter 4,
	Ratio of Γ_h and Γ_c in Chapter 5,
$\mathcal{D}_h, \mathcal{D}_c$	Average dissipation at the hot and cold contacts
H_0	Hamiltonian of three-level system
$V(t)$	Semi-classical Hamiltonian representing matter-field interactions
$\mathcal{L}_h, \mathcal{L}_c$	Lindblad superoperators describing system-bath interactions with
	the hot and cold baths
n_h, n_c	Average number of photons in hot and cold baths
ω_h, ω_c	Control frequencies in three-level system
ρ, ρ_R	Density matrix, density matrix in rotating frame
λ	Matter-field coupling constant
τ	Ratio of T_c and T_h.
R'	Ratio of power lost to power output
$\bar{R}$	Ratio of power at maximum ecological function to optimal power
$U(t), \Lambda(t)$	Time evolution operator, quantum dynamical map

List of Acronyms

Term	Acronym
Ecological function	EF
Efficient power	EP
Efficiency at maximum power	EMP
Efficiency at maximum ecological function	EMEF
Efficiency at maximum efficient power	EMEP
Feynman-Smoluchowski	FS
Curzon-Ahlborn	CA
Low-dissipation	LD
Minimally nonlinear irreversible	MNI
Maximum Omega function	MOF
Scovil and Schulz-DuBois	SSD

Contents

Chapter 1

Introduction

Since the dawn of the industrial revolution, heat engines played a crucial role in the development and progress of the human civilization. In our everyday life, we are surrounded by heat engines (automobiles), refrigerators and air conditioners, among other energy conversion devices. Basically, a heat engine is a device that converts heat into work, operating in a cyclic manner. Historically, the study of heat engines gave birth to the science of Thermodynamics. Impressed by the working of the steam engine and motivated to understand the basic physical principles behind its working, Sadi Carnot, in 1824, introduced the concept of an idealized reversible heat engine (See box 1.1), now known as Carnot engine, operating between two reservoirs at temperatures T_c and T_h ($T_c < T_h$), and showed that the efficiency of such a reversible engine is independent of the properties of working medium, and is given by $\eta_C = 1 - T_c/T_h$ [4]. This is a remarkable result. Carnot efficiency, η_C, sets a theoretical upper bound on the efficiency of all cyclic heat engines working between two heat reservoirs.

The seminal work of Carnot led Clausius [5] to formulate the second law of thermodynamics which introduced the concept of entropy. Carnot's work also motivated Lord Kelvin to introduce the concept of an absolute scale of temperature that is independent of material properties. Although, the abstract concept of reversible Carnot cycle has paramount theoretical importance, it is horribly impractical to implement in real heat engines. The Carnot efficiency is attainable only in reversible limit, whereby the processes occur so slowly that the resulting output power

Box 1.1 Carnot cycle: The Carnot cycle consists of four reversible steps: two isothermal and two adiabatic. Isothermal steps are carried out at constant temperature. In adiabatic steps, no heat exchange takes place between the system and the heat baths, and entropy of the working fluid remains constant. The Carnot cycle for an ideal gas is explained below:

(1) During the isothermal expansion, system absorbs an amount of heat Q_h from the hot reservoir at temperature T_h.

(2) During the adiabatic expansion, gas is cooled downed to a lower temperature T_c.

(3) During the isothermal compression, system rejects an amount of heat Q_c to the cold reservoir at temperature T_c.

(4) Finally the system is brought back to the initial state by adiabatically compressing it.

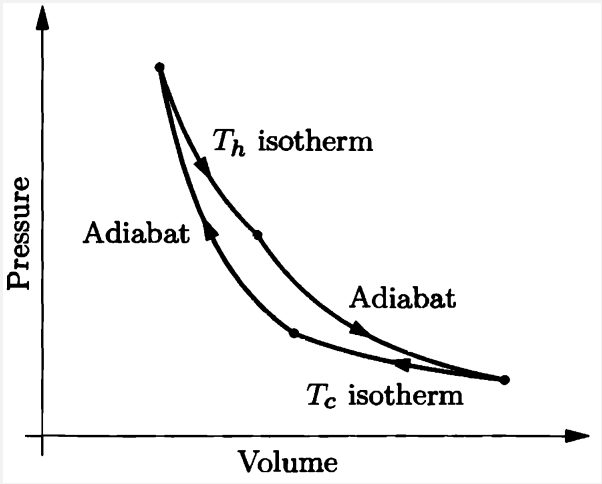

Carnot cycle of an ideal gas

Total work done per cycle and efficiency of the Carnot engine are given by

$$W = Q_h - Q_c, \qquad \eta = \frac{W}{Q_h} = 1 - \frac{Q_c}{Q_h} = 1 - \frac{T_c}{T_h}.$$

is zero. But, real heat engines operate at finite rates and produce finite power per cycle. So it is more useful and practical to optimize the power output of the heat engines by taking into

account the intrinsic irreversibilitities of finite-rate processes. Such an approach was taken by Reitlinger [6], Yvon [7], Chambadal [8], Novikov [9] and Curzon-Ahlbohn (CA) [10]. They all derived the same expression for the efficiency at maximum power (EMP) of a so-called endoreversible [11] heat engine. The form of Reitlinger-Yvon-Chambadal-Novikov-Curzon-Ahlborn efficiency is given by

$$\eta_{CA} = 1 - \sqrt{1 - \eta_C}. \tag{1.1}$$

This is a simple and elegant result as the form of CA efficiency depends upon the ratio of reservoir temperatures only and independent of the properties of working material. Although the formula in Eq. (1.1) was derived first [6] many years before the work of Curzon and Ahlborn, in physics literature it is generally attributed to CA due to the strong impact of their work which stimulated a large number of publications in the field of so-called finite-time thermodynamics.

1.1 Finite-time thermodynamics (FTT)

As mentioned earlier, motivated to find the realistic theoretical bounds on the efficiency of practical heat engines, Curzon and Ahlborn introduced the concept of endoreversible Carnot heat engine and gave birth to FTT. In endoreversible models, the work extracting part of the cycle is assumed to be internally reversible and there are no heak leaks between the reservoirs. The irreversibility arises solely due to the finite rate of heat transfer between the working medium and the external heat baths. Most of the initial papers in FTT analyzed the performance of endoreversible heat engines and refrigerators with a number of different loss mechanisms and various heat transfer laws between the working fluid and heat baths. The number of papers on endoreversible models are so high that one might think that FTT is only about endoreversible heat engines [12]. But it is not true. FTT covers all thermodynamic processes with one added constraint: completion in a finite time. It is a branch of non-equilibrium thermodynamics devoted to explain more realistic irreversible processes happening in finite time. Armed with the tools of optimal control theory, it becomes very powerful theory to study a wide range of physi-

cal phenomena [13, 14]. However, in this thesis, we will focus our attention on the applications of FTT to the optimization of energy conversion devices.

FTT can also be used to analyze the performance of continuous steady state heat engines, coupled simultaneously to the hot and cold reservoirs, operating with finite non-vanishing rates. Historically, Geva and Kosloff were first to apply the theory of FTT to study the performance of a three-level laser heat engine operating in steady state [15, 16]. In 2001, Valesco and coauthors investigated the optimal performance of another steady state continuous heat engine, Feynman's ratchet and pawl model, using the methods of FTT [17]. Since then, many researchers made use of methods of FTT to study engines operating in steady state [18–22].

A brief history of FTT

The ground breaking work of Curzon and Ahlborn inspired many researchers to work along their line. In the late 1970s, a group of scholars working in Chicago university, including Stephen Berry, Bjarne Andresen and Peter Salamon, developed the formal theory of FTT in three back to back publications [23–25]. Two of them were published in the same issue of Physical Review A on 7 September, 1977 [23, 24]; the remaining one was published in Journal of Chemical Physics on 8 September, 1977 [25]. In Ref. [[23]], introducing the concept of step-Carnot cycle, the authors formulated a method to find bounds on process functions, such as heat and work, for processes operating at finite rate in finite time, and then determined the optimal time interval in which a process should be executed to optimize the power output or some other index of optimality. In the second publication, they developed an algorithm to construct thermodynamic potentials for finite-time processes [24]. In Ref. [[25]], focusing on processes of energy conversation, the authors developed a general formalism to find the maxima of power output and efficiency for realistic heat engines.

Another important contributor to the field of FTT is Alexis de Vos. In 1980s, the impact of endoreversible models on FTT was so strong that de Vos termed it as endoreversible thermodynamics [12]. He considered the effect of various heat transfer laws on simple models of

endoreversible engines and discovered various expressions for the EMP, including well known CA efficiency and Cartan's efficiency among others [26]. Orlov also performed same analysis and found a different expression for the efficiency at optimal power of the engine [27]. Later, Yan and Chen considered the same problem and by optimizing power output with the use of Euler-Lagrange equations, they were able to re-derive the results obtained by de Vos and Orlov as the special cases of their general result [28]. Yan and Chen also considered the effect of different heat transfer laws to analyze the optimal performance of a class of endoreversible Carnot refrigerators [29]. In the same paper, they introduced the concept of a new figure of merit, $\chi = \epsilon \dot{Q}_2$, to study the optimal performance of Carnot refrigerator. Here, ϵ is coefficient of performance (COP) of the refrigerator and $\dot{Q}_2$ is cooling rate. χ criterion is a suitable figure of merit to study the performance of refrigerators as Agrawal and Menon showed that cooling power cannot be optimized for an endoreversible Carnot refrigerator employing the same technique used by Curzon and Ahlborn [30].

Another important step towards the study of general class of irreversible heat engines was carried out by Gordon [31, 32]. He investigated the engines operating at maximum power (MP) and undergoing non-isothermal transformations during the process of heat exchange with the reservoirs, and derived the form of optimal driving function that maximizes power. Considering finite-rate heat transfer and internal frictional losses as the only sources of irreversibilities, he concluded that for engines with internal friction, it is better to dissipate frictional losses directly to the environment than to permit dissipative frictional losses to heat the engine's working fluid.

In 1992, for the very first time, Geva and Kosloff applied the theory of FTT to a quantum heat engine whose working material consists of non-interacing spin-half particles [33]. They repeated their analysis by replacing ensemble of spin-half particles by ensemble of non-interacting harmonic oscillators [34]. In both the cases, they were able to obtain the CA efficiency in the high temperature regime. These two systems still maintain their reputation as the standard working fluid to study quantum heat engines. In the spirit of FTT, Geva and Kosloff also investigated the optimal performance of a steady state laser heat engine in the presence of

strong and very fast rotating electromagnetic fields [15, 16]. In doing so, they incorporated the effect of strong fields on the Lindblad dissipators, and for the very first time, derived second law of the thermodynamics in the presence of strong fields. They continued to apply the theory of FTT to quantum heat engines in many subsequent meaningful publications [35–38].

In 2010, a major breakthrough happened in the field of FTT when Esposito and coauthors introduced low-dissipation (LD) model of heat engines [1]. In LD models, the system undergoes a Carnot cycle and entropy production in the isothermal stages is assumed to be inversely proportional to the time of contact of the system with the reservoirs during the heat transfer process. For the extreme dissipative cases, i.e., when heat transfer process at one of the ends (hot or cold) approaches reversible limit, they were able to derive lower and upper bounds on the efficiency of the engine operating at MP. As the icing on the cake, they also derived CA efficiency for the case of symmetric dissipation. The same authors also applied FTT to study a nano-thermoelectric heat engine [39] and a quantum dot Carnot engine [40] in the LD regime.

1.2 Endoreversible heat engine: Curzon-Ahlborn model

In endoreversible models (See Figure 1.1), the internal work extracting part of the cycle is assumed to be reversible. The irreversibility arises solely due to the finite rate of heat transfer between the working medium and the external heat baths. The nature of heat conduction between the working medium and the heat baths is assumed to obey Fourier's law of heat transfer. Hence, the heat fluxes related to the hot and the cold baths are given by

$$\frac{dQ_h}{dt} = \alpha_h(T_h - T_{hW}), \qquad \frac{dQ_c}{dt} = \alpha_c(T_{cW} - T_c), \tag{1.2}$$

where α_h and α_c are heat transfer coefficients which depend upon thermal conductivity and geometry of the heat exchangers; T_{hW} and T_{cW} are the effective temperatures of the working fluid during the isothermal expansion and isothermal compression stages respectively. It is assumed that during the isothermal stages, the temperature of the working fluid remains constant. If t_h

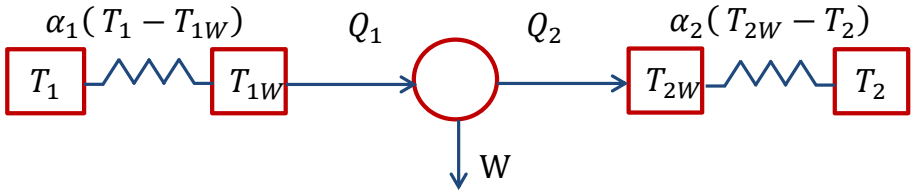

Figure 1.1: Endoreversible heat engine

(t_c) is the time required to transfer an amount Q_h (Q_c) of heat from (to) the hot (cold) reservoir, then

$$Q_h = \alpha_h t_h (T_h - T_{hW}) \Rightarrow t_h = \frac{Q_h}{\alpha_h (T_h - T_{hW})} \tag{1.3}$$

and

$$Q_c = \alpha_c t_c (T_{cW} - T_c) \Rightarrow t_c = \frac{Q_c}{\alpha_c (T_{cW} - T_c)}. \tag{1.4}$$

Further, it is assumed that the time spent on adiabatic branches of the cycle is negligible as compared to the time spent on isothermal branches. This can be justified if relaxation time of the working fluid is fast enough as compared to the duration of the adiabatic branches. So, total duration of the cycle is

$$t_{\text{cycle}} \approx t_h + t_c. \tag{1.5}$$

If W is the work done during one cycle, then power delivered by engine per cycle is given by

$$P = \frac{W}{t_{\text{cycle}}} = \frac{Q_h - Q_c}{t_h + t_c} = \frac{Q_h - Q_c}{\frac{Q_h}{\alpha_h (T_h - T_{hW})} + \frac{Q_c}{\alpha_c (T_{cW} - T_c)}} \tag{1.6}$$

The assumption of endoreversibility (internally reversible) leads to the following equation

$$\frac{Q_h}{T_{hW}} = \frac{Q_c}{T_{cW}}. \tag{1.7}$$

Using Eqs. (1.6) and (1.7), we have

$$P = \frac{T_{hW} - T_{cW}}{\frac{T_{hW}}{\alpha_h(T_h - T_{hW})} + \frac{T_{cW}}{\alpha_c(T_{cW} - T_c)}}. \tag{1.8}$$

To optimize the power output of the heat engine, we define new variables, $x_1 = T_h - T_{hW}$ and $x_2 = T_{cW} - T_c$, and then setting the conditions for extremum of power, $\partial P/\partial x_1 = 0$ and $\partial P/\partial x_2 = 0$, the final form of EMP is found to be

$$\eta_{CA} = 1 - \sqrt{\frac{T_c}{T_h}} = 1 - \sqrt{1 - \eta_C}, \tag{1.9}$$

which depends only on the ratio of bath temperatures. The expression for optimal power is

$$P_{\max} = \frac{\alpha_h \alpha_c}{(\sqrt{\alpha_h} + \sqrt{\alpha_c})^2}(\sqrt{T_h} - \sqrt{T_c}). \tag{1.10}$$

It is worth noting that CA efficiency is obtained for the specific form of heat transfer law, in this case Newton's law, between the working fluid and the heat reservoirs. Yan and Chen studied endoreversible Carnot engine for phenomenological law of linear irreversible thermodynamics [28], $Q = \sigma(1/T - 1/T')$, where σ is coefficient of heat conductance and T and T' are temperatures of working fluid and reservoir, respectively. They found lower and upper bounds on the EMP as follows

$$\frac{\eta_C}{2} \leq \eta_P \leq \frac{\eta_C}{2 - \eta_C}. \tag{1.11}$$

Additionally, they also found the expression for EMP when heat transfer coefficients of heat exchangers at the hot and cold ends are equal. In this case, efficiency is given by

$$\eta_{SS} = \frac{2\eta_C}{4 - \eta_C}. \tag{1.12}$$

The above expression for efficiency was re-derived by Schmiedl and Seifert (SS) for a Brownian heat engine undergoing Carnot cycle [41], and hence named after them.

1.3 Steady-state heat engines

Besides cyclic classical heat engines, there is another class of heat engines which are simultaneously coupled to two heat reservoirs at different temperatures. These are continuous heat engines and operate in steady-state. Feynman-Smoluchowski (FS) engine, three-level laser heat engine and thermoelectric engines are most common examples of steady state heat engines. They consider the fluxes of energy, matter and entropy in steady-state regime and thus these quantities are time-independent. In order to understand the working of a generic model of steady-state engine, we first introduce the framework of linear irreversible thermodynamics.

1.3.1 Linear Irreversible Thermodynamics

The theory of irreversible thermodynamics deals with the states and processes in out of equilibrium systems. In the framework of irreversible thermodynamics, we need to define certain quantities that can appropriately describe irreversible processes. In this regard, the notion of generalized forces and their conjugate fluxes play a fundamental role in the description of irreversible processes. Generalized forces, also known as affinities, drive irreversible processes inside a system and the fluxes represent the response of the system to these forces.

It is very convenient to identify the generalized forces and fluxes in a particular type of system by considering the rate of entropy production. Entropy production in a closed system evolving from a non-equilibrium state can be described by

$$\frac{dS}{dt} = \sum_k \frac{\partial S}{\partial \xi_k} \frac{\partial \xi_k}{\partial t} \equiv \sum_k X_k J_k, \tag{1.13}$$

where the $X_k = \partial S/\partial \xi_k$ are the thermodynamic forces and $J_k = \partial \xi_k/\partial t$ are the conjugate thermodynamic fluxes of the extensive variables ξ_k.

Since the fluxes J_k vanish if the generalized forces vanish, in the linear response regime close to equilibrium, J_k can be represented in terms of generalized forces by the following

equation:

$$J_k = \sum_j L_{kj} X_j, \tag{1.14}$$

where $L_{kj} = \partial J_k / \partial X_j$ are called kinetic coefficients. Substituting Eq. (1.14) in Eq. (1.13), rate of entropy production can be written in bilinear form

$$\frac{dS}{dt} = \sum_{kj} L_{kj} X_k X_j. \tag{1.15}$$

Since $dS/dt \geq 0$, the kinetic coefficients satify $L_{kk} \geq 0$ and $L_{jj} L_{kk} \geq (L_{jk} + L_{kj})/4$. Further based on time reversal symmetry , Onsager proved that $L_{jk} = L_{kj}$.

1.3.2 Linear irreversible heat engine

Van den Broeck [42] studied a generic model of linear irreversible heat engine operating between two reservoirs at temperatures T_c and T_h ($T_c < T_h$). The work is extracted from a heat flux $\dot{Q}_h$ leaving the hot reservoir. The engine is assumed to be operating in the linear response regime, which implies that $T_c \approx T_h \approx T$, and $\Delta T = T_h - T_c$ is small as compared to T. The work done against the fixed external force F is $W = -Fx$, where x is the conjugate variable of F. Then the power is written as $P \equiv \dot{W} = -F\dot{x}$, where the dot denotes the time derivative. A couple of flux-force pairs are identified as follows:

$$J_1 = \dot{x}, \qquad X_1 = \frac{F}{T}, \tag{1.16}$$

$$J_2 = \dot{Q}_h, \qquad X_2 = \frac{1}{T_c} - \frac{1}{T_h} \approx \frac{\Delta T}{T^2}. \tag{1.17}$$

Following Eq. (1.14), we can write each flux as linear combination of available generalized forces

$$J_1 = L_{11} X_1 + L_{12} X_2, \tag{1.18}$$

$$J_2 = L_{21} X_1 + L_{22} X_2, \tag{1.19}$$

where L_{kj} are kinetic coefficients, satisfying Onsager's reciprocity relation, $L_{12} = L_{21}$. Then, the expression for power becomes

$$P = -TJ_1X_1 = -T(L_{11}X_1 + L_{12}X_2)X_1. \tag{1.20}$$

For a given X_2, optimization of power with respect to X_1 yields $X_1^* = -L_{12}X_2/2L_{11}$. Then the efficiency $\eta = P/\dot{Q}_h$ at MP is evaluated to be

$$\eta_P = \frac{\Delta T}{2T}\frac{q^2}{2-q^2}, \tag{1.21}$$

where, $q = L_{12}/\sqrt{L_{11}L_{22}}$, represents the coupling strength between the fluxes, and lies in the range [-1,1]. Tight-coupling condition, $q^2 = 1$, implies that EMP is given as $\eta_P = \Delta T/2T = \eta_C/2$, which is the upper bound to EMP within the linear irreversible framework.

1.4 Different optimization functions

One of the main goals of FTT is the optimization of energy conversion devices: heat engines, refrigerators and heat pumps. Maximization of power is the most studied criterion to analyze the performance of irreversible heat engines operating in finite time. But, heat engines operating at MP are not the most efficient one and, hence, are not very economical. Also, from an environmental point of view, to be ecologically sensitive demands that we should also care about the extent of entropy production which ultimately pollute the environment. In this regard, it has been noted that real thermal plants and practical heat engines should not operate at MP, but in a regime with slightly smaller power output and appreciable larger efficiency [12, 43]. In recent years, a few such alternate measures of performance have been studied. The optimization of ecological function (E) [44, 45] or Omega function (Ω) [46] and efficient power (EP) function (P_η) [47, 48] fall within such a regime, as they pay equal attention to both power and efficiency [49]. Due to contemporary growing need of saving energy resources, relevance of

such optimization criteria deserves serious discussion.

1.4.1 Ecological function (E)

The concept of ecological function (EF) was first proposed by Angulo-Brown in the literature of FTT in order to find the best mode of operation of an endoreversible heat engine [44]. It is defined as follows

$$E = P - T_c \dot{S}_{\rm tot}, \tag{1.22}$$

where P is power output, T_c is the temperature of the cold reservoir and $\dot{S}_{\rm tot}$ is the rate of entropy production. The optimization of the EF represents a compromise between the power output P and the loss of power, $T_c \dot{S}_{\rm tot}$, due to the entropy production. In a later publication, Yan modified the definition of EF by replacing the temperature of cold reservoir by the temperature of the environment [50]. The ecological optimization of a large class of different models of heat conversion devices has been studied in the literature of FTT and linear irreversible thermodynamics [46, 49, 51, 52].

One of the advantages of EF is that it can be applied to study optimal performance of refrigerators too. The EF for the optimization of refrigerators can be written as [53]

$$\mathcal{E} = \dot{\mathcal{Q}}_c - \zeta_C T_0 \dot{\mathcal{S}}_{\rm tot}, \tag{1.23}$$

where $\dot{\mathcal{Q}}_c$ is rate of refrigeration, ζ_C is the Carnot COP of the refrigerator, and T_0 is temperature of the environment.

1.4.2 Unified trade-off function (Ω)

The Ω function represents a compromise between energy benefit and losses for a specific job [51]. It is easy to implement in both heat engines and refrigerators, without the requirement of calculation of entropy production and is independent of environment parameters. For heat

engines, Ω function is defined as [46]

$$\Omega = (2\eta - \eta_{\max})\frac{P}{\eta}, \tag{1.24}$$

where $\eta_{\max}$ is maximum possible efficiency. For the tight coupling heat engines (no heat leaks between the reservoirs), $\eta_{\max}$ is equal to Carnot efficiency η_C, Ω function is equivalent to E[54].

1.4.3 Efficient power (P_η)

EP criterion $P_\eta = \eta P$ represents a trade-off between the efficiency and power output of a heat engine. It was introduced by Stucki in the context of linear irreversible thermodynamics while studying the mitochondrial energetic processes [47]. Later the idea was extended to the regime of FTT by Yan and Chen [55] and given the so-called name "efficient power" by Yilmaz [48]. It is also shown that the EP criterion is well suited to study the optimization of steady and non-steady electric energy converters [56], thermionic generator [57] and biological systems [47, 58, 59] and LD heat engines [60].

1.5 Universal nature of efficiency

Recently, study of universal nature of efficiency attracted a lot of interest [19, 41, 61]. The relevance of the study lies in the observation that it establishes a connection between macroscopic and microscopic models of heat engines [62]. Cleuren et al. [62] investigated the EMP in a general setting for energy conversion machines and demonstrated how symmetries and constraints at the microscopic level, combined with the fluctuation theorems, emerge at macroscopic level via the expression for the EMP. Apart from power optimization, the universal nature of efficiency has been confirmed in the study of some other power-efficiency trade-off optimization criteria [45, 54, 63].

1.5.1 Universality of efficiency at maximum power

Although CA efficiency has paramount importance in the literature of FTT, it is not as universal as Carnot efficiency. It is neither an upper bound nor a lower bound. Efficiencies at MP, not only below but also above CA efficiency, have been reported. However, in many models of heat engines, such as FS engine [19] and Brownian Carnot engine [41], EMP agrees with η_{CA} upto quadratic order in Carnot efficiency as can be seen from the Taylor series expansions of the EMP, near equilibrium:

$$\eta_{CA} = \frac{\eta_C}{2} + \frac{\eta_C^2}{8} + \frac{6\eta_C^3}{96} + O(\eta_C^4), \tag{1.25}$$

$$\eta_{FS} = \frac{\eta_C}{2} + \frac{\eta_C^2}{8} + \frac{7\eta_C^3}{96} + O(\eta_C^4), \tag{1.26}$$

$$\eta_{SS} = \frac{\eta_C}{2} + \frac{\eta_C^2}{8} + \frac{3\eta_C^3}{96} + O(\eta_C^4). \tag{1.27}$$

Clearly the first two terms in the above three expressions for EMP are same. The model dependent differences manifest in the third term only. Using the framework of linear irreversible thermodynamics, Van den Broeck proved that universal EMP for heat engines obeying tight coupling condition is equal to $\eta_C/2$ [42]. The universal nature of second term $\eta_C^2/8$ can be explained by further assuming the presence of some kind of of left-right symmetry in the system in addition to the condition of strongly coupled fluxes [61]. Apart from the above mentioned three models of heat engines, universal nature of EMP also holds true for nano-thermal quantum dot heat engine [39], LD heat engine [1], minimally nonlinear irreversible (MNI) heat engine [64], among other models of heat engines [65].

The universal features of efficiency at the maximum work output, instead of MP, has also been studied for some models of quantum and classical heat engines [66, 67]. Again for the optimization of work, the first two universal terms of efficiency are $\eta_C/2$ and $\eta_C^2/8$.

However it is found that the condition of left-right symmetry in the system is sufficient but not necessary condition for the EMP to show universal behavior [68]. Endoreversible heat engine and FS engine both show universal features of EMP in the lack of any kind of left-right

symmetry in the system. It is ironical that these two heat engines stimulated the discussions about universal nature of EMP. This paradox was resolved by Sheng and Tu by constructing a general constitutive relation in the nonlinear response regime accurate upto the quadratic order for tight coupling heat engines [68]. They showed that in the absence of any kind of left-right symmetry in the system, the EMP shows universal features if the elementary thermal energy flowing through the engine matches the characteristic energy of the engine (energy matching condition). The endoreversible heat engine and FS engine lie in this category and hence recover second order universal term $\eta_C^2/8$ regardless of any symmetry.

1.5.2 Universality of efficiency in the optimization of ecological (or Ω) and efficient power function

The universal features of efficiency are not exclusive to the engines operating at MP; the engines operating at maximum EF, or Ω function and EP function also show same kind of universality [54, 63]. For engines operating at maximum Ω function (or EF) and maximum EP, Taylor's series expansions of the efficiency for the respective functions are given by

$$\eta_\Omega = \frac{3\eta_C}{4} + \frac{\eta_C^2}{32} + O(\eta_C^3), \tag{1.28}$$

and

$$\eta_{P_\eta} = \frac{2\eta_C}{3} + \frac{2\eta_C^2}{27} + O(\eta_C^3). \tag{1.29}$$

Again for both the functions, the first term is universal for the tight coupling heat engines and second term is universal in the presence of an additional left-right symmetry in the system [1, 54, 61, 63]. For the optimization of Ω or E function, the first two terms of Eq. (1.28) have been obtained for various models of heat engines such as LD engines [52], MNI engines [69], FS engines [45] and non-isothermal Carnot engines [70]. However, for engines operating at maximum EP, such universality has been shown only in the case of LD heat engine [60] and FS engine.

1.5.3 Lower and upper bounds on efficiency

Apart from showing universality in efficiency, the abovementioned tight-coupling engines operating at MP (or some other target function), also share common lower and upper bounds on efficiency. For many models of heat engines operating at MP [1, 28, 41], following formula of EMP has been obtained

$$\eta_P = \frac{\eta_C}{2 - \gamma' \eta_C}, \tag{1.30}$$

where γ' is a real parameter and depends upon the details of the particular model and lies in the range $0 \leq \gamma' \leq 1$. The above expression yields $\eta_C/2$ as the lower bound and $\eta_C/(2-\eta_C)$ as the upper bound [See Eq. (1.11)]. For LD models, $\gamma'_{LD} = 1/(1+\sqrt{T_c\Sigma_c/T_h\Sigma_h})$, where Σ_c and Σ_h are the dissipation coefficients at the cold and hot ends, respectively [1]. For endoreversible engines, $\gamma'_{\rm endo} = 1/(1+\sqrt{\alpha_c/\alpha_h})$, where α_h and α_c represent the heat transfer coefficients between the working fluid and the hot or the cold baths, respectively [28]. For a stochastic Carnot engine, $\gamma'_{SS} = 1/(1+\sqrt{A_3/A_1})$, where A_1 and A_3 are known as irreversible "actions" of isothermal processes in contact with the hot and cold baths [41].

For the optimization of Ω function or EP function, no such general expressions analogous to Eq. (1.30) are known, still we can find the corresponding common lower and upperr bounds for various models of heat engines [52, 60, 69–71], and they are given by following equations, respectively

$$\frac{3\eta_C}{4} \leq \eta_\Omega \leq \frac{3-2\eta_C}{4-3\eta_C}\eta_C, \tag{1.31}$$

and

$$\frac{2\eta_C}{3} \leq \eta_{P_\eta} \leq \frac{1}{2}(3-\sqrt{9-8\eta_C}). \tag{1.32}$$

1.6 Thermodynamics, Information and Inference

The relation between thermodynamics and information is subtle. Remarkably, Gibbs expression for thermodynamic entropy and Shannon's information theoretic entropy both have same

form apart from a multiplicative constant. This gives us a useful perspective on the nature of the thermodynamic entropy and forces us to believe that there is a deep connection between thermodynamics and information. In the words of Brillouin "Entropy measures the lack of information about the exact state of a system." To look more into the relation of information with the second law of thermodynamics, we discuss the illustrative example of Maxwell's demon [72].

1.6.1 Maxwell's demon and its exorcism

The story begins with Maxwell who came up with an interesting puzzle via a thought experiment. He considered a hypothetical tiny intelligent being, later dubbed as "Maxwell's demon" by lord Kelvin, guarding a trap door fixed in the middle of a container filled with gas molecules at certain temperature T. The demon has the ability to determine the speed of individual molecules of the gas and is able to watch the molecules bouncing around close to the trap door. The demon separates the faster molecules to one side (say A) of the compartment and slower molecules to the other side (say B) by selectively allowing the molecules to pass through the trap door. This reduces the temperature of side B and increases the temperature of the side A. The overall entropy of the gas decreases, and work can now be extracted from the two compartments because of the temperature gradient. This is in direct contradiction with the second law of thermodynamics. What is the catch to save second law? The answer is hidden in the identification of the information as a physical quantity [73, 74].

Although many distinguished researchers have addressed this problem [72], the issue was finally settled by Bennett [74] who used Landaur's principle of erasure of information to solve the problem of Maxwell's demon. According to Landauer's principle [73], erasure of information is a logically irreversible process. Thus entropy production is inevitable in information eraser process. While making the measurements, the demon must store the results in its memory. And since memory cannot be infinite, the demon must erase the acquired information in order to make room for new measurement results. This erasure of information increases the entropy of

the whole system at least as much as the entropy decreased by the action of the demon. Hence the second law of thermodynamics still holds true.

1.6.2 Bayesian inference

Bayesian inference methods are widely used in physics [75, 76]. Recent applications of Bayesian approach in various fields include human cognition [77], economics [78], cosmology [79], quantum theory [80, 81] and quantum thermodynamics [82, 83]. In Bayesian approach to probability, prior probability distribution, or, simply called a prior, plays a crucial role. Prior is assigned based on the prior information before acquiring the experimental data [84]. After acquiring the new data (D), the prior $P(A)$ is updated to posterior $P(D|A)$ using Bayes theorem [85], given as

$$P(A|D) = \frac{P(D|A)P(A)}{P(D)}, \tag{1.33}$$

where $P(D|A)$ is the probability of observing D given A, and is called the likelihood; $P(D) = \int P(D|A)P(A)dA$ is the normalization constant, sometimes named as marginal likelihood. The choice of prior in Bayesian inference is a crucial step as it incorporates the available partial information as well as uncertainty underlying the problem to be studied. However, choice of an appropriate prior by quantifying the prior information is a subtle issue [84]. The prior is chosen based on certain arguments such as maximum entropy principle [86, 87] or requirement of invariance [84]. The assignment of prior is not based on any frequencies. It is therefore 'subjective' in the sense that it represents the state of knowledge of the observer [84, 88].

1.6.3 Heat engines and prior information approach

It has been shown that using prior probabilities or prior information approach, the optimal characteristics of certain constrained thermodynamic processes can be estimated by inference [82, 89]. In prior information approach to study heat engines, one has only limited or partial information about the control parameters of the system under consideration and a prior proba-

bility distribution quantifies the uncertainty in these parameters. The approach is subjective in the sense that the chosen prior expresses the degree of one's belief in the values taken by the uncertain parameter.

The basic idea of estimating the performance benchmarks of thermal machines, was first proposed in Ref. [82], in the context of a two level quantum heat engine. Later, the idea was extended to treat uncertainty in other thermodynamic processes [20, 45, 83, 89]. To study the optimal performance of thermal machines with prior information approach, a suitable prior is chosen (Jeffreys prior) over the given range of an uncertain control parameter of the system. Then an averaging procedure is performed on the chosen target function (such as power output or EF) using this prior distribution so as to eliminate the uncertain parameter. Following this approach, CA efficiency for engine as well as COP of the refrigerator have been reproduced [20, 90]. In particular, for the problem of maximum work extraction from finite source and sink, the behavior of efficiency at maximum estimate of work shows universal features near equilibrium [89]. Similarly, other expressions for EMP such as in irreversible models of stochastic engines, which obey a different universality near equilibrium, can also be reproduced from the inference based approach [91].

1.7 Thesis layout

In Chapter 2, we optimize the power output of the ratchet engine operating in the high temperature regime, and derive the universality of EMP upto second order, using a non-linear approximation. On the other hand, linear model may be optimized by constraining the internal energy scales in different ways. It is shown that simple constraints lead to well known expressions of thermal efficiency in FTT. Then, by identifying the effective temperatures and coefficients of thermal conductance, we are able to map each case to an effective endoreversible model.

In Chapter 3, we study the optimal performance of Feynmans ratchet and pawl model using two different trade-off objective functions: EF and EP function. We study the model for

both engine and refrigerator modes. The analysis is performed by two different methods: i) a two-parameter optimization over internal energy scales and ii) a one-parameter optimization of the estimate for the objective function, after averaging over the prior probability distribution (Jeffreys prior) for one of the uncertain internal energy scales. We derive expressions for the efficiency/COP at maximum EF. These expressions from the two methods are found to agree in close to equilibrium situations, and show universal features of efficiency at maximum EF. Further, the expressions obtained by the second method (with estimation) agree with the expressions obtained in finite-time thermodynamic models.

Then we repeat our analysis for the optimization of EP function. To study the refrigerator mode, we optimize χ-criterion, which represents a compromise between the cooling load and COP of the refrigerator. First, we perform a two-parameter optimization over the energy scales for the general case and show the universal nature of efficiency at maximum MP. Then exact one parameter optimization is carried out for the linear model of the engine working in high temperature regime by constraining one of the energy scales and well known forms of efficiency are obtained. Further, by using prior information approach, we derive the expression for the efficiency of the engine which concurs with the efficiency of an endoreversible engine. Then prior information analysis is performed in the high temperature limit and we are able to obtain the same forms of efficiency as obtained by exact optimization method. The same analysis is repeated for the optimization of the refrigerator.

In Chapter 4, we study the optimal performance of Carnot-like heat engines working in LD regime using the EP criterion as our objective function. We find lower and upper bounds on the efficiency in case of extreme asymmetric dissipation when the ratio of dissipation coefficients at the cold and the hot contacts approaches, respectively, zero or infinity. In addition, we obtain the form of efficiency for the case of symmetric dissipation. We also discuss the universal features of EMEP and derive the bounds on the efficiency using global linear-irreversible framework introduced recently in Ref. [92]. Finally, we compare the rates of dissipation for LD heat engines under optimal working conditions for power output, Ω function (or EF) and EP function

and show that unlike power output or Ω function, the ratio of rates of dissipation at the hot and cold ends for EP function depends upon the efficiency of the engine.

In Chapter 5, we study a three-level laser quantum heat engine operating at maximum EF. We derive analytic expressions for efficiency under the assumptions of strong matter-field coupling and high bath temperatures. Upper and lower bounds on the efficiency exist in case of extreme asymmetric dissipation when the ratio of system-bath coupling constants at the hot and the cold contacts respectively approaches, zero or infinity. These bounds have been established previously for various classical models of Carnot-like engines. We conclude that while the engine produces at least 75% of the power output as compared with the MP conditions, the fractional loss of power is appreciably low in case of the engine operating at maximum EF, thus making this objective function relevant from an environmental point of view.

Chapter 6 is devoted to summarizing the content of this thesis and possible extensions of our research work.

Chapter 2

Feynman-Smoluchowski Engine at High Temperatures and the Role of Constraints

2.1 Introduction

In order to shed some light on the nature of second law of thermodynamics, Feynman, in his famous *Lectures on Physics*, proposed a simple mechanical device that can rectify thermal fluctuations to extract work from a setup of two reservoirs at different temperatures. Feynman's model was inspired by the work of Smoluchowski on Maxwell's demon. Hence we name this device after Feynman-Smoluchowski (FS). The device consists of an axle coupled on one side to a vane (paddles) immersed in a gas at a fixed temperature T_1 while the other end is coupled to a ratchet wheel, with asymmetric teeth profile, immersed in a gas kept at temperature T_2. In the center of the axle, there is a wheel from which a small weight is hanged. Feynman first considered the case when both the thermal baths have same temperature, that is, $T_1 = T_2$. Because of the collisions of gas molecules, the vane is subjected to Brownian fluctuations. But the ratchet is restricted to rotate in one direction only due to the pawl which in turn is connected to a spring. This breaks the rotational symmetry and the wheel will turn slowly and in doing so might even lift some weight (say a fly). This is a direct violation of the second

law of thermodynamics. However, Feynman showed that it is not possible as the pawl is also subjected to the Brownian fluctuations. This releases the pawl and the wheel is free to rotate in the backward direction too. Feynman showed that the probability of the backward motion is equal to the probability of the forward motion, thus no net motion of the wheel is possible, which in turn implies that no net work can be extracted from a single heat reservoir using the ratchet and pawl mechanism. This saves the second law.

However, Feynman also showed that ratchet and pawl system can operate as a heat engine as well as a refrigerator if the reservoirs are at different temperatures. In FS engine, processes of heat and work transfer are assumed to occur at finite rates, thus generating a finite output power. Feynman's analysis [93] concluded that the device could operate with reversible efficiency in the quasi-static limit which implies a vanishing output power. Based on this analysis, we shall also assume a strong coupling between the fluxes, i.e., there is no heat leakage between the heat baths (see [94–96] for contrasting views).

In this chapter, we focus on the performance of FS ratchet at MP in the regime where thermal energy of a bath is much higher than the internal energy scale excited by the bath. We highlight new features of the device in this regime, not discussed earlier in literature. We note that it is not possible to optimize power—simultaneously over both internal scales—within the linear regime. However, a two-parameter optimization is possible if one extends the operational domain to non-linear approximation. Interestingly, one is able to then recover EMP that retains the same universality up to second order as for the EMP of the original problem, Eq. (2.10) below. We then impose some simple constraints over the internal energy scales, such that the optimization of power over a single parameter can be performed using the linear model. These constrained optimization problems yield some well-known forms of EMP found in other finite-time models. Moreover, under each of these constraints, it is possible to give an effective finite-time thermodynamic model for the FS engine.

The plan of the chapter is as follows. In Section 2.2, we briefly describe the model of FS engine and discuss its optimal performance. In Section 2.3, two-parameter optimization of

ratchet engine in high temperatures limit is discussed. Section 2.4 is devoted to optimization of the ratchet in linear regime, subject to constraints. In Section 2.5, FS engine is mapped to effective thermodynamic models depending on the constraints used in the previous section. Section 2.6 is devoted to a discussion of the results, with concluding remarks.

2.2 Feynman's ratchet and pawl model as a heat engine

Let ϵ_2 be the amount of energy required to overcome the elastic energy of the spring. Let in each step, the wheel rotate an angle ϕ and the torque induced by the weight be Z. Then the system requires a minimum of $\epsilon_1 = \epsilon_2 + Z\phi$ energy to lift the weight hanging from the axle. Hence the rate of forward jumps of the ratchet is given as $R_{\rm F} = r_0 e^{-\epsilon_1/k_{\rm B}T_1}$, where r_0 is a rate constant and $k_{\rm B}$ is Boltzmann's constant, which we set equal to unity. In other words, temperature has the dimensions of energy. A part of the energy ϵ_1 is converted into work $Z\phi$, and other is transferred as heat ϵ_2 to the cold thermal bath through the interaction between the ratchet and the pawl. Similarly, the rate of the backward jumps is $R_{\rm B} = r_0 e^{-\epsilon_2/T_2}$. One may regard $Z\phi$ and $-Z\phi$ as the work done by and on the system, respectively. If $R_{\rm F} > R_{\rm B}$, this system works as two-reservoir heat engine. Then, the rates of heat related to the hot and the cold reservoirs, are given as

$$\dot{Q}_1 = r_0\epsilon_1 \left(e^{-\epsilon_1/T_1} - e^{-\epsilon_2/T_2}\right) > 0, \tag{2.1}$$

$$\dot{Q}_2 = r_0\epsilon_2 \left(e^{-\epsilon_1/T_1} - e^{-\epsilon_2/T_2}\right) > 0. \tag{2.2}$$

According to the model, $\epsilon_1 > \epsilon_2$, and so positivity of the fluxes implies: $\epsilon_2/T_2 > \epsilon_1/T_1$. The power output, $P = \dot{Q}_1 - \dot{Q}_2$, is given by:

$$P = r_0(\epsilon_1 - \epsilon_2) \left(e^{-\epsilon_1/T_1} - e^{-\epsilon_2/T_2}\right). \tag{2.3}$$

2.2.1 Performance of the engine in the presence of heat leaks

Velasco and co-workers made a careful study of FS engine working in the MP and maximum efficiency regime with heat leakage using the methods of FTT [17]. The form of heat leaks between the reservoirs is assumed to obey Fourier's law:

$$\dot{Q}_L = \sigma(T_h - T_c), \tag{2.4}$$

Where σ is the thermal conductance. In the presence of the heat leaks, the efficiency of the engine is given by

$$\eta = \frac{P}{\dot{Q}_1 + \dot{Q}_L}. \tag{2.5}$$

For different values of σ, they plotted power versus efficiency curves and and obtained the closed loop curves, typical of real irreversible heat engines operating in finite-time. Further assuming the high temperature regime and optimizing power output over the single parameter ϵ_1, they obtained EMP as $\eta'_{FS} = \eta_C/(2 - \eta_C)$.

2.2.2 Ratchet engine at maximum power

Going one step further, Tu carried out a two parameter optimization of the power output of the engine over the internal energy scales ϵ_1 and ϵ_2 in the absence of heat leaks. In this case, efficiency of the engine is given by

$$\eta = \frac{P}{\dot{Q}_1} = 1 - \frac{\epsilon_2}{\epsilon_1} \quad \leq \quad \eta_C. \tag{2.6}$$

For given bath temperatures, optimization of the power output with respect to ϵ_1 and ϵ_2, yields the following solution [19]

$$\epsilon_1^* = T_1 \eta_C^{-1} \left[\eta_C - (1 - \eta_C)\log(1 - \eta_C)\right], \tag{2.7}$$

$$\epsilon_2^* = T_1 \eta_C^{-1}(1 - \eta_C)(\eta_C - \log(1 - \eta_C)), \tag{2.8}$$

with the expressions for the optimal power and EMP [19] as given by

$$P^* = r_o e^{-1} T_1 \eta_C^2 (1-\eta_C)^{(1-\eta_C)/\eta_C}, \tag{2.9}$$

$$\eta_{FS} = \frac{\eta_C^2}{\eta_C - (1-\eta_C)\ln(1-\eta_C)}. \tag{2.10}$$

Notably, η_{FS} depends only on the ratio of the reservoir temperatures. Further, the above expression of efficiency also holds for EMPs of a two-level atomic system [97] and a simple model of classical particle transport [98]. η_{FS} can be expanded in Taylor's series, near equilibrium, to give

$$\eta_{FS} = \frac{\eta_C}{2} + \frac{\eta_C^2}{8} + \frac{7\eta_C^3}{96} + O(\eta_C^4). \tag{2.11}$$

Clearly, the EMP of the ratchet engine shows universal features of efficiency upto second order term in η_C [61]. In the next section, we will show that this universality of efficiency also appears in case of optimization of FS engine in the high temperature regime.

2.3 Ratchet in high temperatures regime

In the following, we are interested in the regime, where the energies associated with forward and backward jumps are very small compared to the temperatures of reservoirs. Therefore, we can expand $e^{-\epsilon_1/T_1}(e^{-\epsilon_2/T_2})$ as Taylor series, say, up to first or second order. First, we look for a possible two-parameter power optimization in this regime. Keeping terms up to the first order, we have the approximate expression for power as

$$P = r_0(\epsilon_1 - \epsilon_2)\left(\frac{\epsilon_2}{T_2} - \frac{\epsilon_1}{T_1}\right). \tag{2.12}$$

We address the above approximation as the linear model [17]. Similarities between the above model and a thermoelectric generator were recently discussed in Ref. [95].

Now, a two-parameter optimization of the above expression, over ϵ_1 and ϵ_2, yields the trivial solution $\epsilon_1 = 0$ and $\epsilon_2 = 0$, which is clearly not a meaningful result. Therefore, we go a step

further and retain terms up to second order in the exponentials, then power is given by

$$P = r_0(\epsilon_1 - \epsilon_2)\left(\frac{\epsilon_2}{T_2} - \frac{\epsilon_1}{T_1} + \frac{\epsilon_1^2}{2T_1^2} - \frac{\epsilon_2^2}{2T_2^2}\right). \tag{2.13}$$

Now, optimizing the above expression over ϵ_1 and ϵ_2, we get following solution (see Appendix A)

$$\epsilon^*_{1_{hot}} = T_1\frac{(4-3\eta_C)}{3(2-\eta_C)}, \quad \epsilon^*_{2_{hot}} = T_1\frac{(1-\eta_C)(4-\eta_C)}{3(2-\eta_C)}. \tag{2.14}$$

It is clear that the expression for efficiency remains as in Eq. (2.6). Thus, we obtain the expressions for optimal power and EMP in the high temperatures regime

$$P^*_{\rm hot} = \frac{2r_oT_1\eta_C^2}{27(2-\eta_C)}, \tag{2.15}$$

$$\eta^*_{\rm hot} = \frac{2-\eta_C}{4-3\eta_C}\eta_C. \tag{2.16}$$

If we expand η^*_{hot} in Taylor series near equilibrium, we obtain

$$\eta^*_{hot} = \frac{\eta_C}{2} + \frac{\eta_C^2}{8} + \frac{9\eta_C^3}{96} + O(\eta_C^4). \tag{2.17}$$

The above series shows that the universality of EMP up to second order [19, 61] survives in the high temperatures limit, using a non-linear approximation in the power output. The above form of efficiency is compared with Eq. (2.10) in Figure 2.1, where we also compare the optimal power, Eq. (2.9), with the optimal power in high temperatures non-linear regime, Eq. (2.15). It is to be noted that whereas the latter approximation overestimates EMP, the power output is underestimated as compared to optimal power.

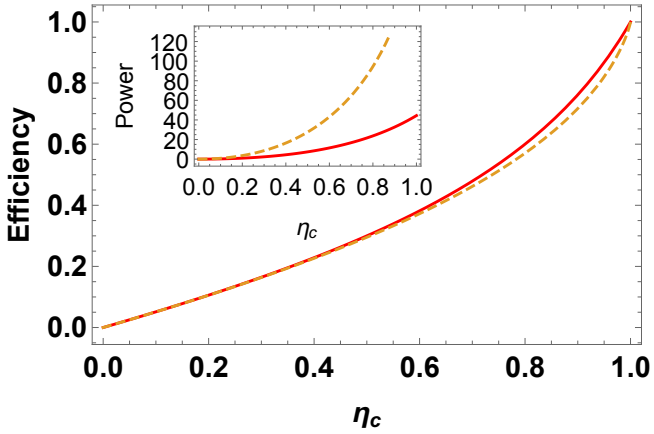

Figure 2.1: The efficiency of FS ratchet plotted against η_C. Dashed curve and upper solid curves correspond to equations (2.10) and (2.16) respectively, with the corresponding optimal power versus η_C, using $r_o = 1$ and $T_1 = 600$.

2.4 Linear regime with constraints

In this section, we impose simple constraints on the energy scales of the ratchet system in the linear regime. This allows us to define a single-parameter optimization problem for power output, Eq. (2.12). These constraints may be interpreted as a form of control on the design of the device. We are interested in the form of EMP under the following constraints [66].

(a) $\epsilon_1 = k_1 > 0$. Then optimizing power (Eq. (2.12)) with respect to ϵ_2, we get $\epsilon_2^* = k_1(2-\eta_C)/2$ and EMP as

$$\eta_{\epsilon_1} = \frac{\eta_C}{2}, \tag{2.18}$$

a universal expression independent of the chosen k_1 value.

(b) On the other hand, consider setting $\epsilon_2 = k_2 > 0$. On optimization of power, we obtain $\epsilon_1^* = k_2(2-\eta_C)/(2-2\eta_C)$, and EMP as

$$\eta_{\epsilon_2} = \frac{\eta_C}{2-\eta_C}, \tag{2.19}$$

which is again a universal formula depending only on the ratio of bath temperatures, but independent of the chosen constant k_2. Of course, the expressions for optimal power do depend on

the chosen constant.

(c) A more general constraint $\gamma\epsilon_1 + (1-\gamma)\epsilon_2 = k_3$ where $0 \leq \gamma \leq 1$. Here, the constraint involves two fixed parameters. Optimization of power subject to this constraint, leads to the following optimal values:

$$\epsilon_1^* = \frac{k_3(2-(1-\gamma)\eta_C)}{2(1-(1-\gamma)\eta_C)}, \quad \epsilon_2^* = \frac{k_3(2-(2-\gamma)\eta_C)}{2(1-(1-\gamma)\eta_C)} \tag{2.20}$$

and the EMP is Schmiedl-Seifert (SS) efficiency [41]

$$\eta_{SS} = \frac{\eta_C}{2-(1-\gamma)\eta_C}. \tag{2.21}$$

Clearly, (a) and (b) are special cases, with $\gamma = 1$ and $\gamma = 0$, respectively. Here, EMP is independent of k_3, but depends on γ. The above form has been obtained in Refs. [1, 41, 67, 99–101], where the parameter γ may be defined, for example, in terms of the ratio of the dissipation constants or thermal conductivities of the thermal contacts [1, 99].

(d) If the constraint $\epsilon_1\epsilon_2 = k_4$ is imposed, the optimal power is obtained at CA efficiency [10]:

$$\eta_{CA} = 1 - \sqrt{1-\eta_C}, \tag{2.22}$$

at optimal values of ϵ_1 and ϵ_2:

$$\epsilon_1^* = \sqrt{k_4}(1-\eta_C)^{1/4}, \quad \epsilon_2^* = \frac{\sqrt{k_4}}{(1-\eta_C)^{1/4}}. \tag{2.23}$$

2.5 Mapping to effective thermodynamic model

The expressions for EMP, obtained in the above, are also encountered in many thermodynamic models based on different assumptions [1, 41, 99–101]. They are obtained in finite-time as well as quasi-static models [67, 102] of heat engines. Thus, it is natural to enquire about the thermodynamic underpinning of the constrained FS model. In this section, we show that FS engine

in the linear regime can be mapped to a specific endoreversible model, under the constraints described above. In the endoreversible approximation [10, 26, 103], the work-extracting part of the engine operates in a reversible way, and any irreversibility in the cycle is attributed solely to thermal contacts with the reservoirs due to finite conductance of the heat exchangers.

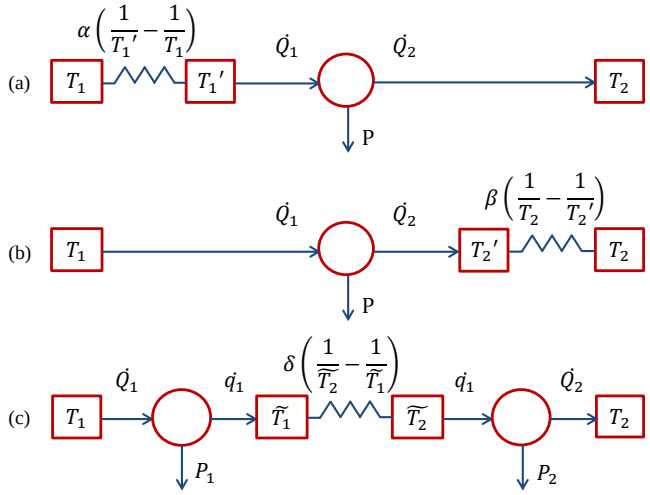

Figure 2.2: Effective models of FS engine. Here α, β and δ are coefficients of heat conductance. (a) Engine with resistance to incoming heat flux only; (b) Engine with resistance to outgoing heat flux only; (c) Two coupled reversible engines where the heat flow between the engines experiences resistance.

(a) In the linear regime, the heat flux entering from the hot reservoir $\dot{Q}_1$, Eq. (3.1), is given by

$$\dot{Q}_1 = r_0\epsilon_1\left(\frac{\epsilon_2}{T_2}-\frac{\epsilon_1}{T_1}\right). \tag{2.24}$$

$$\equiv r_0\epsilon_1^2\left(\frac{1-\eta}{T_2}-\frac{1}{T_1}\right). \tag{2.25}$$

Here, we identify $T_1' = T_2/(1-\eta)$ as an effective temperature, satisfying $T_2 < T_1' < T_1$. Therefore, when we impose $\epsilon_1 =$ constant, the heat flux satisfies $\dot{Q}_1 \propto (1/T_1' - 1/T_1)$, i.e. the flux is proportional to thermodynamic force as in linear irreversible thermodynamics (see Figure 2.2(a)). Then, it is assumed that the power is extracted between the temperatures T_1' and

T_2, with reversible efficiency given by $\eta = 1 - T_2/T_1'$. Therefore,

$$P = \eta \dot{Q}_1 = r_0 \eta \epsilon_1^2 \left(\frac{1-\eta}{T_2} - \frac{1}{T_1} \right). \tag{2.26}$$

Optimizing power with respect to η ($\partial P/\partial \eta = 0$), we can obtain EMP as in Eq. (3.53).

(b) Similarly, in terms of ϵ_2, the heat flux into the cold bath can be written as

$$\begin{aligned} \dot{Q}_2 &= r_0 \epsilon_2^2 \left(\frac{1}{T_2} - \frac{1}{T_1(1-\eta)} \right) \\ &\equiv r_0 \epsilon_2^2 \left(\frac{1}{T_2} - \frac{1}{T_2'} \right), \end{aligned}$$

where $T_2' = T_1(1-\eta)$ is an effective temperature, lying between values T_1 and T_2. Thus, for a fixed value of ϵ_2, the heat flux $\dot{Q}_2$ is proportional to $(1/T_2 - 1/T_2')$, which plays the role of thermodynamic force (see Figure 2.2(b)). In this case, power is extracted at Carnot efficiency between T_1 and T_2': $\eta = 1 - T_2'/T_1$. Therefore,

$$P = \frac{\eta}{1-\eta} \dot{Q}_2 = r_0 \epsilon_2^2 \frac{\eta}{1-\eta} \left(\frac{1}{T_2} - \frac{1}{T_1(1-\eta)} \right). \tag{2.27}$$

Optimizing the above equation with respect to η, we obtain Eq. (3.54).

(c) For the linear constraint $\gamma \epsilon_1 + (1-\gamma)\epsilon_2 = k_3$, the effective thermodynamic model is more interesting. In terms of η, this constraint equation can be written as

$$\epsilon_1 = \frac{k_3}{\gamma + (1-\gamma)(1-\eta)} \equiv \frac{k_3}{A}. \tag{2.28}$$

Then the expression for power becomes

$$P = r_0 k_3^2 \frac{\eta}{A^2} \left(\frac{1-\eta}{T_2} - \frac{1}{T_1} \right), \tag{2.29}$$

which can be rewritten as follows:

$$P = r_0 k_3^2 \frac{\eta}{A} \left(\frac{1}{\tilde{T}_2} - \frac{1}{\tilde{T}_1} \right), \tag{2.30}$$

where the effective temperatures are defined as

$$\tilde{T}_1 = T_1 A, \qquad \tilde{T}_2 = \frac{T_2 A}{1-\eta}. \tag{2.31}$$

Now we show that FS system in the linear regime, and under the general constraint, is equivalent to a system of two coupled Carnot engines in which heat flux leaving the first engine ($\dot{q}_1$), serves as input heat flux for the second engine, through a finite heat conductance (see Figure 2.2(c)). Thus consider the power output from the first engine:

$$P_1 = \frac{\eta_1}{1-\eta_1} \dot{q}_1, \tag{2.32}$$

where η_1 is the reversible efficiency of engine 1 working between T_1 and $\tilde{T}_1$:

$$\eta_1 = 1 - \frac{\tilde{T}_1}{T_1} = 1 - A, \tag{2.33}$$

and

$$\dot{q}_1 = r_0 k_3^2 \left(\frac{1}{\tilde{T}_2} - \frac{1}{\tilde{T}_1} \right), \tag{2.34}$$

is the heat flux leaving engine 1. Thus $r_0 k_3^2 \equiv \delta$ is the heat transfer coefficient of the heat exchanger connecting engines 1 and 2. So, we can rewrite Eq. (5.5) as

$$P_1 = r_0 k_3^2 \frac{1-A}{A} \left(\frac{1}{\tilde{T}_2} - \frac{1}{\tilde{T}_1} \right). \tag{2.35}$$

Now, engine 2 operates at Carnot efficiency η_2 between temperatures $\tilde{T_2}$ and T_2:

$$\eta_2 = 1 - \frac{T_2}{\tilde{T_2}} = 1 - \frac{1-\eta}{A}, \tag{2.36}$$

with the input heat flux as $\dot{q}_1$. Hence, power of engine 2, $P_2 = \eta_2 \dot{q}_1$ can be written as

$$P_2 = r_0 k_3^2 \left(1 - \frac{1-\eta}{A}\right)\left(\frac{1}{\tilde{T_2}} - \frac{1}{\tilde{T_1}}\right). \tag{2.37}$$

Adding equations (2.35) and (2.37), we get

$$P_1 + P_2 = P, \tag{2.38}$$

which is the total power, Eq. (2.30). Alternately, we can write $P_1 = (1-\gamma)P$ and $P_2 = \gamma P$. Optimizing P with respect to η, we obtain Eq. (2.21). It is clear that the maximum of P_1 and P_2 is also reached at the same value of η as of P. Thus optimality of P for the overall engine implies optimal power output of the sub-engines.

Now, the values $\gamma = 0$ and $\gamma = 1$ correspond to the special cases (a) and (b), respectively. Using $A = \gamma + (1-\gamma)(1-\eta)$, we can write

$$\eta_1 = (1-\gamma)\eta, \qquad \eta_2 = \frac{\gamma\eta}{1-\eta+\eta\gamma}. \tag{2.39}$$

Also, the manner in which the two sub-engines are coupled, implies that the efficiencies of the sub-engines are related to the overall efficiency as: $\eta = 1 - (1-\eta_1)(1-\eta_2)$.

Finally, using Eq. (2.21), the EMPs for engine 1 and 2 are given by

$$\eta_1^* = \frac{(1-\gamma)\eta_C}{2-(1-\gamma)\eta_C}, \qquad \eta_2^* = \frac{\gamma\eta_C}{2-2(1-\gamma)\eta_C}. \tag{2.40}$$

(d) For the constraint $\epsilon_1\epsilon_2 = k_4$, Eq. (2.12) for power becomes simplified as

$$P = r_0 k_4 \eta \left(\frac{1}{T_2} - \frac{1}{T_1(1-\eta)} \right). \tag{2.41}$$

$$\equiv r_0 k_4 \frac{\eta}{\sqrt{1-\eta}} \left(\frac{1}{\bar{T}_2} - \frac{1}{\bar{T}_1} \right), \tag{2.42}$$

where we have defined

$$\bar{T}_1 = T_1\sqrt{1-\eta}, \qquad \bar{T}_2 = \frac{T_2}{\sqrt{1-\eta}}, \tag{2.43}$$

as the effective temperatures. Further, it is useful to decompose $\eta/\sqrt{1-\eta}$ as follows:

$$\frac{\eta}{\sqrt{1-\eta}} = \frac{1-(1-\eta)}{\sqrt{1-\eta}} = \frac{1}{\sqrt{1-\eta}} - \sqrt{1-\eta}. \tag{2.44}$$

Thus, we can express Eq. (2.42) in the following form

$$P = r_0 k_4 \left(\frac{1}{\sqrt{1-\eta}} - 1 \right) \left(\frac{1}{\bar{T}_2} - \frac{1}{\bar{T}_1} \right) + r_0 k_4 (1 - \sqrt{1-\eta}) \left(\frac{1}{\bar{T}_2} - \frac{1}{\bar{T}_1} \right), \tag{2.45}$$

which can be rewritten as

$$P = \frac{\eta_1'}{1-\eta_1'} \dot{q}_1' + \eta_2' \, \dot{q}_1' \equiv P_1 + P_2, \tag{2.46}$$

where $\eta_1'(\eta_2')$ is Carnot efficiency of engine 1(2) operating between the temperatures $T_1(\bar{T}_2)$ and $\bar{T}_1(T_2)$, defined as

$$\eta_1' = 1 - \frac{\bar{T}_1}{T_1} = 1 - \sqrt{1-\eta}, \tag{2.47}$$

$$\eta_2' = 1 - \frac{T_2}{\bar{T}_2} = 1 - \sqrt{1-\eta}, \tag{2.48}$$

and

$$\dot{q}_1' = r_0 k_4 \left(\frac{1}{\bar{T}_2} - \frac{1}{\bar{T}_1} \right) \tag{2.49}$$

is the heat flux leaving engine 1 and entering engine 2 (see Figure 2.3(a)). Here $r_0 k_4$ is heat transfer coefficient of the heat exchanger connecting engines 1 and 2. We note that engine 1 and engine 2 deliver power at same efficiency. Then, the expressions for η_1' and η_2', at optimal power, are given by:

$$\eta_1'^{*} = \eta_2'^{*} = 1 - (1 - \eta_C)^{1/4}. \tag{2.50}$$

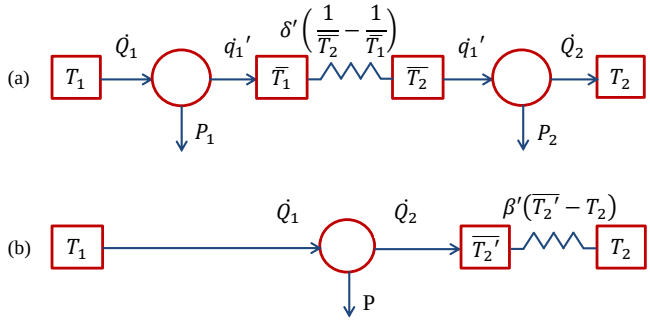

Figure 2.3: Two different thermodynamic models of FS ratchet for the constraint $\epsilon_1 \epsilon_2 = k_4$. (a) Two Carnot engines connected by thermal conductance $\delta' = r_0 k_4$. (b) Carnot engine subjected to finite thermal conductance β' for the outgoing heat flux obeying Newton's law.

2.6 Discussion and Summary

Our choice of constraints is motivated by the fact that both ϵ_1 and ϵ_2 are the control parameters of the ratchet system. It is possible to tune either of them to obtain a desired performance of the engine. In other words, energy constraints can be imposed by setting a design goal. On the other hand, it is not straightforward to appreciate the nature of control with the general linear constraint (c), though one can consider the equivalent thermodynamic model with effective temperatures as in Eq. (2.31). For a given value of γ, we can tune these temperatures and thus the efficiencies of engines 1 and 2. For $\eta = 0$, we have $\tilde{T}_1 = T_1$ and $\tilde{T}_2 = T_2$. In the reversible limit, when $\eta = \eta_C$, we have $\tilde{T}_1 = \tilde{T}_2 = \gamma T_1 + (1-\gamma) T_2$, see Figure 2.4. From Eqs. (2.35) and (2.37), it is also clear that the power vanishes as $\tilde{T}_1 \to \tilde{T}_2$. Similar considerations can be made

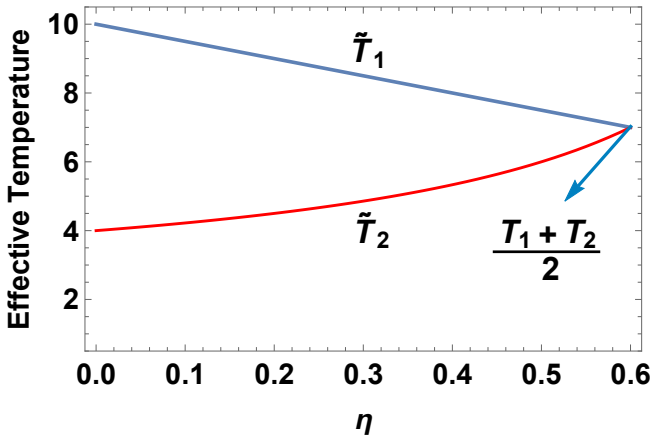

Figure 2.4: Effective temperatures $\tilde{T}_1(\tilde{T}_2)$ with constraint (c), as plotted against the efficiency of the ratchet engine. Here $T_1 = 10$, $T_2 = 4$ and $\eta_C = 0.6$. The upper curve represents the effective temperature of engine 1 and the lower curve represents the effective temperature of engine 2.

regarding the control of the effective temperatures in the case of constraint (d).

However, note that the proposed thermodynamic model for the constrained FS system may not be unique. This may be shown by considering the case (d). We have mapped this model to two coupled reversible engines connected by a heat flow with an inverse-temperature law. It has been shown that the EMP in this model is CA-efficiency. Usually, CA-value is associated with EMP for endoreversible models with Newtonian heat flows, i.e. heat flux is proportional to the difference of temperatures between which the heat flow takes place [10, 26]. In fact, it is possible to imagine an alternate model as follows (see Figure 2.3(b)). By rewriting the power output, we get

$$\begin{aligned} P &= \frac{r_0 k_4}{T_1 T_2} \frac{\eta}{1-\eta} \left(T_1(1-\eta) - T_2\right) \\ &\equiv k' \frac{\eta}{1-\eta} (\bar{T}_2' - T_2), \end{aligned} \tag{2.51}$$

where we define $\bar{T}_2' = T_1(1-\eta)$ as the effective temperature and $k' = r_0 k_4 / T_1 T_2$ as the coefficient of the exiting heat flux $\dot{Q}_2 = k'(\bar{T}_2' - T_2)$, between temperatures $\bar{T}_2'$ and T_2.

Concluding, we have considered the optimization of output power in FS ratchet in the high

temperatures regime, when the internal energy scales are much smaller in comparison to bath temperatures. A two-parameter optimization is possible if one includes the quadratic terms in the expansion of the exponentials. For the linear model, we have considered simple constraints on the internal scales, and obtained some well-known forms of EMP, such as SS-efficiency and CA-efficiency. The reason for these similarities is appreciated by showing that the constrained FS system can be mapped to a finite-time endoreversible model with appropriately defined heat flows, using effective temperatures. Finally, due to a formal analogy between FS system in the linear regime and thermoelectric models [95], and also specific types of quantum heat engines in the hot temperatures regime [66], the present analysis can provide a useful perspective on a broader class of energy conversion systems.

Chapter 3

Optimization of Feynman's model with two different trade-off objective functions and estimation with prior information

3.1 Introduction

A standard method of optimization assumes a complete knowledge of the model, in the sense that the variables over which optimization is performed, such as intrinsic energy scales [17, 19], or the intermediate temperatures of the working medium [104], or the times spent on the thermal contacts with the reservoirs [1], take on definite values; one just has to tune them to specific value(s) in order to optimize the objective function. Recently, one of the authors and coworkers [82, 83, 89, 91], introduced a novel method of optimization, by which some variables can be assigned values, only in a probabilistic sense. This approach is based on interpreting the limited prior information about the system in the sense of subjective probability [84, 105], and a prior distribution quantifies the uncertainty in these parameters. Then an averaging procedure is performed on the target function using this probability distribution so as to eliminate these parameters. Following this approach, CA-efficiency for engine as well as COP of the refrig-

erator [20, 90], have been reproduced. Using the inference based prior information approach, many other significant results of FTT have been reproduced and universal nature of efficiency has also been addressed using this approach.

Thus, the latter approach provides an effective way of analyzing the performance of energy conversion systems. Here, the limited information can be interpreted in the sense of a limited control of the observer over the system. So, this approach also points towards an entirely different origin of the figures of merit at optimal performance, which are usually obtained by an exact tuning of the variable parameters.

In this chapter, we apply and compare the above mentioned two approaches for optimization: the standard one-parameter or two-parameter optimization, and the alternate, one-parameter optimization which also involves estimation based on prior information. We use Feynman's ratchet model [93, 94] as the paradigmatic example for our investigation. We study the model for both engine and refrigerator modes.

For the heat engine mode, we use two different trade-off objective functions:EF [44] and EP function (P_η) [47, 48].EF can also be used to analyze the performance of Feynman's model operating as a refrigerator. Complimentary to EP function, we also use χ function to study the refrigerator mode. It is defined as: $\chi = \zeta \dot{\mathcal{Q}}_2$, where ζ is COP of the refrigerator and $\dot{\mathcal{Q}}_2$ is the rate of refrigeration. Optimization of χ-criterion represents a compromise between the COP and rate of refrigeration of the refrigerator.

The chapter is organized as follows. In Section 3.2, we describe the model of Feynman's ratchet as heat engine and discuss its optimal performance with ecological criterion. In Subsection 3.2.1, two parameter optimization of the ratchet is carried out. In Subsection 3.2.2, the approach based on prior information is applied to the case when the efficiency of the engine is fixed, but one of the internal energy scales is uncertain. The analysis is extended to the refrigerator mode in Section 3.3 where we discuss performance based on two-parameter optimization of ecological criterion as well as the estimation based on prior information. In Section 3.4, we optimize the performance of the engine operating at maximum EP, by carrying out two parameter

optimization for the general case as well as one parameter optimization in the high temperature limit. Section 3.5 is devoted to the prior information analysis in which we reproduce the results obtained in the last section. In Section 3.6, we repeat the analysis performed in Sections 3.4 and 3.5, to study the refrigerator mode operating at maximum χ function. The final Section 3.7 is devoted to results and conclusions.

3.2 Optimal performance of the heat engine

The model of Feynman's ratchet [93] consists of a vane, immersed in a hot reservoir at temperature T_1, and connected through an axle with a ratchet in contact with a cold reservoir at T_2. The ratchet is restricted to rotate in one direction due to a pawl which in turn is connected to a spring. Let ϵ_2 be the amount of energy to overcome the elastic energy of the spring. Let in each step, the wheel rotate an angle δ and the torque induced by the weight be Z. Then the system requires a minimum of $\epsilon_1 = \epsilon_2 + Z\delta$ energy to lift the weight hanging from the axle. Hence the rate of forward jumps of the ratchet is given as $R_{\rm F} = r_0 e^{-\epsilon_1/T_1}$, where r_0 is a rate constant and we have set Boltzmann's constant $k_{\rm B} = 1$. In other words, temperature has the dimensions of energy. Similarly, the rate of the backward jumps is $R_{\rm B} = r_0 e^{-\epsilon_2/T_2}$. One may regard $Z\delta$ and $-Z\delta$ as the work done by and on the system, respectively. Then, the rates of heat absorbed from the hot and the cold reservoirs, are given as

$$\dot{Q}_1 = r_0\epsilon_1 \left(e^{-\epsilon_1/T_1} - e^{-\epsilon_2/T_2}\right), \tag{3.1}$$

$$\dot{Q}_2 = r_0\epsilon_2 \left(e^{-\epsilon_1/T_1} - e^{-\epsilon_2/T_2}\right). \tag{3.2}$$

The power output and efficiency of the engine are given by following two equations, respectively

$$P = \dot{Q}_1 - \dot{Q}_2 = r_0(\epsilon_1 - \epsilon_2) \left(e^{-\epsilon_1/T_1} - e^{-\epsilon_2/T_2}\right), \tag{3.3}$$

$$\eta = \frac{P}{\dot{Q}_1} = 1 - \frac{\epsilon_2}{\epsilon_1}. \tag{3.4}$$

The rate of total entropy production in this energy conversion is:

$$\dot{S}_{\rm tot} = -\frac{\dot{Q}_1}{T_1} + \frac{\dot{Q}_2}{T_2}. \tag{3.5}$$

Then the ecological criterion has been defined as [44]:

$$E = P - T_2 \dot{S}_{\rm tot}. \tag{3.6}$$

3.2.1 Two parameter ecological optimization of heat engine

Using Eqs. (3.1)-(3.6), the EF E can be written as:

$$E = 2P - \eta_C \dot{Q}_1 = r_o \left(e^{-\epsilon_1/T_1} - e^{-\epsilon_2/T_2}\right) [2(\epsilon_1 - \epsilon_2) - \eta_C \epsilon_1]. \tag{3.7}$$

On optimizing E with respect to ϵ_1 and ϵ_2, i.e., setting $\partial E/\partial \epsilon_1 = 0$ and $\partial E/\partial \epsilon_2 = 0$, we get the following two equations respectively,

$$T_1(2-\eta_C)\left(e^{-\epsilon_1/T_1} - e^{-\epsilon_2/T_2}\right) = e^{-\epsilon_1/T_1}[2(\epsilon_1-\epsilon_2) - \eta_C\epsilon_1], \tag{3.8}$$

$$2T_2\left(e^{-\epsilon_1/T_1} - e^{-\epsilon_2/T_2}\right) = e^{-\epsilon_2/T_2}[2(\epsilon_1-\epsilon_2) - \eta_C\epsilon_1]. \tag{3.9}$$

Upon dividing Eq. (3.8) by Eq. (3.9), we can obtain

$$\frac{\epsilon_2}{T_2} - \frac{\epsilon_1}{T_1} = \ln\left[\frac{(2-\eta_C)}{2(1-\eta_C)}\right] \equiv k. \tag{3.10}$$

Eliminating $e^{\epsilon_2/T_2 - \epsilon_1/T_1}$ from Eq. (3.9) by using Eq. (3.10), we get

$$T_2\eta_C = (1-\eta_C)[2(\epsilon_1-\epsilon_2) - \eta_C\epsilon_1]. \tag{3.11}$$

The solution of Eqs. (3.10) and (3.11) is

$$\epsilon_1^* = \frac{T_2[\eta_C + 2k(1-\eta_C)]}{\eta_C(1-\eta_C)}, \qquad \epsilon_2^* = \frac{T_2[\eta_C + (2-\eta_C)k]}{\eta_C}. \tag{3.12}$$

Substituting from Eq. (3.12) into Eq. (3.4), we obtain the efficiency at maximum ecological function (EMEF)

$$\eta^* = \frac{\eta_C + (1-\eta_C)k}{\eta_C + 2(1-\eta_C)k}\,\eta_C. \tag{3.13}$$

Close to equilibrium (small values of η_C), η^* behaves as follows

$$\eta^* = \frac{3\eta_C}{4} + \frac{\eta_C^2}{32} + \frac{19\eta_C^3}{768} + \mathcal{O}(\eta_C^4). \tag{3.14}$$

Note that the above value of efficiency depends only on η_C, or the ratio of the reservoir temperatures. The behavior of η^* close to equilibrium, will be discussed below. Eq. (3.13) is plotted in Figure 3.1. Similarly, from Eq. (3.7), we obtain the maximum value of the EF

$$E^* = \frac{r_o T_1 \eta_C^2 [2(1-\eta_C)]^{2(1-\eta_C)/\eta_C}}{e(2-\eta_C)^{(2-\eta_C)/\eta_C}}. \tag{3.15}$$

3.2.2 Prior information and estimation for heat engine

Now we consider a situation where the efficiency of the engine has some pre-specified value η, but the energy scales (ϵ_1, ϵ_2) are not given to us in *a priori* information. Since η is known, the problem is reduced to a single uncertain parameter, due to Eq. (3.4). One can cast the problem either in terms of ϵ_1 or ϵ_2. In terms of the latter, we can write EF as

$$E(\eta, \epsilon_2) = \frac{r_0 \epsilon_2}{(1-\eta)}(2\eta - \eta_C)\left(e^{-\epsilon_2/(1-\eta)T_1} - e^{-\epsilon_2/T_2}\right). \tag{3.16}$$

Based on the notion of prior information in Bayesian statistics, we assign a prior probability distribution for ϵ_2 in some arbitrary, but a finite range of positive values: $[\epsilon_{\min}, \epsilon_{\max}]$. Later we consider an asymptotic range in which the analysis becomes simplified and we observe

universal features.

Now consider two observers A and B who respectively assign a prior for ϵ_1 and ϵ_2. Taking the simplifying assumption that each observer is in an equivalent state of knowledge, we can write [20, 84, 89]

$$\Pi(\epsilon_1) = \Pi(\epsilon_2) \left| \frac{d\epsilon_2}{d\epsilon_1} \right|, \tag{3.17}$$

where Π is the prior distribution function, taken to be of the same form for each observer. At a fixed known value of efficiency, it implies that $\Pi(\epsilon_2) \propto 1/\epsilon_2$. This is also well-known as Jeffreys prior for a one-dimensional scale parameter [84, 105].

Now, we define the expected value of function E, over this prior, as

$$\begin{aligned} \overline{E}(\eta) &= \int_{\epsilon_{\min}}^{\epsilon_{\max}} E(\eta, \epsilon_2) \Pi(\epsilon_2) d\epsilon_2 \\ &= \frac{C}{(1-\eta)} (2\eta - \eta_C) \int_{\epsilon_{\min}}^{\epsilon_{\max}} \left(e^{-\epsilon_2/(1-\eta)T_1} - e^{-\epsilon_2/T_2} \right) d\epsilon_2, \end{aligned} \tag{3.18}$$

where

$$C = r_0 \left[\ln \left(\frac{\epsilon_{\max}}{\epsilon_{\min}} \right) \right]^{-1}. \tag{3.19}$$

Upon performing the integration, we get

$$\overline{E}(\eta) = CT_1(2\eta - \eta_C) \left(e^{-\epsilon_{\min}/(1-\eta)T_1} - e^{-\epsilon_{\max}/(1-\eta)T_1} \right) + \frac{CT_2(2\eta - \eta_C)}{(1-\eta)} \left(e^{-\epsilon_{\max}/T_2} - e^{-\epsilon_{\min}/T_2} \right). \tag{3.20}$$

We are interested in the value of the efficiency at maximum of $\overline{E}$. Hence, on optimizing $\overline{E}(\eta)$ with respect to η, we get

$$\begin{aligned} \frac{\partial \overline{E}}{\partial \eta} &\equiv 2T_1 \left(e^{-\epsilon_{\min}/(1-\eta)T_1} - e^{-\epsilon_{\max}/(1-\eta)T_1} \right) + \frac{T_2(2-\eta_C)}{(1-\eta)^2} \left(e^{-\epsilon_{\max}/T_2} - e^{-\epsilon_{\min}/T_2} \right) \\ &\quad - \frac{2\eta - \eta_C}{(1-\eta)^2} \left(\epsilon_{\min} e^{-\epsilon_{\min}/(1-\eta)T_1} - \epsilon_{\max} e^{-\epsilon_{\max}/(1-\eta)T_1} \right) = 0. \end{aligned} \tag{3.21}$$

Now, we consider the asymptotic limit [20, 82], in which the maximal allowed range for ϵ_2 is considered. In particular, we require $\epsilon_{\max} >> T_1$ and $\epsilon_{\min} << T_2$. In this limit, Eq. (3.21)

reduces to:

$$2T_1 - \frac{2T_2}{(1-\eta)^2} + \frac{T_2\eta_C}{(1-\eta)^2} = 0. \tag{3.22}$$

Putting $T_2/T_1 = 1 - \eta_C$ and solving Eq. (3.22) for η, we get

$$\tilde{\eta} = 1 - \sqrt{\frac{(1-\eta_C)(2-\eta_C)}{2}}. \tag{3.23}$$

The above expression is identical to the one obtained by Angulo-Brown for the ecological optimization of an endoreversible engine [44]. Although the above expression for $\tilde{\eta}$ is different

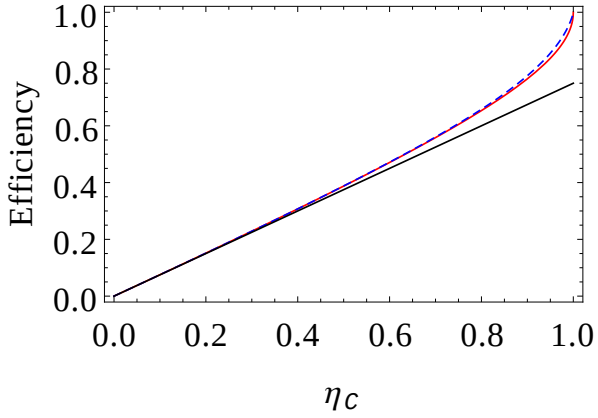

Figure 3.1: The EMEF obtained from two different methods, is plotted versus η_C. The dashed curve represents the efficiency obtained from two-parameter optimization [Eq. (3.13)]. The solid curve is the corresponding efficiency when prior information approach is used [Eq. (3.23)]. The bottom straight line is $3\eta_C/4$. See also Eq. (3.24).

from the one obtained via the two-parameter optimization [Eq. (3.13)], we note that, near equilibrium, i.e., η_C close to zero,

$$\tilde{\eta} = \frac{3\eta_C}{4} + \frac{\eta_C^2}{32} + \frac{3\eta_C^3}{128} + \mathcal{O}(\eta_C^4), \tag{3.24}$$

which shows the same universality upto second order in η_C [51, 54], as Eq.(3.14). The interpretation of this result viz-a-viz the result from exact optimization is the following. If the experimentalist is unable to tune an internal parameter, or has a limited control over it, then it makes sense to consider an expected value of E, suitably averaged over the uncertain parame-

ter. Then it has been observed in the above that this average value, $\overline{E}$, takes its maximum value at a certain efficiency $\tilde{\eta}$, which is also the one obtained in purely thermodynamic models. We observe that the behavior of $\tilde{\eta}$ is very similar to η^*, as a function of η_C close to equilibrium.

3.3 Optimal performance as a refrigerator

Ratchet and pawl system can also be operated as a refrigerator [20, 45, 106, 107]. It is analogous to Büttiker-Landauer model of particle transport [108, 109]. In this section, we consider the function of Feynman's ratchet as a refrigerator [20, 106]. We will optimize the corresponding ecological criterion [53]:

$$\mathcal{E} = \dot{\mathcal{Q}}_2 - \zeta_C T_1 \dot{\mathcal{S}}_{\rm tot}. \tag{3.25}$$

where $\dot{\mathcal{S}}_{\rm tot}$ is the rate of entropy production and $\zeta_C = T_2/(T_1 - T_2)$ is Carnot COP. The rate of refrigeration and rate of heat added to the hot reservoir are given respectively as:

$$\dot{\mathcal{Q}}_2 = r_0 \epsilon_2 \left(e^{-\epsilon_2/T_2} - e^{-\epsilon_1/T_1} \right), \tag{3.26}$$

$$\dot{\mathcal{Q}}_1 = r_0 \epsilon_1 \left(e^{-\epsilon_2/T_2} - e^{-\epsilon_1/T_1} \right). \tag{3.27}$$

Further, for refrigerator, rate of entropy production and COP are given by:

$$\dot{\mathcal{S}}_{\rm tot} = \frac{\dot{\mathcal{Q}}_1}{T_1} - \frac{\dot{\mathcal{Q}}_2}{T_2}, \tag{3.28}$$

$$\zeta = \frac{\dot{\mathcal{Q}}_2}{\dot{\mathcal{Q}}_1 - \dot{\mathcal{Q}}_2} = \frac{\epsilon_2}{\epsilon_1 - \epsilon_2}. \tag{3.29}$$

3.3.1 Two parameter ecological optimization for the refrigerator

Using Eqs. (3.26)-(3.28), the EF in Eq. (3.25) can be written as

$$\mathcal{E} = r_o \left(e^{-\epsilon_2/T_2} - e^{-\epsilon_1/T_1} \right) [(2 + \zeta_C)\epsilon_2 - \zeta_C \epsilon_1]. \tag{3.30}$$

On optimizing $\mathcal{E}$ with respect to ϵ_1 and ϵ_2, that is, setting $\partial\mathcal{E}/\partial\epsilon_1 = 0$ and $\partial\mathcal{E}/\partial\epsilon_2 = 0$, we get following two equations respectively,

$$T_1\zeta_C\left(e^{-\epsilon_2/T_2} - e^{-\epsilon_1/T_1}\right) = e^{-\epsilon_1/T_1}[(2+\zeta_C)\epsilon_2 - \zeta_C\epsilon_1], \tag{3.31}$$

$$T_2(2+\zeta_C)\left(e^{-\epsilon_2/T_2} - e^{-\epsilon_1/T_1}\right) = e^{-\epsilon_2/T_2}[(2+\zeta_C)\epsilon_2 - \zeta_C\epsilon_1]. \tag{3.32}$$

Comparing Eqs. (3.31) and (3.32), we can obtain

$$\frac{\epsilon_2}{T_2} - \frac{\epsilon_1}{T_1} = \ln\left(\frac{1+\zeta_C}{2+\zeta_C}\right) \equiv k'. \tag{3.33}$$

Using Eqs. (3.32) and (3.33), we get

$$(2+\zeta_C)\epsilon_2 - \zeta_C\epsilon_1 = T_2. \tag{3.34}$$

Finally, solving the Eqs. (3.33) and (3.34), we obtain optimal values of ϵ_1^* and ϵ_2^*:

$$\epsilon_1^* = \frac{(1+\zeta_C)(1-(2+\zeta_C)k')}{\zeta_C}; \qquad \epsilon_2^* = T_2[1-(1+\zeta_C)k']. \tag{3.35}$$

Using Eq. (3.35) in (3.29), we derive COP at the maximum EF

$$\zeta^* = \frac{1-(1+\zeta_C)k'}{1-2(1+\zeta_C)k'}\zeta_C. \tag{3.36}$$

We can write series expansion of ζ^* with respect to ζ_C as follows

$$\frac{\zeta^*}{\zeta_C} = \frac{2}{3} + \frac{1}{18\zeta_C} - \frac{2}{27\zeta_C^2} + O\left(\frac{1}{\zeta_C}\right)^3. \tag{3.37}$$

Substituting Eq. (3.35) in (3.30), we get the maximum EF

$$\mathcal{E} = \frac{r_o T_2(1+\zeta_C)^{1+\zeta_C}}{e(2+\zeta_C)^{2+\zeta_C}}. \tag{3.38}$$

3.3.2 Prior information and estimation for refrigerator

Similar to the case of heat engine, we now obtain, using the prior based approach, the COP at optimal performance of Feynman's ratchet as refrigerator. Again, we suppose that the figure of merit ζ is fixed at some value and ϵ_2 is uncertain, within the range $[\epsilon_{\min}, \epsilon_{\max}]$. Then Jeffreys prior for ϵ_2 can be argued, similar to Eq. (3.17). In terms of ζ and one of the scales say, ϵ_2, the ecological-criterion $\mathcal{E} = \dot{\mathcal{Q}}_2(2+\zeta_C) - \zeta_C \dot{\mathcal{Q}}_1$, is given by

$$\mathcal{E} = r_0 \left(2 - \frac{\zeta_C}{\zeta}\right) \epsilon_2 \left(e^{-\epsilon_2/T_2} - e^{-\epsilon_2(1+\zeta)/\zeta T_1}\right). \tag{3.39}$$

Then, we define the expected value of $\mathcal{E}$ as

$$\begin{aligned} \overline{\mathcal{E}}(\zeta) &= \int_{\epsilon_{\min}}^{\epsilon_{\max}} \mathcal{E}(\zeta, \epsilon_2) \Pi(\epsilon_2) d\epsilon_2 & (3.40) \\ &= C \left(2 - \frac{\zeta_C}{\zeta}\right) \int_{\epsilon_{\min}}^{\epsilon_{\max}} \left(e^{-\epsilon_2/T_2} - e^{-\epsilon_2(1+\zeta)/\zeta T_1}\right) d\epsilon_2, & (3.41) \end{aligned}$$

where C is given by Eq. (3.19). Upon integrating the above equation, we get

$$\begin{aligned} \overline{\mathcal{E}}(\zeta) &= CT_2 \left(2 - \frac{\zeta_C}{\zeta}\right) \left(e^{-\epsilon_{\min}/T_2} - e^{-\epsilon_{\max}/T_2}\right) \\ &\quad + CT_1 \left(2 - \frac{\zeta_C}{\zeta}\right) \frac{\zeta}{(1+\zeta)} \left(e^{-\epsilon_{\max}(1+\zeta)/\zeta T_1} - e^{-\epsilon_{\min}(1+\zeta)/\zeta T_1}\right). \end{aligned} \tag{3.42}$$

Then the maximum of $\overline{\mathcal{E}}$ with respect to ζ, is evaluated as

$$\begin{aligned} \frac{\partial \overline{\mathcal{E}}}{\partial \zeta} &\equiv \frac{\zeta_C T_2}{\zeta^2} \left(e^{-\epsilon_{\min}/T_2} - e^{-\epsilon_{\max}/T_2}\right) + \frac{(2+\zeta_C)T_1}{(1+\zeta)^2} \left(e^{-\epsilon_{\max}(1+\zeta)/\zeta T_1} - e^{-\epsilon_{\min}(1+\zeta)/\zeta T_1}\right) \\ &\quad + \frac{2\zeta - \zeta_C}{\zeta^2(1+\zeta)} \left(\epsilon_{\max} e^{-\epsilon_{\max}(1+\zeta)/\zeta T_1} - \epsilon_{\min} e^{-\epsilon_{\min}(1+\zeta)/\zeta T_1}\right) = 0 \end{aligned} \tag{3.43}$$

In the asymptotic limit mentioned earlier, the above equation reduces to

$$\frac{\zeta_C T_2}{\zeta^2} = \frac{(2+\zeta_C)T_1}{(1+\zeta)^2}. \tag{3.44}$$

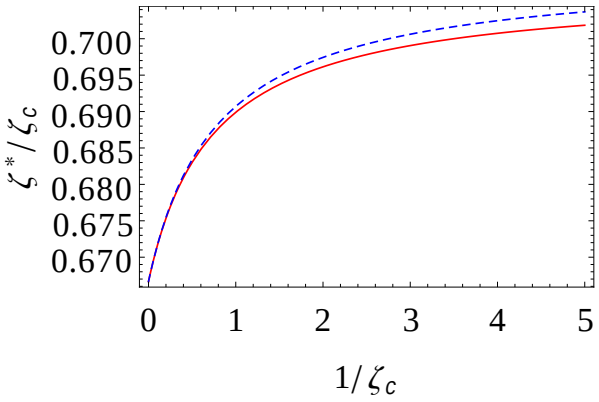

Figure 3.2: The COP (relative to ζ_C) at maximum EF, obtained from two different methods, is plotted versus $1/\zeta_C$. The dashed curve represents the COP obtained from two parameter optimization [Eq. (3.36)]. The solid curve is the corresponding COP when prior information approach is used [Eq. (3.45)].

Putting $T_1/T_2 = (1+\zeta_C)/\zeta_C$ and solving for ζ, we get

$$\tilde{\zeta} = \left(\frac{1+\zeta_C}{\zeta_C} \sqrt{\frac{2+\zeta_C}{1+\zeta_C}} - 1 \right)^{-1} . \tag{3.45}$$

This is the same equation as obtained by Yan [53] when we take the environment temperature equal to the temperature of the hot reservoir. In near-equilibrium regime, the Carnot COP ζ_C, as well as ζ^* become large in magnitude. One can then write the series expansion for ζ^* relative to ζ_C as follows:

$$\frac{\zeta^*}{\zeta_C} = \frac{2}{3} + \frac{1}{18\zeta_C} - \frac{17}{216\zeta_C^2} + \mathcal{O}\left(\frac{1}{\zeta_C}\right)^3 , \tag{3.46}$$

which is similar to the Eq. (3.37) upto first two terms. In Figure 3.2, we compare the expressions from Eqs. (3.36) and (3.45). Before closing, we point out that upon performing the same analysis in terms of ϵ_1 as the uncertain scale, we obtain a similar behavior in the asymptotic range of values, and the same figures of merit, as $\tilde{\eta}$ and $\tilde{\zeta}$, are obtained with the choice of Jeffreys' prior.

3.4 Ratchet engine at maximum efficient power

3.4.1 Two parameter optimization

In this section, we study the optimization of EP function which is product of efficiency (η) and power (P) of the heat engine. Using Eqs. (3.3) and (3.4), it can be written as

$$P_\eta = \eta P = \frac{(\epsilon_1 - \epsilon_2)^2}{\epsilon_1} \left(e^{-\epsilon_1/T_1} - e^{-\epsilon_2/T_2} \right). \tag{3.47}$$

Optimizing Eq. (3.47) with respect to ϵ_1 and ϵ_2, we get following equations:

$$e^{\epsilon_1/T_1 - \epsilon_2/T_2} = 1 - \frac{\epsilon_1(\epsilon_1 - \epsilon_2)}{T_1(\epsilon_1 + \epsilon_2)}, \tag{3.48}$$

$$e^{\epsilon_1/T_1 - \epsilon_2/T_2} = \frac{2T_2}{\epsilon_1 - \epsilon_2 + 2T_2}. \tag{3.49}$$

These two equations cannot be solved analytically for ϵ_1 and ϵ_2. However combining Eqs. (3.4), (3.48) and (3.49), we can obtain following transcendental equation,

$$\frac{(2\eta_C - \eta)(\eta - \eta_C)}{\eta(1 - \eta_C)} = \ln\left[\frac{2(1 - \eta_C)}{2 - \eta}\right], \tag{3.50}$$

from which it is clear that efficiency is independent of system parameters and depends on η_C only. Eq. (3.50) is plotted in Figure 3.3 (dashed curve). Since an analytic solution of this equation is not possible, we first look for perturbative solutions for η_C near equilibrium, by substituting $\eta = a_1\eta_C + a_2\eta_C^2 + a_3\eta_C^3 + O(\eta_C^4)$ in Eq. (3.50) and expanding the resulting equation in η_C. The coefficients a_1, a_2 and a_3 are found recursively by solving order by order in η_C. We find the first order term as $a_1 = 2/3$. At second order and third order, we find $a_2 = 2/27$ and $a_3 = 11/243$, respectively. So near equilibrium, EMEP behaves as follows

$$\eta'^* = \frac{2\eta_C}{3} + \frac{2\eta_C^2}{27} + \frac{11\eta_C^3}{243} + O(\eta_C^4). \tag{3.51}$$

The first two terms in the above equation were also derived for the EMEP of a LD heat engine [60] and a nonlinear irreversible heat engine [63], both working in strong-coupling limit under the condition of symmetric dissipation. This confirms the assertion of Esposito and co-authors that for a strong-coupling system, first two terms in η_C are of universal nature and third term is model dependent [61, 63].

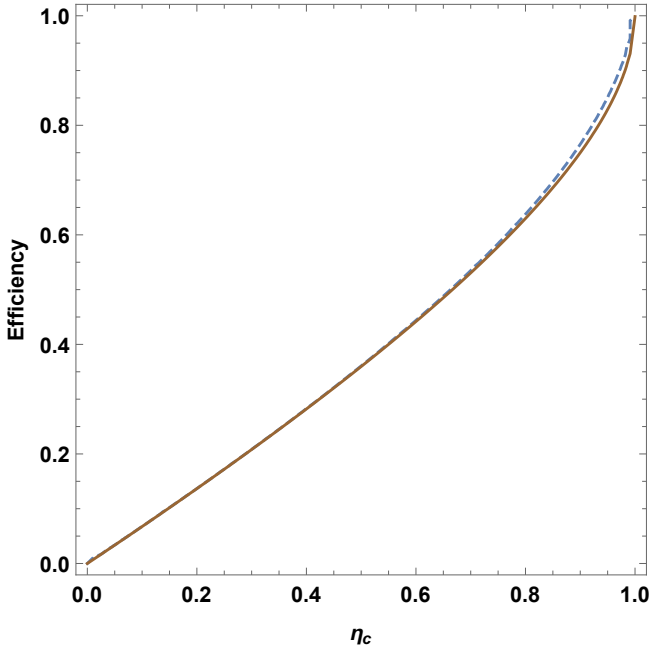

Figure 3.3: The EMEP obtained under two different optimization schemes, is plotted versus η_C. The dashed (upper) and solid (lower) curves represent Eqs. (3.50) and (3.60), respectively.

3.4.2 One parameter optimization in high temperature limit

In order to get analytical expressions for EMEP, we will study Feynman ratchet in high temperature regime [17, 110]. In this regime, energies associated with forward and backward jumps are very small compared to the temperatures of reservoirs. Therefore we can expand $e^{-\epsilon_1/T_1}(e^{-\epsilon_2/T_2})$ upto first order in temperature only. Then the form of the EP is

$$P_\eta = \frac{(\epsilon_1 - \epsilon_2)^2}{\epsilon_1}\left(\frac{\epsilon_2}{T_2} - \frac{\epsilon_1}{T_1}\right) \tag{3.52}$$

Optimization of P_η with respect to ϵ_1 and ϵ_2 yields the solution $\epsilon_1 = 0$ and $\epsilon_2 = 0$, which is clearly not a useful result. Therefore, we impose some simple constraints on the internal energy scales of the system to define a one parameter optimization problem for linear model of ratchet and pawl system. We will consider following two cases:

(a) $\epsilon_1 = k_1 > 0$. Then optimizing EP with respect to ϵ_2, we get

$$\eta_{\epsilon_1} = \frac{2}{3}\eta_C, \tag{3.53}$$

which is the lower limit on efficiency for the LD heat engines operating at MEP [60, 71].

(b) On the other hand by fixing $\epsilon_2 = k_2$, we obtain

$$\eta_{\epsilon_2} = \frac{1}{2}(3 - \sqrt{9 - 8\eta_C}), \tag{3.54}$$

which is the upper limit on efficiency for the LD heat engines operating at MEP [60, 71].

3.5 Prior information approach

3.5.1 Engine at maximum efficient power

Now, we estimate the performance of FS engine using the prior information approach. As mentioned earlier, in this approach, we only have limited information about the control parameters (here ϵ_1 and ϵ_2) of the system. First, we treat ϵ_2 as the uncertain variable. Using Eq. (3.4), we eliminate ϵ_1 from Eq. (3.47) and recast it in terms of η and ϵ_2.

$$P_\eta(\eta, \epsilon_2) = \frac{r_0 \epsilon_2 \eta^2}{1-\eta}\left(e^{-\epsilon_2/(1-\eta)T_1} - e^{-\epsilon_2/T_2}\right). \tag{3.55}$$

Jeffreys prior on ϵ_2 : Assigning Jeffreys prior, $\Pi(\epsilon_2) \propto 1/\epsilon_2$, to uncertain variable ϵ_2 and taking average over the prior distribution, the expected value of EP is given by

$$\begin{aligned}\overline{P_\eta}(\eta) &= \int_{\epsilon_{\min}}^{\epsilon_{\max}} P_\eta(\eta,\epsilon_2)\Pi(\epsilon_2)d\epsilon_2 \\ &= \frac{C\eta^2}{1-\eta}\int_{\epsilon_{\min}}^{\epsilon_{\max}} \left(e^{-\epsilon_2/(1-\eta)T_1} - e^{-\epsilon_2/T_2}\right) d\epsilon_2. \end{aligned} \tag{3.56}$$

Upon performing the integration, we get

$$\begin{aligned}\overline{P_\eta}(\eta) &= CT_1\eta^2\left(e^{-\epsilon_{\min}/(1-\eta)T_1} - e^{-\epsilon_{\max}/(1-\eta)T_1}\right) \\ &\quad + \frac{CT_2\eta^2}{1-\eta}\left(e^{-\epsilon_{\max}/T_2} - e^{-\epsilon_{\min}/T_2}\right). \end{aligned} \tag{3.57}$$

Now, to show that the averaged models behave in thermodynamic fashion, we maximize $\overline{P_\eta}(\eta)$ with respect to η to get following equation:

$$\begin{aligned}\frac{\partial\overline{P}}{\partial\eta} &\equiv 2\eta T_1\left(e^{-\epsilon_{\min}/(1-\eta)T_1} - e^{-\epsilon_{\max}/(1-\eta)T_1}\right) \\ &\quad - \frac{\eta^2}{(1-\eta)^2}\left(\epsilon_{\min}e^{-\epsilon_{\min}/(1-\eta)T_1} - \epsilon_{\max}e^{-\epsilon_{\max}/(1-\eta)T_1}\right) \\ &\quad - T_2\left(e^{-\epsilon_{\min}/T_2} - e^{-\epsilon_{\max}/T_2}\right)\left(\frac{2\eta}{1-\eta} + \frac{\eta^2}{(1-\eta)^2}\right) = 0. \end{aligned} \tag{3.58}$$

Now, we consider the so-called asymptotic limit as defined in Refs. [20, 82]. In this limit, $\epsilon_{\max} >> T_1$ and $\epsilon_{\min} << T_2$. Hence Eq. (3.58) reduces to:

$$2\eta T_1 - \frac{T_2(2\eta-\eta^2)}{(1-\eta)^2} = 0 \tag{3.59}$$

Solving this equation in terms of $\eta_C = 1 - T_2/T_1$, we have

$$\eta^* = 1 - \frac{1}{4}(1-\eta_C)\left(1 + \sqrt{1 + \frac{8}{1-\eta_C}}\right), \tag{3.60}$$

which can be expanded in power series in η_C to reveal universality of the first two terms in the series,

$$\eta^* = \frac{2\eta_C}{3} + \frac{2\eta_C^2}{27} + \frac{9\eta_C^3}{243} + O(\eta_C^4). \tag{3.61}$$

The same expression also holds for the efficiency of a LD heat engine operating at MEP under the conditions of tight system-bath coupling and symmetric dissipation at the hot and the cold baths. The result also holds for the EMEP of an endoreversible heat engine [48].

Alternatively, we may also treat ϵ_1 as the uncertain parameter. Again in this case, we derive Eq. (3.60) in the asymptotic limit.

Uniform Prior: On the other hand, when we have maximal ignorance about the likely values of a parameter, a uniform prior density, $\Pi_u = 1/(\epsilon_{\max} - \epsilon_{\min})$, may be assigned to the uncertain parameter. By considering the uniform prior over the energy ϵ_2 and repeating the steps of above analysis, we obtain the following form of efficiency in the asymptotic limit:

$$\eta^u_{\epsilon_2} = \frac{1}{9}\left(8 - \frac{2^{1/3}K}{\left(M + \sqrt{M^2 - 4K^3}\right)^{1/3}} - \frac{\left(M + \sqrt{M^2 - 4K^3}\right)^{1/3}}{2^{1/3}}\right), \tag{3.62}$$

where $K = 9\eta_C^2 - 18\eta_C + 10$ and $M = 270\eta_C^2 - 540\eta_C + 272$.

Alternatively, we may consider the uniform prior over the energy scale ϵ_1 and in this case, the form of efficiency is found to be

$$\eta^u_{\epsilon_1} = 1 - (1 - \eta_C)^{2/3}, \tag{3.63}$$

Eqs. (3.62) and (3.63) can be expanded in Taylor's series near equilibrium and we have following two equations:

$$\eta^u_{\epsilon_2} = \frac{2\eta_C}{3} + \frac{\eta_C^2}{27} + \frac{4\eta_C^3}{243} + O\left(\eta_C^4\right), \tag{3.64}$$

$$\eta^u_{\epsilon_1} = \frac{2\eta_C}{3} + \frac{\eta_C^2}{9} + \frac{4\eta_C^3}{81} + O\left(\eta_C^4\right). \tag{3.65}$$

Clearly the above equations contains first universal term $2\eta_C/3$ only. Hence we conclude that $2\eta_C/3$ term in the series expansion of EMEP can be faithfully reproduced by the expected EP irrespective of the chosen prior. However, the second order term $2\eta_C^2/27$ follows from the use of Jeffreys prior.

3.5.2 Prior information analysis in the high temperature regime

In this section, we use the prior information approach to study FS in the high temperature limit and re-derive Eqs. (3.53) and (3.54).

Jeffreys prior on ϵ_2: In Subsection 3.5.1, we derived Eq. (3.60) by averaging the EP function over the Jeffreys prior on ϵ_2 and then optimizing the averaged EP with respect to given efficiency. Here, in order to derive the form of optimal efficiency, we consider high temperature limit instead of considering asymptotic limit. In high temperature limit, $\epsilon_{\min}/T_2 << 1$. We put $\epsilon_{\max} = \epsilon_{\min} + \Delta$, where Δ is considered to be a small parameter. As $\epsilon_{\min}/T_2 << 1$, in Eq. (3.58), we can ignore terms containing $\epsilon_{\min}/T_2$ and approximate terms $e^{-\epsilon_{\min}/T_2}$ and $e^{-\epsilon_{\min}/(1-\eta)T_2}$ as unity. The resulting equation is

$$\frac{\eta^2}{(1-\eta)^2}\left[\Delta e^{-\Delta/(1-\eta)T_1} - T_2\left(1-e^{-\Delta/T_2}\right)\right] + 2\eta T_1\left(1-e^{-\Delta/(1-\eta)T_1}\right) - \frac{2\eta T_2}{1-\eta}\left(1-e^{-\Delta/T_2}\right) = 0. \tag{3.66}$$

Since Δ is small, we expand the above equation upto second order in Δ to get

$$\left(\frac{2-\eta}{2T_2} - \frac{1}{(1-\eta)T_1}\right)\Delta^2 = 0. \tag{3.67}$$

Solving the above equation for η, we have

$$\eta_+ = \frac{1}{2}(3-\sqrt{9-8\eta_C}), \tag{3.68}$$

which is the same efficiency as obtained in Eq. (3.54).

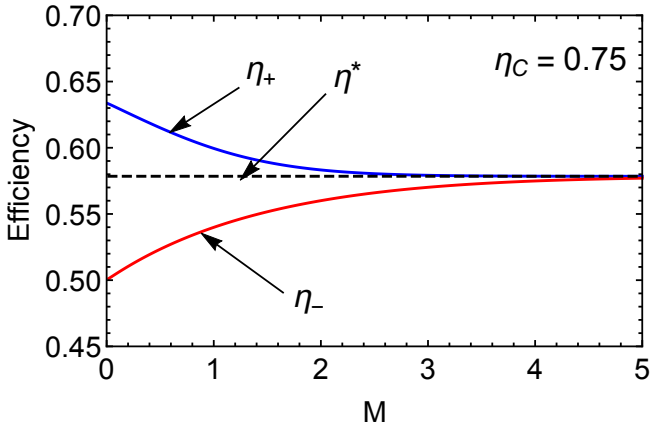

Figure 3.4: The efficiency at maximum expected EP is plotted versus M (M is scaled $\epsilon_{\max}$: $M = \epsilon_{\max}/T_1$), for given $m = \epsilon_{\min}/T_1 = 0.01$, and $\eta_C = 0.75$. The upper (blue) curve is obtained with ϵ_2 as the uncertain variable. For small values of M, the efficiency approaches the upper bound $\eta_+ = (3 - \sqrt{9 - 8\eta_C})/2$. The lower (red) curve implies that ϵ_1 is the uncertain variable, and the efficiency approaches the lower bound $2\eta_C/3$. For large M values, both curves approach $\eta^* = 1 - (1 - \eta_C)(1 + \sqrt{1 + 8/(1 - \eta_C)})/4$.

Jeffreys prior on ϵ_1: In this case, the EP function can be written in terms of η and ϵ_1 as follows

$$P_\eta = \eta^2 \epsilon_1 \left(e^{-\epsilon_1/T_1} - e^{-\epsilon_1(1-\eta)/T_1} \right). \tag{3.69}$$

Integration of the above equation with respect to Jeffreys prior yields

$$\overline{P_\eta}(\eta) = \eta^2 T_1 \left(e^{-\epsilon_{\min}/T_1} - e^{-\epsilon_{\max}/T_2} \right) - \frac{\eta^2 T_2}{1-\eta} \left(e^{-\epsilon_{\min}(1-\eta)/T_2} - e^{-\epsilon_{\max}(1-\eta)/T_2} \right) \tag{3.70}$$

Optimizing the above equation with respect to η, i.e. setting $\partial\overline{P_\eta}/\partial\eta = 0$, we have

$$\begin{aligned} \frac{\partial \overline{P_\eta}}{\partial \eta} &= 2\eta T_1 \left(e^{-\epsilon_{\min}/T_1} - e^{-\epsilon_{\max}/T_1} \right) \\ &\quad - \frac{\eta^2}{1-\eta} \left(\epsilon_{\min} e^{-\epsilon_{\min}(1-\eta)/T_2} - \epsilon_{\max} e^{-\epsilon_{\max}(1-\eta)/T_2} \right) \\ &\quad - \left(e^{-\epsilon_{\min}(1-\eta)/T_2} - e^{-\epsilon_{\max}(1-\eta)/T_2} \right) T_2 \left(\frac{2\eta}{1-\eta} + \frac{\eta^2}{(1-\eta)^2} \right) = 0. \end{aligned} \tag{3.71}$$

In high temperature limit, $\epsilon_{\min}/T_2 << 1$, above equation reduces to

$$2\eta T_1\left(1-e^{-\Delta/T_1}\right)+\frac{\eta^2\Delta}{1-\eta}e^{-\Delta(1-\eta)/T_2}$$
$$-\left(1-e^{-\Delta(1-\eta)/T_2}\right)T_2\left(\frac{2\eta}{1-\eta}+\frac{\eta^2}{(1-\eta)^2}\right)=0. \tag{3.72}$$

Expanding the above equation upto second order term in Δ, we have

$$\eta(3\eta T_1+2T_2-2T_1)\Delta^2=0, \tag{3.73}$$

which can be solved to give

$$\eta_-=\frac{2\eta_C}{3}. \tag{3.74}$$

Again, using the prior information approach, we are able to reproduce the same form of efficiency as obtained in Eq. (3.53) using the one parameter optimization of constrained FS model.

It is worth noting that the expressions $\eta_-=2\eta_C/3$ and $\eta_+=(3-\sqrt{9-8\eta_C})/2$ can also be obtained using the uniform prior over ϵ_1 and ϵ_2, respectively.

The above analysis is valid in the high temperature regime. To understand the general behavior of efficiency, we numerically plot Eqs. (3.58) and (3.71) between efficiency (η) and $M\equiv\epsilon_{\max}/T_1$, for a fixed small value of $m\equiv\epsilon_{\min}/T_1$ at given η_C (see Figure 3.4). In Figure 3.4, blue curve represents Eq. (3.58) when ϵ_2 is uncertain parameter, and red curve represents Eq. (3.71) for uncertain parameter ϵ_1. At large values of M, both curves (red and blue) approach $\eta^*=1-(1-\eta_C)(1+\sqrt{1+8/(1-\eta_C)})/4$.

3.6 Refrigerator at maximum χ function

3.6.1 Two parameter optimization

In section 3.3, we have studied ecological optimization of FS refrigerator. Here, we choose to optimize the function $\chi=\zeta\dot{\mathcal{Q}}_2$, known as χ-criterion [29]. Using Eqs. (3.26) and (3.29), χ

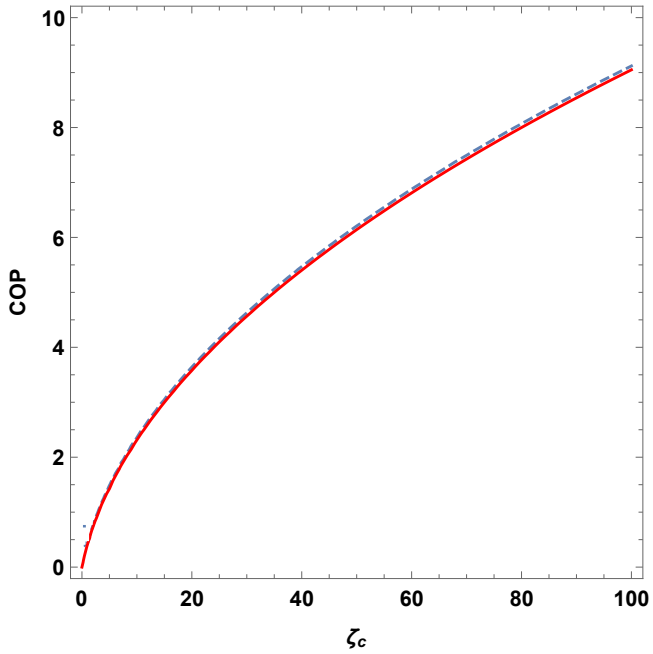

Figure 3.5: The COP at maximum χ function, obtained under two different optimization schemes, is plotted versus ζ_C. The dashed and solid curves represent Eqs. (3.78) and (3.82), respectively.

function can be expressed as

$$\chi = \frac{\epsilon_2^2}{\epsilon_1 - \epsilon_2}\left(e^{-\epsilon_2/T_2} - e^{-\epsilon_1/T_1}\right). \tag{3.75}$$

From $\partial\chi/\partial\epsilon_1 = 0$ and $\partial\chi/\partial\epsilon_2 = 0$, we have following two equations

$$e^{\epsilon_1/T_1 - \epsilon_2/T_2} = 1 + \frac{\epsilon_2\zeta_C}{T_2\zeta(1+\zeta_C)}, \tag{3.76}$$

$$e^{\epsilon_1/T_1 - \epsilon_2/T_2} = \frac{T_2(2+\zeta)}{T_2(2+\zeta) - \epsilon_2}. \tag{3.77}$$

Combining Eqs. (3.29), (3.76) and (3.77), we get following transcendental equation [106],

$$\frac{(\zeta_C - \zeta)(2\zeta_C - \zeta)}{\zeta_C(1+\zeta_C)\zeta} = \ln\left[\frac{\zeta_C(2+\zeta)}{(1+\zeta_C)\zeta}\right], \tag{3.78}$$

which cannot be solved analytically. Eq. (3.78) is plotted in Figure 3.5 (dashed curve). The solution can be approximated by an interpolation formula [106]

$$\bar{\zeta} = \sqrt{\zeta_C + (0.954)^2} - 0.954. \tag{3.79}$$

Similar to the case of heat engine, we analyze the performance of refrigerator in the high temperature regime to get the analytical solution.

3.6.2 One parameter optimization in high temperature regime

Analogous to the case of engine, we will carry out one parameter optimization of the linear model of FS refrigerator, for which χ function is approximated as

$$\chi = \frac{\epsilon_2^2}{\epsilon_1 - \epsilon_2}\left(\frac{\epsilon_1}{T_1} - \frac{\epsilon_2}{T_2}\right). \tag{3.80}$$

We consider following two cases:

(a) $\epsilon_2 = k_3$, optimization of χ function with respect to ϵ_1 fails to provide us optimal value of ϵ_1 rather it implies $\epsilon_2 = k_3 = 0$, which further implies that $\zeta_- = 0$.

(b) $\epsilon_1 = k_4$, optimizing χ with respect to ϵ_2, that is, setting $\partial\chi/\partial\epsilon_2 = 0$, the COP at maximum χ function is given by

$$\zeta_+ = \frac{1}{2}(\sqrt{9 + 8\zeta_C} - 3), \tag{3.81}$$

which serves as an upper bound for the LD refrigerators [111], MNI refrigerators [112]. The same bound can be derived for a two-level system working as a refrigerator in the high temperature regime [113].

3.6.3 Prior information approach

For refrigerator mode of FS model operating at maximum χ function, the prior information study has already been carried out in the Ref. [20], and COP at optimal χ is found to be:

$$\zeta^* = \zeta_{CA} = \sqrt{1+\zeta_C} - 1, \tag{3.82}$$

which is considered to be equivalent to CA efficiency, applicable to the case of refrigerators. Notably, $\zeta_{CA} = \sqrt{1+\zeta_C} - 1$, can also be derived in the optimization of endoreversible [114], symmetric LD [111] and MNI models of refrigerator [112].

Jeffreys prior on ϵ_2: To estimate the performance of the refrigerator in high temperature regime using prior information approach, we express χ in terms of ϵ_2 and average over Jeffreys prior for the given range $[\epsilon_{\min}, \epsilon_{\max}]$ of ϵ_2. So we have following equations for χ and average value of χ:

$$\chi(\zeta, \epsilon_2) = r_0 \zeta \epsilon_2 \left(e^{-\epsilon_2/T_2} - e^{-\epsilon_2(1+\zeta)/\zeta T_1} \right) \tag{3.83}$$

and

$$\bar{\chi}(\zeta) = \int_{\epsilon_{\min}}^{\epsilon_{\max}} \chi(\zeta, \epsilon_2) \Pi(\epsilon_2) d\epsilon_2 = C \int_{\epsilon_{\min}}^{\epsilon_{\max}} \zeta \left(e^{-\epsilon_2/T_2} - e^{-\epsilon_2(1+\zeta)/\zeta T_1} \right), \tag{3.84}$$

Upon integrating the above equation, we get

$$\begin{aligned} \bar{\chi}(\zeta) = C T_1 \Big[\quad & \frac{\zeta T_2}{T_1} \left(e^{-\epsilon_{\min}/T_2} - e^{-\epsilon_{\max}/T_2} \right) \\ & + \frac{\zeta^2}{(1+\zeta)} \left(e^{-\epsilon_{\max(1+\zeta)}/\zeta T_1} - e^{-\epsilon_{\min}(1+\zeta)/\zeta T_1} \right) \Big] \end{aligned} \tag{3.85}$$

In the following, we focus on COP at maximal $\bar{\chi}$ in the high temperature limit. So the maximum of $\bar{\chi}$with respect to ζ is evaluated as $\partial\bar{\chi}/\partial\zeta = 0$,

$$\frac{T_2}{T_1}\left(e^{-\epsilon_{\min}/T_2} - e^{-\epsilon_{\max}/T_2}\right) + \frac{\zeta(\zeta+2)}{(1+\zeta)^2}\left(e^{-\epsilon_{\max}(1+\zeta)/\zeta T_1} - e^{-\epsilon_{\min}(1+\zeta)/\zeta T_1}\right)$$
$$+\frac{1}{T_1(1+\zeta)}\left(\epsilon_{\max}e^{-\epsilon_{\max}(1+\zeta)/\zeta T_1} - \epsilon_{\min}e^{-\epsilon_{\min}(1+\zeta)/\zeta T_1}\right) = 0. \tag{3.86}$$

Following the same procedure as for the engine, it is not possible to find analytical expression for COP in the high temperature limit. However, we can still guess the behavior of COP by numerically plotting Eq. (3.86) for COP (ζ) versus $M \equiv \epsilon_{\max}/T_1$, by considering small value of $m \equiv \epsilon_{\min}/T_1$ for a fixed ζ_C (see Figure 3.6). It is clear from blue curve in Figure 3.6 that for small values of M, COP approaches lower bound $\zeta_- = 0$. Similar graph (red curve in Figure 3.6) can be plotted by treating ϵ_1 as the uncertain variable [see Eq. (3.88)].

Jeffreys prior on ϵ_1: The second method considers ϵ_1 as the uncertain variable and defines

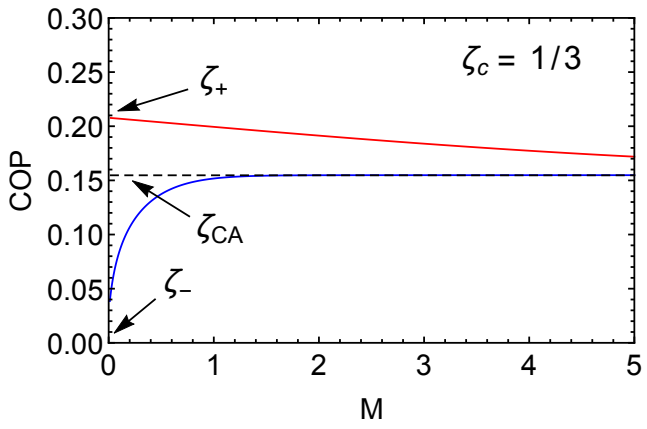

Figure 3.6: The COP at maximum expected χ function is plotted versus M for given $m = 0.01$, and $\zeta_C = 1/3$. The lower (blue) curve is obtained with ϵ_2 as the uncertain variable. For small values of M, the COP approaches the lower bound $\zeta_- = 0$. The upper (red) curve implies that ϵ_1 is the uncertain variable, and the COP approaches the upper bound $\zeta_+ = (\sqrt{9+8\zeta_C})/2$. For large M values, both curves approach CA value, $\zeta_{CA} = \sqrt{1+\zeta_C} - 1 = 0.155$.

$$\bar{\chi}(\zeta) = \int_{\epsilon_{\min}}^{\epsilon_{\max}} \chi(\zeta, \epsilon_1)\Pi(\epsilon_1)d\epsilon_1. \tag{3.87}$$

So the maximum of $\bar{\chi}(\zeta, \epsilon_1)$ with respect to ζ, is evaluated as $\partial\bar{\chi}/\partial\zeta = 0$,

$$\begin{aligned}&\frac{\zeta(2+\zeta)}{1+\zeta}\left(e^{-\epsilon_{\min}/T_1} - e^{-\epsilon_{\max}/T_1}\right) - \frac{T_2}{T_1}\left(e^{-\epsilon_{\min}\zeta/(1+\zeta)T_2} - e^{-\epsilon_{\max}\zeta/(1+\zeta)T_2}\right)\\ &-\frac{\zeta}{T_1(1+\zeta)^2}\left(\epsilon_{\min}e^{-\epsilon_{\min}\zeta/(1+\zeta)T_2} - \epsilon_{\max}e^{-\epsilon_{\max}\zeta/(1+\zeta)T_2}\right) = 0.\end{aligned} \tag{3.88}$$

Again following the approach applied in the last paragraph, upper bound on COP can be obtained as,

$$\zeta_+ = \frac{1}{2}(\sqrt{9+8\zeta_C} - 3), \tag{3.89}$$

which we have already obtained from the exact analysis in Subsection 3.6.2.

3.7 Conclusions

We have studied optimal of performance of FS engine using the ecological criterion and efficient power criterion. Our choice of the objective functions is motivated by the fact that they represent a compromise between the power output and efficiency of the engine. We have performed our analysis by recourse to two methods: i) the standard approach of two-parameter optimization over the two internal energy scales. We derive explicit expressions for the efficiency and coefficient of performance at the maximum of EF. ii) We also perform an estimation over one uncertain energy scale followed by a single-parameter optimization. The latter approach is based on the quantification of (limited) prior information as in the Bayesian probability theory. Here also, we are able to find exact expressions for efficiency, in some well-defined asymptotic limit. Remarkably, we obtain the well-known expressions of FTT models where EF is optimized. Further, we observe that the behavior of efficiency as predicted in the two methods are quite similar. In fact, close to equilibrium, the corresponding expressions match upto the second term.

The analysis is repeated for the optimization of EP function. First, we perform a two-parameter optimization for the general case and show that analytical solution is not possible for this case. However, we are able to find a transcendental equation, which shows that EMEP depends upon Carnot efficiency only. By employing perturbative solution close to equilibrium, we confirm the presence of the first two universal terms of EMEP. Although we are not able to obtain analytical expression for efficiency for exact two parameter optimization; by using prior information approach, we derive the expression for the efficiency of the engine which concurs with the efficiency of an endoreversible engine. We also carry out one parameter optimization for the engine working in high temperature regime by constraining one of the energy scales and obtain well known forms of efficiency. Again, by performing prior information analysis in the high temperature limit, we are able to obtain the same forms of efficiency as obtained by exact optimization method. The same analysis is repeated for the optimization of the refrigerator. To this end, we want to emphasize one point. We optimize χ function to study FS refrigerator, since two-parameter optimization of the cooling power $\dot{Q}_2$ is not possible in this case. Further, prior information analysis also fails to estimate the performance of refrigerator when optimization of average cooling power is carried out. Thus χ function is suitable figure of merit to analyze the optimal performance of FS refrigerator.

Since, the presence of limited information may also be interpreted in the sense of limited control over the system, the agreement of figures of merit by the two methods, suggests that an exact knowledge of the variable parameters is not essential to infer the optimal behavior. Thus, the present results provide a further evidence that the estimation based approach can provide a robust and effective method to indicate the figures of merit at optimal performance of heat devices.

Chapter 4

Low-Dissipation Carnot-Like Heat Engines at Maximum Efficient Power

4.1 Introduction

In 2010, complementary to Curzon-Ahlborn's endoreversible model, a new heat engine model, known as LD model, was proposed by Esposito and coworkers. It consists of a Carnot-like engine with small deviation from the reversible Carnot cycle through dissipations at isothermal branches which occur at finite time. The nature of the dissipation is incorporated in some generic dissipative coefficients and dissipation is assumed to be proportional to the time duration of the isotherms. For LD heat engines, they derived upper and lower bounds for the EMP of Carnot-like heat engines. In addition, for the symmetric dissipation, they were able to reproduce the CA result. The LD models [1, 2, 41, 52, 71, 111, 115–122] have some advantages over the endoreversible models. It does not make use of any specific heat transfer law and also valid beyond the linear-response regime. A good comparison of LD models and endoreversible models is given in the Refs. [101, 123–125]. LD models are also closely related to irreversible heat engines [64, 126]. Izumida and Okuda investigated the optimal performance of MNI heat engines and showed that LD models can be described by MNI heat engines [64]. Going one step

further, Sheng and Tu constructed a generic model of engine under the tight-coupling conditions abiding by a linear constitutive relation between the generalized thermodynamic forces and fluxes [126]. They showed that their model is equivalent to LD heat engines and obtained same lower and upper bounds on EMP as obtained for LD engines. Further, LD models were used to investigate the optimal performance of Carnot-like refrigerators [111, 116, 122], quantum heat engines [40, 120, 121, 127] and for the optimization of target functions other than power output [2, 52, 71]. Guo et. al. investigated the optimal performance of LD heat engines for different types of heat cycles other than Carnot cycle [117].

As mentioned earlier, in order to achieve the optimal performance of an energy converter, an appropriate objective function (or target function) must be introduced and optimized. EP function, $P_\eta = \eta P$, is such a function, which represents a trade-off between the power and efficiency of a heat engine. In this chapter, we analyze the optimal performance of general class of LD Carnot-like heat engines using EP function as the objective function. In Section 4.2, we discuss model of LD heat engine undergoing Carnot cycle. In Section 4.3, we find the general expression for EMEP and obtain lower and upper bound on the efficiency. We also discuss universal features of EMEP in this section. Section 4.4 is devoted to the comparison of rates of dissipation at hot and cold contacts for three different objective functions. In Section 4.5, using a different optimization scheme, we obtain the same bounds on the EMEP as obtained for LD heat engines. We conclude in Section 4.6 by highlighting the key results.

4.2 Model of low-dissipation Carnot engine

As in the case of usual Carnot cycle, heat cycle in our case consists of two adiabatic and two isothermal steps. Adiabatic steps are assumed to be instantaneous and there is no entropy production along these branches [11]. Let t_h and t_c be the time durations of the isothermal branches during which the system remains in contact with the hot and cold reservoirs respectively. During the heat exchange process with the hot (cold) bath, the change in entropy of the system can

be split into two parts as follows [101, 115]

$$\Delta S_j = \Delta S_j^{\rm ex} + \Delta S_j^{\rm ir}, \qquad j = h, c \tag{4.1}$$

where $\Delta S_j^{\rm ex}$ is change in entropy of the system due to heat exchange and $\Delta S_j^{\rm ir}$ accounts for irreversible entropy production during the process. The first term is Q_h/T_h for the heat absorbed from the hot reservoir at temperature T_h and Q_c/T_c for the heat transferred to cold reservoir at temperature T_c. In LD limit, it is assumed that irreversible entropy production $\Delta S_j^{\rm ir}$ during the heat transfer step is inversely proportional to the time duration for which the system remains in contact with the bath. Hence entropy production along the isothermal branch is given by $\Delta S_j^{\rm ir} = \Sigma_j/t_j$, $(j = h, c)$. Here Σ_h and Σ_c are dissipation coefficients, containing the information about the irreversibilities induced in the model as we deviate away from the reversible limit. It is self evident that the cycle approaches reversible limit as $t_h \to \infty$ and $t_c \to \infty$. Thus, at hot and cold contacts, we have respectively [52, 115]

$$\Delta S_h = \frac{Q_h}{T_h} + \frac{\Sigma_h}{t_h}, \tag{4.2}$$

$$\Delta S_c = -\frac{Q_c}{T_c} + \frac{\Sigma_c}{t_c}, \tag{4.3}$$

where $Q_h, Q_c > 0$. Since after undergoing the full cycle, the system returns to its initial state, the total entropy change of the working substance in the whole cycle is zero: $\Delta S_h + \Delta S_c = 0$. Therefore we have $\Delta S_h = -\Delta S_c = \Delta S > 0$. Then the amount of heat exchanged with each reservoir can be written as

$$Q_h = T_h\left(\Delta S - \frac{\Sigma_h}{t_h}\right) \equiv T_h(\Delta S - x_h\Sigma_h), \tag{4.4}$$

$$Q_c = T_c\left(\Delta S + \frac{\Sigma_c}{t_c}\right) \equiv T_c(\Delta S + x_c\Sigma_c), \tag{4.5}$$

where we have used $x_h \equiv 1/t_h$ and $x_c \equiv 1/t_c$ for our convenience. The work extracted in a cycle with time period $t = t_c + t_h$ is $W = Q_h - Q_c$. So the efficiency η and average output

power P per cycle is defined as

$$\eta = \frac{W}{Q_h} = 1 - \frac{Q_c}{Q_h} = 1 - \frac{T_c(\Delta S + x_c\Sigma_c)}{T_h(\Delta S - x_h\Sigma_h}, \tag{4.6}$$

$$P = \frac{Q_h - Q_c}{t_h + t_c} \equiv \frac{(Q_h - Q_c)x_h x_c}{x_c + x_h}. \tag{4.7}$$

Low-dissipation heat engine at maximum power

By optimizing power in Eq. (4.7) over contact times t_c and t_h, Esposito and coauthors derived the following form of efficiency for the LD engines operating in the MP regime [1]:

$$\eta^P = \frac{\eta_C(1 + \sqrt{\gamma(1-\eta_C)})}{(1 + \sqrt{\gamma(1-\eta_C)})^2 + (1-\eta_C)(1-\gamma)}. \tag{4.8}$$

where $\gamma = \Sigma_c/\Sigma_h$. For the limiting cases $\gamma \to 0$ and $\gamma \to \infty$, EMP converges to the upper bound $\eta^P_+ = \eta_C/(2-\eta_C)$ and to the lower bound $\eta^P_- = \eta_C/2$, respectively. Hence EMP lies in the range:

$$\frac{\eta_C}{2} \leq \eta^P \leq \frac{\eta_C}{2-\eta_C}. \tag{4.9}$$

4.3 Efficient power in low-dissipation regime

To study the optimal performance of a LD Carnot engine, we will use EP $P_\eta = \eta P$ as the target function. Here, the EP represents the compromise between the efficiency and average power of the engine. Using Eqs. (4.6) and (4.7) in the expression for P_η, we have

$$P_\eta = \eta P = \frac{(Q_h - Q_c)^2}{Q_h}\frac{x_c x_h}{x_c + x_h}. \tag{4.10}$$

In order to optimize the EP function P_η, we first substitute Eqs. (5.6) and (5.9) in Eq. (4.10) and then set the partial derivatives of P_η with respect to x_c and x_h equal to zero. Then rearranging the terms and writing left hand side of both equations again in terms of $(Q_h - Q_c)^2/Q_h$, we

obtain following two equation:

$$\frac{(Q_h - Q_c)^2}{Q_h} x_h = 2T_c\Sigma_c(x_c + x_h)x_c \left[1 - \frac{T_c(\Delta S + x_c\Sigma_c)}{T_h(\Delta S - x_h\Sigma_h)}\right], \tag{4.11}$$

and

$$\frac{(Q_h - Q_c)^2}{Q_h} x_c = T_h\Sigma_h(x_c + x_h)x_h \left[1 - \frac{T_c^2}{T_h^2}\frac{(\Delta S + x_c\Sigma_c)^2}{(\Delta S - x_h\Sigma_h)^2}\right]. \tag{4.12}$$

Using Eqs. (5.6) and (5.9) in Eqs. (4.11) and (4.12), we solve for x_h and get the following expression (see Appendix B.1) for x_h

$$x_h = -\frac{\Delta S}{\Sigma_h}\left[\frac{N}{8B} + \frac{1}{2}\sqrt{K} + \frac{1}{2}\sqrt{K' - \frac{G}{4\sqrt{K}}}\right] \tag{4.13}$$

where we used the following notation

$$\begin{aligned}
K &= \frac{N^2}{16B^2} - \frac{M}{6B} + \frac{(A + \sqrt{A^2 - 4A'^3})^{1/3}}{12 \times 2^{1/3}B} + \frac{F}{6 \times 2^{2/3}B(A + \sqrt{A^2 - 4A'^3})^{1/3}}, \\
K' &= \frac{N^2}{8B^2} - \frac{M}{3B} - \frac{(A + \sqrt{A^2 - 4A'^3})^{1/3}}{12 \times 2^{1/3}B} - \frac{F}{6 \times 2^{2/3}B(A + \sqrt{A^2 - 4A'^3})^{1/3}}, \\
G &= \frac{12\eta_C}{B} - \frac{N^3}{8B^3} + \frac{MN}{2B^2}, \\
N &= (1 - \eta_C)(6 - \eta_C)\gamma - 6, \\
B &= -(1 - \eta_C)\gamma + 1, \\
M &= -3(1 - \eta_C)(3 - \eta_C)\gamma + (4\eta_C + 9), \\
F &= 9(1 - \eta_C)^2(3 - \eta_C)^2\gamma^2 - 6(1 - \eta_C)(3 - 2\eta_C)(9 - 5\eta_C)\gamma + (9 - 8\eta_C)^2, \\
A &= 2M^3 + 108\eta_C MN + 108\eta_C^2 N^2 + 3888\eta_C^2 B - 288\eta_C^2 MB, \\
A' &= M^2 + 36\eta_C N + 48\eta_C^2 B.
\end{aligned} \tag{4.14}$$

Now we seek the form of EMEP $\eta^* = W/Q_h$, which is found to be (see Appendix B.2)

$$\eta^* = \frac{2\eta_C}{3 - 2x_h\Sigma_h/\Delta S}. \tag{4.15}$$

Using Eqs. (4.13) and (4.14) in Eq. (4.15), we can obtain a closed-form expression for EMEP. The resulting form is too lengthy to be reproduced here. However, a couple of points about this expression need to be noted. Firstly, it depends only upon Carnot efficiency $\eta_{\rm C}$ and parameter γ. For some limiting cases, it reduces to well known forms for the efficiency obtained in literature (see Appendix B.3). In the extreme asymmetric limit $\gamma \to 0$, the EMEP converges to the upper bound $\eta_+ = (3 - \sqrt{9 - 8\eta_{\rm C}})/2$, while for $\gamma \to \infty$, it reduces to the lower bound $\eta_- = 2\eta_{\rm C}/3$ (See Figure 4.1). Thus

$$\eta_- \equiv \frac{2}{3}\eta_{\rm C} \leq \eta^* \leq \frac{1}{2}(3 - \sqrt{9 - 8\eta_{\rm C}}) \equiv \eta_+. \tag{4.16}$$

These upper and lower bounds on the efficiency were previously obtained by Holubec and Ryabov [2] for the case of overdamped brownian particle undergoing a Carnot-like cycle using the framework of stochastic thermodynamics [41].

We pay special attention to the case of symmetric dissipation in which $\Sigma_c = \Sigma_h$, or $\gamma = 1$. Under this condition, Eq. (4.15) reduces to

$$\eta_{\rm sym} = 1 - \frac{1}{4}(1 - \eta_{\rm C}) \left(1 + \sqrt{1 + \frac{8}{1 - \eta_{\rm C}}}\right). \tag{4.17}$$

The same result was obtained in Refs. [48, 55] for the endoreversible model of Carnot heat engine operating at MEP, under the tight-coupling condition. We expand Eq. (4.17) in Taylor's series near equilibrium to reveal universal features of the EMEP.

$$\eta_{sym} = \frac{2}{3}\eta_{\rm C} + \frac{2}{27}\eta_{\rm C}^2 + O(\eta_{\rm C}^3). \tag{4.18}$$

The first two terms in the above equation were also derived for the EMEP of a nonlinear irreversible heat engine [63] working in strong coupling limit under the symmetric condition by using master equation model [54, 61]. In Ref. [63], it is also shown that EMEP is given by $2\eta_{\rm C}/3$ in linear response regime. Hence, we confirm that universal features of efficiency

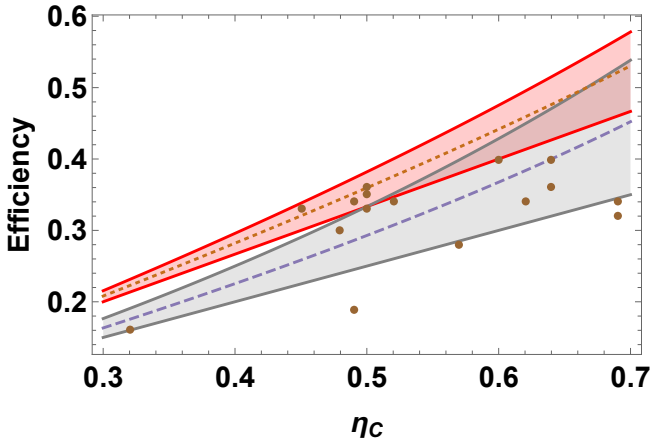

Figure 4.1: Comparison of the bounds on efficiency with observed data. Red curves show the bounds for the EMEP. Gray lines represents the same for the EMP [1]. Brown circles represent the observed efficiencies of various power plants as analyzed in Refs. [1–3]. Dashed and dotted lines stand for $\eta_{\rm CA}$ and $\eta_{\rm sym}$ respectively.

[54, 61, 110] are not exclusive to the conditions of MP and MOF but also extend to the engines operating in MEP regime.

4.4 Rates of dissipation

Now we compare the average rates of dissipation for LD heat engines under optimal working conditions for power output, EP function and Omega (Ω) function. In general, the average rates of dissipation for the LD model, at hot and cold contacts are given by [101]:

$$\mathcal{D}_h^{(f)} = \frac{T_h \Sigma_h}{t_h^2} \equiv T_h \Sigma_h x_h^2, \tag{4.19}$$

$$\mathcal{D}_c^{(f)} = \frac{T_c \Sigma_c}{t_c^2} \equiv T_c \Sigma_c x_c^2, \tag{4.20}$$

where $f(\equiv P,\ P_\eta,\ \Omega)$ is the function being optimized. In case of LD engines operating at MP, the relation between x_h and x_c is given by [1]

$$\frac{x_c}{x_h} = \sqrt{\frac{T_h \Sigma_h}{T_c \Sigma_c}}, \tag{4.21}$$

from which it follows that the average rates of dissipation at two thermal contacts are equal:

$$\mathcal{D}_c^{(P)} = \mathcal{D}_h^{(P)}. \tag{4.22}$$

Similarly for the case of maximum Ω function, which represents a trade-off between the useful energy and the lost energy of heat engines, we have [52]

$$\frac{x_c}{x_h} = \sqrt{\frac{\Sigma_h(2-\eta_{\rm C})}{2\Sigma_c(1-\eta_{\rm C})}}. \tag{4.23}$$

So, we obtain

$$\mathcal{D}_c^{(\Omega)} = \mathcal{D}_h^{(\Omega)} \left(1 - \frac{\eta_{\rm C}}{2}\right). \tag{4.24}$$

Since the factor $(1 - \eta_{\rm C}/2)$ is always smaller than 1, the rate of dissipation is higher at the hot contact. Now we find the relation between rates of dissipation for the case of LD engines operating at MEP. From Eqs. (B.4) and (B.7), we have

$$\frac{x_c}{x_h} = \sqrt{\frac{\Sigma_h(2-\eta^*)}{2\Sigma_c(1-\eta_{\rm C})}}, \tag{4.25}$$

which can be solved to give

$$\mathcal{D}_c^{(P_\eta)} = \mathcal{D}_h^{(P_\eta)} \left(1 - \frac{\eta^*}{2}\right). \tag{4.26}$$

Comparing Eqs. (4.22), (4.24) and (4.26), it is clear that ratio of cold to hot dissipation is smallest in the case of Omega function:

$$\frac{\mathcal{D}_c^{(\Omega)}}{\mathcal{D}_h^{(\Omega)}} < \frac{\mathcal{D}_c^{(P_\eta)}}{\mathcal{D}_h^{(P_\eta)}} < \frac{\mathcal{D}_c^{(P)}}{\mathcal{D}_h^{(P)}} = 1. \tag{4.27}$$

Here, we emphasize that as the ratio of the rates of dissipation at the cold and the hot ends decreases, the efficiency of the engine increases, which is clear from the fact that in strong coupling limit, engines operating at MOF are the most efficient ones and the engines working in the MP regime are the least efficient [49]. We also note that in the cases of MP and MOF,

the ratio of rates of dissipation is independent of dissipation constants Σ_c and Σ_h, whereas for MEP it depends upon γ as the general form of EMEP is a function of γ (See Figure 4.2).

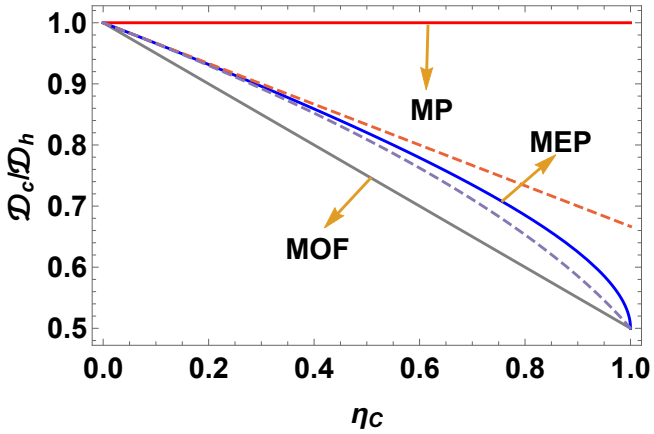

Figure 4.2: Solid lines MP and MOF represent the ratio of the rates of dissipation at cold and hot contacts of the indicated functions. Solid line MEP represents the same for MEP under symmetric dissipation, $\gamma = 1$. Dashed upper and lower curves represent the ratio $\mathcal{D}_c^{(P_\eta)}/\mathcal{D}_h^{(P_\eta)}$ for the extreme asymmetric dissipation $\gamma \to \infty$ and $\gamma \to 0$, respectively.

4.5 Global linear-irreversible principle

We noted in the above that the bounds on EMEP have also been obtained with other models such as the endoreversible model. The similarities and differences between endoreversible and LD models have been discussed recently [101, 123–125]. While different such models assume a particular functional form or a mechanism for irreversible entropy generation, we discuss in the following a different formulation that has been recently proposed in Ref. [92] and show that the same lower and upper bounds as obtained in Eq. (4.16) and (4.17) can be obtained using a different optimization scheme. In this so-called global linear-irreversible principle framework, we do not assume stepwise details of the cycle. Rather, the validity of LIT is assumed globally, *i.e.*, for the complete cycle. Here, the thermal machine is considered as an irreversible channel with an effective heat conductivity λ, with an associated passage of a mean heat $\bar{Q}$ from hot to cold reservoir in the total cycle time τ. Thereby, the relation between total cycle time τ and $\bar{Q}$

is given by [92]

$$\tau = \frac{\bar{Q}^2}{\lambda \Delta S_{\rm tot}}, \tag{4.28}$$

where $\Delta S_{\rm tot} = Q_c/T_c - Q_h/T_h$, is the total entropy generated per cycle, which is non-zero. Using the basic definitions and Eq. (4.28), the average EP is given by

$$P_\eta = \eta \frac{W}{\tau} = \frac{\lambda (Q_h - Q_c)^2}{Q_h \bar{Q}^2} \Delta S_{\rm tot} = \frac{\lambda (Q_h - Q_c)^2}{Q_h \bar{Q}^2} \left(\frac{Q_c}{T_c} - \frac{Q_h}{T_h} \right). \tag{4.29}$$

Defining $\nu = Q_c/Q_h$, we can rewrite Eq. (4.29) in terms of $\eta_{\rm C}$ and ν:

$$P_\eta = \frac{\lambda}{T_c} (1 - \nu)(\nu + \eta_{\rm C} - 1) \frac{Q_h^2}{\bar{Q}^2}. \tag{4.30}$$

Now, in order to optimize the above objective function, we have to specify the form of $\bar{Q}$ which is assumed to be a mean value lying in the range $Q_c \leq \bar{Q} \leq Q_h$. We will discuss here only the extreme cases. Substituting $\bar{Q} = Q_h$ in Eq. (4.30) and optimizing with respect to ν, EMEP comes out to be $\eta_- = 2\eta_{\rm C}/3$. Similarly, for $\bar{Q} = Q_c$, the form of EMEP is $\eta_+ = (3 - \sqrt{9 - 8\eta_{\rm C}})/2$. Alternately, if we use the geometric mean $\bar{Q} = \sqrt{Q_c Q_h}$, the optimization of Eq. (4.30) yields the EMEP as in Eq. (4.17).

4.6 Conclusions

We have discussed the efficiency of a LD heat engine operating at MEP. In the limit of extremely asymmetric dissipation, we are able to obtain the lower and upper bounds on the efficiency of the engine, as well as the expression η_{sym} for the symmetric case. The universal features of EMEP are highlighted. We also note that ratio of average dissipation rates at cold and hot contacts depends upon γ, see Eq. (4.26), whereas in the case of MP and MOF, the same ratio is independent of γ, see Eqs. (4.22) and (4.24). The derivation of forms of EMEP, similar to those obtained for LD Carnot-like engines, using the global principle of LIT, confirms the validity of our analysis.

Although the real power plants do not operate in a Carnot cycle, and the assumption of LD may not be valid for them, it is compelling to compare the upper and lower bounds with the observed efficiencies. In Figure 4.1, we have compared the observed data with the bounds obtained for LD engines operating at MP and MEP. Although not shown in Figure 4.1, it is important to know that the area between the lower and upper bounds of MOF does not contain any observed data points [2], whereas five and eight data points respectively lie within the areas bounded by the lower and upper bounds of EMEP and EMP. However, it is interesting to observe that the density of points (number of data points per unit area between the upper and lower bounds for the respective objective function shown in Figure 4.1), is higher in the case of MEP criterion than for MP.

Chapter 5

Three-level laser heat engine at optimal performance with ecological function

5.1 Introduction

The study of quantum heat engines (QHEs) started with the seminal work of Scovil and Schulz-Dubois (SSD) [128]. In their work, they investigated the thermodynamics of three-level maser and showed its equivalence to classical Carnot engine. Three level laser heat engine [128] is one of the simplest steady-state heat engine. It converts the incoherent thermal energy of heat reservoirs to a coherent laser output. It has been studied extensively in the literature. Three-level systems are also employed to study quantum absorption refrigerators [129–132]. The model proposed by Scovil and DuBois was further analyzed by Geva and Kosloff [15, 16] in the spirit of FTT. In the presence of strong time dependent external fields, they optimized the power output of the amplifier with respect to different control parameters. In their model, the second law of thermodynamics is generally satisfied if one incorporates the effect of external field on the dissipative superoperator. In a series of papers [133–135], Boukobza and Tannor formulated a new way to partition energy into heat and work. They applied their analysis to a three level amplifier continuously coupled to two reservoirs and to a classical single mode field [135].

Their formulation is quite general and one does not need to incorporate the effect of external field on the dissipative term of the Liouvillian, and yet the second law of thermodynamics is always satisfied at steady state. In this work, we use the formalism of [135] to study the optimal performance of a three-level QHE operating in high temperature regime.

It has been 60 years since the first paper appeared in the field of quantum thermodynamics and QHEs. Since then, there has been a lot of progress in this field on the theoretical as well as experimental front. Various models of QHEs have been proposed employing a quantum mechanical system as the working fluid, such as spin systems [33–35, 136–141], harmonic oscillators [34, 38, 142–144], two-level or multilevel systems [15, 16, 145–154], single ion or two ion systems [155–157], cavity quantum electrodynamics systems [158–162], optomechanical cavities [163–165] etc.

On the other hand, rising concerns about the harmful effects of human activity towards the environment and ecology make it pertinent to enquire if the new technologies are better from ecological point of view. Most comparisons that are usually studied between quantum [138–142, 144, 145, 149, 150, 156, 158, 166] and classical macroscopic models of heat engines [1, 10, 64], focus on the optimization of power output [1, 22, 40, 155, 167]. However, to be ecologically sensitive demands that we also care about the extent of entropy production these machines inevitably lead to and which ultimately impacts the environment.

In this regard, we study the optimization of EF. We analyze the performance of a three-level steady state laser heat engine operating at maximum EF. In the context of classical models, this function suggests optimal working conditions which lead to a drop of about 20% in power output (compared to MP output), but on the other hand, reduce the entropy generation by about 70% [44].

Our second motivation for this analysis is to study the correspondence between classical and quantum heat engines. In most of the studies done so far, QHEs can show exotic behavior only when we use additional resources such as quantum coherence [22, 168–170], quantum entanglement [171–174] and squeezed baths [143, 160, 175]. In many cases, when QHEs do not

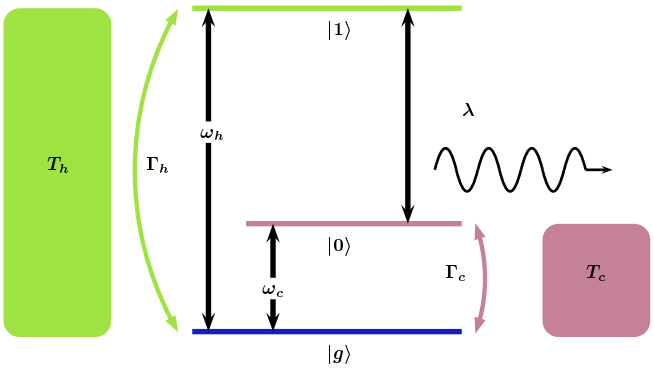

Figure 5.1: Model of three-level laser heat engine continuously coupled to two reservoirs of temperatures T_h and T_c having coupling constants Γ_h and Γ_c, respectively. The system is interacting with a classical single mode field. λ represents the strength of matter-field coupling.

employ additional resources mentioned above, they show remarkable similarity to macroscopic heat engines. In such cases, the Carnot efficiency provides an upper bound on the efficiencies of QHEs operating between two heat reservoirs. For the optimal performance of many models of classical and quantum heat engines operating at finite power, the form of efficiency comes out to be similar for both types of engines. The irreversible operation of quantum engines with finite power output has many similarities to macroscopic endoreversible engines. In the LD regime [1], the behavior of quantum and classical heat engines are quite similar [40]. Also in high temperature limit, QHEs are expected to behave like classical heat engines [33, 34].

The chapter is organised as follows. In Section 5.2, we discuss the model of three-level laser quantum heat engine. In Section 5.3, we obtain the general expression for the efficiency of the engine operating at maximum EF and find lower and upper bounds on the efficiency for two different optimization schemes. In Sections 5.4 and 5.5, we compare the performance of heat engine operating at maximum EF to the engine operating at MP. We conclude in Section 5.6 by highlighting the key results.

5.2 Model of Three Level Quantum Laser Heat Engine

The model consists of a three level system continuously coupled to two thermal reservoirs and to a single mode classical field (See Figure 5.1). A hot reservoir at temperature T_h drives the transition between the ground level $|g\rangle$ and top level $|1\rangle$, whereas the transition between the intermediate level $|0\rangle$ and ground level $|g\rangle$ is constantly de-excited by a cold reservoir at temperature T_c. The power output mechanism is modeled by coupling the levels $|0\rangle$ and $|1\rangle$ to a classical single mode field. The Hamiltonian of the system is given by: $H_0 = \hbar \sum \omega_k |k\rangle\langle k|$ where the summation runs over all three states and ω_k represents the relevant atomic frequency. The interaction with the single mode lasing field of frequency ω, under the rotating wave approximation, is described by the semiclassical hamiltonian: $V(t) = \hbar\lambda(e^{i\omega t}|1\rangle\langle 0| + e^{-i\omega t}|0\rangle\langle 1|)$; λ is the field-matter coupling constant. The time evolution of the system is described by the following master equation (Appendix C):

$$\dot{\rho} = -\frac{i}{\hbar}[H_0 + V(t), \rho] + \mathcal{L}_h[\rho] + \mathcal{L}_c[\rho], \tag{5.1}$$

where $\mathcal{L}_{h(c)}$ represents the dissipative Lindblad superoperator describing the system-bath interaction with the hot (cold) reservoir:

$$\begin{aligned} \mathcal{L}_h[\rho] &= \Gamma_h(n_h+1)(2|g\rangle\langle g|\rho_{11} - |1\rangle\langle 1|\rho - \rho|1\rangle\langle 1|) \\ &\quad + \Gamma_h n_h(2|1\rangle\langle 1|\rho_{gg} - |g\rangle\langle g|\rho - \rho|g\rangle\langle g|), \end{aligned} \tag{5.2}$$

$$\begin{aligned} \mathcal{L}_c[\rho] &= \Gamma_c(n_c+1)(2|g\rangle\langle g|\rho_{00} - |0\rangle\langle 0|\rho - \rho|0\rangle\langle 0|) \\ &\quad + \Gamma_c n_c(2|0\rangle\langle 0|\rho_{gg} - |g\rangle\langle g|\rho - \rho|g\rangle\langle g|). \end{aligned} \tag{5.3}$$

Here Γ_h and Γ_c are the Weisskopf-Wigner decay constants, and $n_{h(c)} = 1/(\exp[\hbar\omega_{h(c)}/k_B T_{h(c)}] - 1)$ is average occupation number of photons in hot (cold) reservoir satisfying the relations $\omega_c = \omega_0 - \omega_g$, $\omega_h = \omega_1 - \omega_g$.

In our model, it is possible to find a rotating frame in which the steady-state density matrix ρ_R is time independent [135]. Defining $\bar{H} = \hbar(\omega_g|g\rangle\langle g| + \frac{\omega}{2}|1\rangle\langle 1| - \frac{\omega}{2}|0\rangle\langle 0|)$, an arbitrary operator A in the rotating frame is given by $A_R = e^{i\bar{H}t/\hbar}Ae^{-i\bar{H}t/\hbar}$. It can be seen that $\mathcal{L}_h[\rho]$ and $\mathcal{L}_c[\rho]$ remain unchanged under this transformation. Time evolution of the system density matrix in the rotating frame can be written as

$$\dot{\rho_R} = -\frac{i}{\hbar}[H_0 - \bar{H} + V_R, \rho_R] + \mathcal{L}_h[\rho_R] + \mathcal{L}_c[\rho_R] \tag{5.4}$$

where $V_R = \hbar\lambda(|1\rangle\langle 0| + |0\rangle\langle 1|)$.

For a weak system-bath coupling, the output power, heat flux and efficiency of the engine can be defined, using the formalism of Ref. [135], as follows:

$$P = \frac{i}{\hbar}\mathrm{Tr}([H_0, V_R]\rho_R), \tag{5.5}$$

$$\dot{Q}_h = \mathrm{Tr}(\mathcal{L}_h[\rho_R]H_0), \tag{5.6}$$

$$\eta = \frac{P}{\dot{Q}_h}. \tag{5.7}$$

Plugging the values of H_0, V_R and $\mathcal{L}_h[\rho_R]$, and calculating the traces (Appendix D.1) appearing in right hand side of the Eqs. (5.5) and (5.6), the power and heat flux can be written as:

$$P = i\hbar\lambda(\omega_1 - \omega_0)(\rho_{01} - \rho_{10}) = i\hbar\lambda(\omega_h - \omega_c)(\rho_{01} - \rho_{10}), \tag{5.8}$$

$$\dot{Q}_h = i\hbar\lambda\omega_h(\rho_{01} - \rho_{10}), \tag{5.9}$$

where $\rho_{01} = \langle 0|\rho_R|1\rangle$ and $\rho_{10} = \langle 1|\rho_R|0\rangle$. Then, the efficiency is given by

$$\eta = 1 - \frac{\omega_c}{\omega_h}. \tag{5.10}$$

From Eq.(D.17), the positive power production condition implies that $\omega_c/\omega_h \geq T_c/T_h$. Hence $\eta \leq \eta_C$.

5.3 Optimization of Ecological Function

In this work, we choose to optimize the EF which represents a trade-off between power output and loss of power in the system. The optimal performance of SSD engine at MP has already been studied recently [22]. According to our sign convention, EF is defined as

$$E = P - T_c \dot{S}_{tot}, \tag{5.11}$$

where

$$\dot{S}_{tot} = \frac{\dot{Q}_c}{T_c} - \frac{\dot{Q}_h}{T_h}, \tag{5.12}$$

is the total rate of entropy production in the reservoirs. In the steady state, the entropy of the system remains constant. Substituting Eq. (5.12) in Eq. (5.11) and writing in terms of ratio of temperatures of hot and cold reservoirs ($\tau = T_c/T_h$), the EF can be written as

$$E = 2P - (1-\tau)\dot{Q}_h. \tag{5.13}$$

Using Eqs. (5.8) and (5.9), we recast Eq. (5.13) as follows

$$E = i\hbar\lambda(\rho_{01} - \rho_{10})[2(\omega_h - \omega_c) - (1-\tau)\omega_h] \tag{5.14}$$

Now we optimize E w.r.t. the transition frequencies ω_h and ω_c, and then calculate the corresponding EMEF. In order to obtain analytic expressions in a closed form for the EMEF, we will work in the high temperature regime and assume that matter-field coupling is very strong as compare to the system-bath coupling ($\lambda >> \Gamma_{h,c}$). In the high temperature limit, we set $n_h \simeq k_B T_h/\hbar\omega_h$ and $n_c \simeq k_B T_h/\hbar\omega_c$. In high temperature regime, E can be written in the following form (Appendix D.2)

$$E \simeq \frac{2\hbar\Gamma_h(\omega_c - \tau\omega_h)[2(\omega_h - \omega_c) - (1-\tau)\omega_h]}{3(\omega_c\gamma + \tau\omega_h)}. \tag{5.15}$$

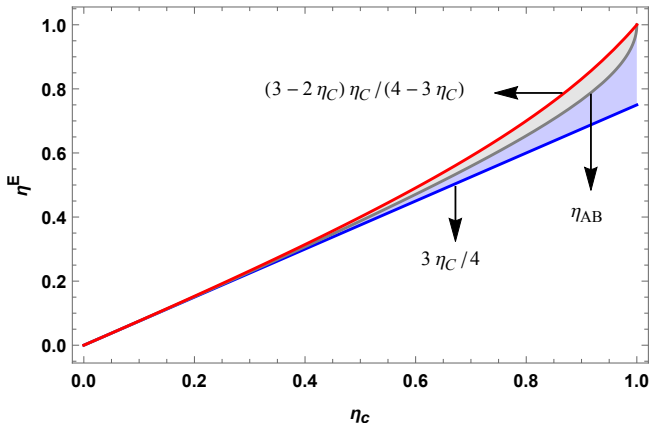

Figure 5.2: Efficiency η^E versus the Carnot efficiency η_C for the SSD engine. η_{AB} serves as upper bound for fixed ω_h and lower bound for fixed ω_c.

Here we choose frequencies ω_h and ω_c as control parameters. It is important to note that it is not possible to optimize E given in Eq. (5.15) with respect to ω_c and ω_h simultaneously. Such two parameter optimization scheme yields the trivial solution, $\omega_c = \omega_h = 0$, which is clearly not a useful result. Therefore we will perform optimization with respect to one parameter only while keeping the other one fixed at some constant value. First we keep ω_h fixed, then optimizing EF [Eq.(5.15)] w.r.t. ω_c, i.e., setting $\partial E/\partial\omega_c = 0$, we evaluate EMEF as

$$\eta^E_{\omega_h} = 1 + \frac{\tau}{\gamma} - \frac{\sqrt{(1+\gamma)\tau[\gamma+(2+\gamma)\tau]}}{\sqrt{2}\gamma}, \tag{5.16}$$

where $\gamma = \Gamma_h/\Gamma_c$. We note that $\eta^E_{\omega_h}$ is monotonic increasing function of γ. Therefore we can calculate lower and upper bounds on EMEF by putting $\gamma \to 0$ and $\gamma \to \infty$, respectively. Further, writing in terms of $\eta_C = 1-\tau$, we have (see Figure 5.2)

$$\frac{3}{4}\eta_C \leq \eta^E_{\omega_h} \leq 1 - \sqrt{\frac{(1-\eta_C)(2-\eta_C)}{2}}. \tag{5.17}$$

Lower bound $3\eta_C/4$ obtained here also serves as the lower bound for the LD heat engines [52] and MNI heat engines [69]. Upper bound $\sqrt{(1-\eta_C)(2-\eta_C)/2}$ obtained here was first derived by Angulo-Brown for a classical endoreversible heat engine [44]. Henceforth we call it Angulo-

Brown (AB) efficiency η_{AB}. Under the conditions of tight-coupling and symmetric dissipation, η_{AB} can also be obtained for the LD heat engines [52] and MNI heat engines [69].

Alternately, we may fix the value of ω_c and optimize EF w.r.t ω_h, thus obtaining EMEF in the following form

$$\eta^E_{\omega_c} = \frac{\gamma(1-\tau^2) + 2(1+\gamma)\tau - \sqrt{(1+\gamma)\tau^2(1+\tau)[\gamma + (2+\gamma)\tau]}}{\gamma + 2\tau + 3\gamma\tau}. \tag{5.18}$$

Again $\eta^E_{\omega_c}$ is monotonic increasing functions of γ. So we obtain lower and upper bounds on EMEF in the limiting cases $\gamma \to 0$ and $\gamma \to \infty$, respectively. In terms of η_C, we have (see Figure 5.2)

$$\eta_{AB} \leq \eta^E_{\omega_c} \leq \frac{3-2\eta_C}{4-3\eta_C}\eta_C. \tag{5.19}$$

Under the conditions of extreme dissipation, upper bound $(3-2\eta_C)\eta_C/(4-3\eta_C)$ reported here, also serves as the upper bound for the LD [1] and MNI [69] heat engines.

5.4 Fractional loss of power at maximum ecological function and maximum power output

In this section, we compare the performance of three level heat engine operating at maximum EF to the engine operating at MP. We derive the expressions for the loss of power in both cases. It can be done by using the very definition of EF $E = P - T_2\dot{S}_{\rm tot}$, where $T_2\dot{S}_{\rm tot}$ represents the loss of power. So we write the EF as $E = P - P_{\rm lost}$ and after rearranging terms, we can write

$$R' \equiv \frac{P_{\rm lost}}{P} = 1 - \frac{E}{P} \equiv 1 - R. \tag{5.20}$$

We calculate the ratio of power lost to power gain for four different cases discussed in Appendix D.3. All the relevant quantities are derived there. For the optimization of EF wrt ω_c keeping ω_h fixed, the ratio of optimal EF, $E^{*(\omega_h)}_{\rm eco}$, to power at maximum EF, $P^{*(\omega_h)}_{\rm eco}$, is given in Eq. (D.23).

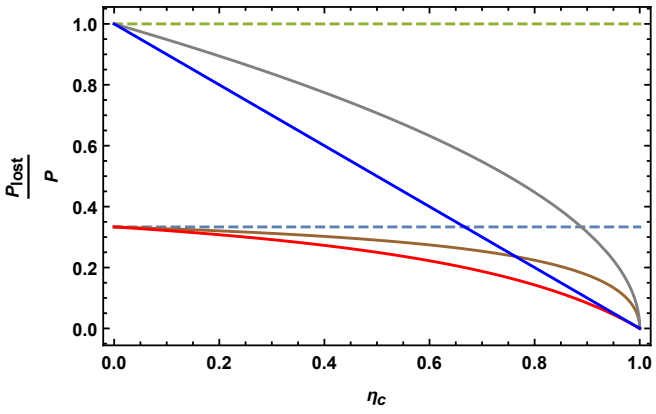

Figure 5.3: Comparison of the ratios of power lost to power gained for the optimization of two different target functions - EF and power output (see Figure 5.3). The lower lying curves [Eqs. (5.21) and (5.22)] represent the case when EF is optimized whereas the upper lying curves [Eqs. (5.23) and (5.24)] represent the case for the optimization of power output. The dashed curves implies that rate of power dissipation is independent of η_C.

We will discuss only the limiting cases $\gamma \to 0$ and $\gamma \to \infty$, for which respective equations for R' can be derived using Eqs. (5.20) and (D.24):

$$R'^{\omega_h}_{\text{eco}(0)} = \frac{1}{3}, \quad R'^{\omega_h}_{\text{eco}(\infty)} = \frac{\sqrt{\tau}}{\sqrt{\tau} + \sqrt{2(1+\tau)}} \tag{5.21}$$

Similar equations for the optimization of E wrt ω_h, while keeping ω_c fixed, are given by

$$R'^{\omega_c}_{\text{eco}(0)} = \frac{\sqrt{\tau}}{\sqrt{\tau} + \sqrt{2(1+\tau)}}, \quad R'^{\omega_c}_{\text{eco}(\infty)} = \frac{\tau}{1+2\tau} \tag{5.22}$$

Next we calculate the ratio of power loss to power gain in the cases when we optimize power output. First we discuss the case when optimization is performed over ω_c. As seen from Eq. (D.33), $R^{\omega_h}_{\text{pow}(0)} = 0$, which indicates that corresponding EF is zero in this case, which in turn implies that loss of power is equal to gain of power. The ratios R' for the extreme cases $\gamma \to 0$ and $\gamma \to \infty$ are given by

$$R'^{\omega_h}_{\text{pow}(0)} = 1, \quad R'^{\omega_h}_{\text{pow}(\infty)} = \sqrt{\tau} \tag{5.23}$$

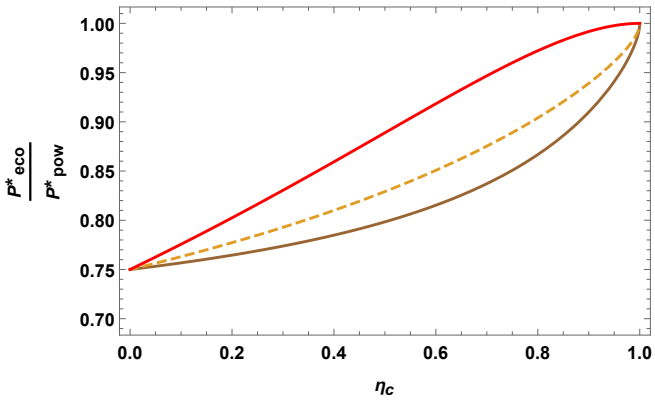

Figure 5.4: Comparison of the ratios of power output at maximum EF and optimal power [Eqs. (5.25) and (5.26)].

The corresponding expressions the optimization of power wrt ω_h are given by

$$R'^{\omega_c}_{\mathrm{pow}(0)} = \sqrt{\tau}, \quad R'^{\omega_c}_{\mathrm{pow}(\infty)} = \tau. \tag{5.24}$$

5.5 Ratio of power at maximum ecological function to maximum power

Figure 5.3 clearly indicates that the fractional loss of power is larger when our three level laser heat engine operates at MP as compared to the engine operating at maximum EF. So, it is useful to evaluate the ratio of power at maximum EF to optimal power. Dividing $P^{*(\omega_h)}_{\mathrm{eco}}$ by $P^{*(\omega_h)}_{\mathrm{pow}}$ (see Eqs. (D.22) and (D.30)), and by taking limits $\gamma \to 0$ and $\gamma \to \infty$, we have following two equations, respectively

$$\bar{R}^{\omega_h}_0 = \frac{1+3\tau-\frac{\tau(3+5\tau)}{\sqrt{1+3\tau}}}{1+3\tau-2\sqrt{2\tau(1+\tau)}}, \bar{R}^{\omega_h}_\infty = \frac{1+\tau-\frac{\tau(3+\tau)}{\sqrt{2\tau(1+\tau)}}}{(1-\sqrt{\tau})^2} \tag{5.25}$$

Similar equations can be obtained for fixed ω_c by dividing $P^{*(\omega_c)}_{\mathrm{eco}}$ with $P^{*(\omega_c)}_{\mathrm{pow}}$ (see Eqs. (D.26)

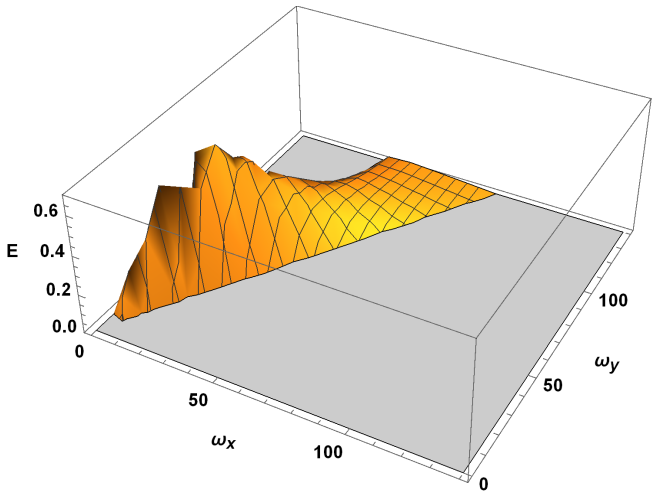

Figure 5.5: 3D-plot of EF [Eq. (D.14)] in terms of control frequencies ω_c and ω_h for $\hbar = 1, k_B = 1, \Gamma_h = \Gamma_c = 1, \lambda = 1, T_h = 20, T_c = 5$.

and (D.35)) and repeating the above mentioned step. Thus we have

$$\bar{R}_0^{\omega_c} = \frac{1+\tau-\frac{\tau(3+\tau)}{\sqrt{2\tau(1+\tau)}}}{(1-\sqrt{\tau})^2}, \quad \bar{R}_\infty^{\omega_c} = \frac{1+2\tau}{(1+\tau)^2}. \tag{5.26}$$

Note that $\bar{R}_\infty^{\omega_h} = \bar{R}_0^{\omega_c}$. Plotting the Eqs. (5.25) and (5.26) in Figure 5.4, we observe that at least 75 percentage of the optimal power is produced in maximum EF regime. The ratio P_{eco}/P increases with increasing η_C and approaches 1 for $\eta_C = 1$. This is expected as with increasing η_C, the efficiency of the engine also increases while dissipation decreases.

5.6 Concluding Remarks

We have analyzed and optimized the thermodynamic performance of SSD heat engine with EF. Here we performed one parameter optimization of EF alternatively with respect to ω_c (ω_h fixed) and ω_h (ω_c fixed) and obtained the general expression for the EMEF. In the limit of extremely asymmetric dissipation, lower and upper bounds on the efficiency are obtained. η_{AB} serves as the upper bound in the former case and lower bound in the later case, thus separating the entire parameter regime of η^E into two parts. To this end, we want to emphasize one point. Although

for the strong matter-field coupling ($\lambda >> \Gamma_{h,c}$) in the high temperature limit, global maximum of EF does not exist for two parameter optimization scheme; for the general case when λ is comparable to $\Gamma_{h,c}$, global maximum of EF exists (See Figure 5.5). But it is not possible to find the analytic expression for EMEF in this case. We have plotted the 3D-graph of EF [Eq. (D.14)] in Figure 5.5.

Next we have compared the performance of SSD engine operating at maximum EF to the engine operating at MP. It is clear from Figures 5.3 and 5.4 that fraction of power lost is appreciably low in case of engine operating at MF. At the same time, engine at maximum EF produce at least 75% of the power produced by the engine working in MP regime. The same analysis also holds true for the for the optimal performance of a classical endoreversible heat engine operating in the ecological regime [44]. Hence we conclude that classical as well as quantum heat engines operating at maximum EF are much more efficient and environment friendly than the engines operating at MP. Therefore it is more reasonable to design real heat engines along the lines of maximizing EF for economical and ecological purposes.

Chapter 6

Conclusions and future outlook

The main motivation of this thesis was to study the optimal performance of different classes of heat engines, including classical, mesoscopic and quantum heat engines, using different objective functions such as power output, ecological function, Omega (Ω) function and efficient power function. In particular, we have focused on the optimization of ecological and efficient power functions which represent a trade-off between the power output and efficiency of a heat engine. We have paid special attention to the universal nature of efficiency at optimal performance of abovementioned objective functions.

In chapter 2, we studied Feynman's ratchet and pawl model, a simple mechanical device of mesoscopic size that can rectify thermal fluctuations to extract work from a setup of two reservoirs at different temperatures using a ratchet and pawl mechanism. We optimized the power output of the ratchet engine operating in the high temperature regime using a non-linear approximation and derived the expression for efficiency at maximum power, which shows the universal nature of efficiency upto second order in η_C. We also optimized the linear model of ratchet engine by constraining the internal energy scales in different ways and obtained well known expressions of thermal efficiency in finite-time thermodynamics. We discussed four cases and by identifying the effective temperatures and coefficients of thermal conductance, we were able to map each case to an effective endoreversible model.

However, we mapped only linear model of the engine to effective endoreversible models.

It is an interesting problem to explore whether the non-linear model can be mapped to effective endoreversible models. A possible mapping beyond the assumptions of linear irreversible thermodynamics (linear flux-force formalism) may be attempted. It may shed light on general connection between various finite-time models beyond the linear response regime.

In Chapter 3, we studied the optimal performance of Feynman's model for both engine and refrigerator modes. For engine mode, we optimized two different objective functions: ecological function and efficient power function. Similarly, for refrigerator mode, we optimized ecological function and χ function. We employed two different optimization methods to carry out our study: the first one involves the standard technique of two parameter optimization over the energy scales of the engine and the second one uses prior information analysis based on Bayesian approach to estimate the expected performance of the engine. Based on a few simple assumptions, the prior probability distribution was found to be of the form $\Pi(\epsilon_k) = 1/\epsilon_k$, known as Jeffreys prior, where ϵ_k is assumed to take values in the range $[\epsilon_{\min}, \epsilon_{\max}]$. The derived expressions for the efficiency/coefficient of performance (COP) at maximum ecological function from the abovementioned two methods were found to agree with each other close to equilibrium.

The analysis was repeated for the optimization of efficient power function and χ function. In addition, we also studied one parameter optimization of the engine and refrigerator modes in the high temperature limit. Again the results obtained from two different optimization schemes (exact approach and prior information approach) were found to agree close to equilibrium. Moreover, the forms of efficiency obtained from exact one parameter optimization of efficient power function and χ function were re-derived using the prior information approach.

While addressing the problem using prior information approach, we assumed that one of the energy scales is fixed and considered prior distribution over the remaining energy scale. By doing so, we were able to recast the problem in terms of one uncertain variable only. It is remaining to explore the problem in terms of two uncertain variables (energy scales here). It is a nontrivial problem since assignment of prior probability distribution is not straight forward in

this case.

In Chapter 4, we studied the optimization of a low-dissipation Carnot like heat engine operating in the maximum efficient power regime. We derived the expression for efficiency at maximum efficient power in a closed form and were able to obtain the lower and upper bounds on efficiency in the case of extreme asymmetric dissipation when the ratio of dissipation constants (coefficients) at the hot and cold reservoirs approaches zero or infinity respectively. In addition, for the symmetric dissipation, we obtained expression for the efficiency which concurs with the efficiency of an endoreversible heat engine. We confirmed the universality of the first two terms of the efficiency at maximum efficient power by expanding it in Taylor's series near equilibrium. We also compared the ratio of average dissipations at the cold and hot contacts for three different objective functions: power output, Ω function and efficient power functions.

Interestingly enough, whereas in case of power and Ω function, the ratio is independent of efficiency of the engine, it depends upon efficiency for the optimization of efficient power function. It hints that efficient power function belongs to different class of functions than power output and Ω function. In our future work, we would like to work along this direction and try to find common or dissimilar features among these objective functions.

In Chapter 5, we optimized the performance of a three-level lase heat engine operating at maximum ecological function. Under the assumptions of strong matter-field coupling and high bath temperatures, we derived analytic expressions for efficiency for two different optimization schemes. In both cases, upper and lower bounds on efficiency were obtained in the case of extreme asymmetric dissipation when the ratio of system-bath coupling constants at the hot and cold reservoirs approaches zero and infinity respectively. Then we compared the performance of the engine operating at maximum ecological function to the engine operating at maximum power. Our analysis showed that engines operating at maximum ecological function are much more efficient than those operating at maximum power, thus making them more suitable for economical and environmental considerations. Our analysis also sheds light on the correspondence between quantum and classical heat engines, and the classical features observed in quantum

machines. This work can be extended to study the optimal performance of a three-level system operating as a refrigerator.

Appendix A

Feynman-Smoluchowski engine at high temperatures

In Chapter 2, we have optimized the power output of non-linear model model of FS engine. The optimal values of ϵ_1 and ϵ_2 at maximum power are given by

$$\epsilon^*_{1_{hot}} = T_1\frac{(4-3\eta_C)}{3(2-\eta_C)}, \quad \epsilon^*_{2_{hot}} = T_1\frac{(1-\eta_C)(4-\eta_C)}{3(2-\eta_C)}. \tag{A.1}$$

Evaluating the second order derivatives of P with respect to ϵ_1 and ϵ_2 at optimal values, we have

$$A \equiv \frac{\partial^2 P}{\partial \epsilon_1^2} = \frac{3\epsilon_1 - \epsilon_2 - 2T_1}{T_1^2} = -\frac{T_1(4-2\eta_C+\eta_C^2)}{3(2-\eta_C)T_1^2} < 0, \tag{A.2}$$

$$B \equiv \frac{\partial^2 P}{\partial \epsilon_2^2} = \frac{3\epsilon_2 - \epsilon_1 - 2T_2}{T_2^2} = -\frac{T_1(4-6\eta_C+3\eta_C^2)}{3(2-\eta_C)T_2^2} < 0, \tag{A.3}$$

$$C \equiv \frac{\partial^2 P}{\partial \epsilon_1 \partial \epsilon_2} = \frac{T_1-\epsilon_1}{T_1^2} - \frac{T_2-\epsilon_2}{T_2^2} = \frac{16T_1^2(1-\eta_C)^2}{9(2-\eta_C)^2T_1^2T_2^2} \tag{A.4}$$

We plot $D \equiv AB/C^2$ versus η_C in Figure A.1, from which it is clear that $D > 1$. Thus, we have a maximum in this case.

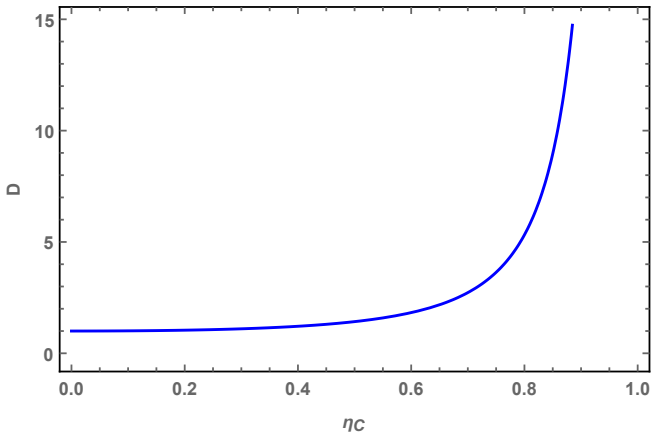

Figure A.1: $D \equiv AB/C^2$ versus η_C.

Appendix B

Low-dissipation heat engine

B.1 Derivation of x_c and x_h

Substituting the values of Q_h and Q_c from Eqs. (5.6) and (5.9) into the Eqs. (4.11) and (4.12) and then adding, we have

$$\begin{aligned} &T_h(\Delta S - x_h\Sigma_h) - 2T_c(\Delta S + x_c\Sigma_c) - 2T_c x_c\Sigma_c\left[1 - \frac{T_c(\Delta S + x_c\Sigma_c)}{T_h(\Delta S - x_h\Sigma_h)}\right] \\ &+T_h\left[1 - \frac{T_c^2(\Delta S + x_c\Sigma_c)^2}{T_h^2(\Delta S - x_h\Sigma_h)}\right] - x_h\Sigma_h T_h\left[1 - \frac{T_c^2(\Delta S + x_c\Sigma_c)^2}{T_h^2(\Delta S - x_h\Sigma_h)^2}\right] = 0. \end{aligned} \tag{B.1}$$

Further writing the above equation in terms of $\eta_{\rm C} = 1 - T_c/T_h$, we have

$$\begin{aligned} \Delta S \quad &-2x_h\Sigma_h - 4(1-\eta_{\rm C})x_c\Sigma_c - 2(1-\eta_{\rm C})\Delta S \\ &+2(1-\eta_{\rm C})^2 x_c\Sigma_c\frac{\Delta S + x_c\Sigma_c}{\Delta S - x_h\Sigma_h} + \Delta S(1-\eta_{\rm C})^2\frac{(\Delta S + x_c\Sigma_c)^2}{(\Delta S - x_h\Sigma_h)^2} = 0. \end{aligned} \tag{B.2}$$

Solving Eq. (B.2) for x_c, we have

$$x_c = \frac{1}{\Sigma_c(1-\eta_{\rm C})}\left[\frac{\Delta S^2\eta_{\rm C}}{3\Delta S - 2x_h\Sigma_h} - x_h\Sigma_h\right]. \tag{B.3}$$

Dividing Eqs. (4.11) and (4.12) and writing in terms of $\eta_{\rm C}$, we get

$$\frac{x_c^2}{x_h^2} = \frac{\Sigma_h}{2\Sigma_c}\left[\frac{\Delta S + x_c\Sigma_c}{\Delta S - x_h\Sigma_h} + \frac{1}{1-\eta_{\rm C}}\right]. \tag{B.4}$$

Again solving Eq. (B.4) for x_c and writing in terms of γ, we have

$$\begin{aligned} x_c \;=\; & \frac{1}{4(1-\eta_{\rm C})\Sigma_c(\Delta S - x_h\Sigma_h)}\Big[\gamma x_h^2\Sigma_h^2(1-\eta_{\rm C}) - x_h\Sigma_h\sqrt{\gamma(1-\eta_{\rm C})} \\ & \times\sqrt{8\Delta S^2(2-\eta_{\rm C}) - 8\Delta S x_h\Sigma_h(3-\eta_{\rm C}) + \gamma x_h^2\Sigma_h^2(1-\eta_{\rm C}) + 8x_h^2\Sigma_h^2}\Big] \end{aligned} \tag{B.5}$$

Comparing Eqs. (B.3) and (B.5), we have the final expression for x_h as given by Eq. (4.13).

B.2 Derivation of Eq. (4.15)

Efficiency of the engine is given by:

$$\eta = \frac{W}{Q_h} = 1 - \frac{Q_c}{Q_h}. \tag{B.6}$$

Using Eq. (5.6) and (5.9) and writing in terms of $\eta_{\rm C}$, the expression for efficiency becomes

$$\eta = 1 - (1-\eta_{\rm C})\frac{\Delta S + x_c\Sigma_c}{\Delta S - x_h\Sigma_h}. \tag{B.7}$$

Rearranging the terms in Eq. (B.3), we obtain under conditions of MEP

$$(\Delta S + x_c\Sigma_c)(1-\eta_{\rm C}) = \frac{\Delta S^2\eta_{\rm C}}{3\Delta S - 2x_h\Sigma_h} + \Delta S - x_h\Sigma_h - \Delta S\eta_{\rm C}. \tag{B.8}$$

Substituting Eq. (B.8) in Eq. (B.7), we obtain following form of efficiency

$$\eta^* = \frac{2\eta_{\rm C}}{3 - 2x_h\Sigma_h/\Delta S}. \tag{B.9}$$

.

B.3 Derivation of η_-, η_+ and $\eta_{\rm sym}$

Upper bound: For $\gamma \to 0$, using Eq. (4.14), $K = 9/4 - 2\eta_{\rm C}$, $K' = 0$, $G = 0$. Substituting these values in Eq. (4.13), we obtain $x_h = (3 - \sqrt{9 - 8\eta_{\rm C}})\Delta S/4\Sigma_h$. Then using Eq. (4.15), we obtain the upper bound on efficiency $\eta_+ = 1(3 - \sqrt{9 - 8\eta_{\rm C}})/2$.

EMEP for symmetric dissipation ($\gamma = 1$): In this case, $K = (1 + \eta_{\rm C})^2/16$, $K' = (1 - \eta_{\rm C})(9 - \eta_{\rm C})/8$, $G = -(9 - \eta_{\rm C})(1 - \eta_{\rm C}^2)/8$ (See Eq. (4.14)). Putting these values in Eq. (4.13), we have $x_h = (3 - \eta_{\rm C} - \sqrt{(1 - \eta_{\rm C})(9 - \eta_{\rm C})})\Delta S/4\Sigma_h$. Substitution of x_h in Eq. (12) will yield $\eta_{\rm sym} = 1 - (1 - \eta_{\rm C})\left(1 + \sqrt{1 + 8/(1 - \eta_{\rm C})}\right)/4$.

Lower bound: We first calculate K, K' and G by pulling out γ from the numerator and denominator of each term and then taking the limit $\gamma \to \infty$. Thus we have $K = (6 - \eta_{\rm C})^2/16$, $K' = \eta_{\rm C}^2/8$ and $G = (6 - \eta_{\rm C})\eta_{\rm C}^2/8$. Repeating the steps used to derive η_+ and $\eta_{\rm sym}$, we obtain $x_h = 0$ and $\eta_- = 2\eta_{\rm C}/3$.

Appendix C

Dynamics of open quantum systems

In order to understand the dynamics of open quantum systems, we first introduce the dynamics of closed systems.

C.1 Dynamics of closed quantum systems

In non-relativistic quantum mechanics, state of a quantum system is represented by a state ket $|\psi\rangle$ in the Hilbert space $\mathcal{H}$. The time evolution of the closed quantum system is described by the Schrodinger equation:

$$H(t)\,|\psi(t)\rangle = i\hbar\frac{d\,|\psi(t)\rangle}{dt}, \tag{C.1}$$

where $H(t)$ is the Hamiltonian of the system. The formal solution of Schrodinger equation is given by

$$|\psi(t)\rangle = U(t,t_0)\,|\psi(t_o)\rangle\,, \tag{C.2}$$

where $U(t,t_0)$ is unitary time evolution operator satisfying the relation $U(t,t_0)^\dagger U(t,t_0) = U(t,t_0)U(t,t_0)^\dagger = I$, and $|\psi(t_o)\rangle$ is state of the system at some initial time t_0.

Substitution of Eq. (C.2) in Eq. (C.1) leads to an operator equation for $U(t,t_0)$:

$$H(t)U(t,t_0) = i\hbar\frac{\partial U(t,t_0)}{\partial t}, \tag{C.3}$$

subjected to the initial condition $U(t_0, t_0) = I$. For a closed and isolated quantum system, Hamiltonian is time independent and Eq. (C.3) is integrated to yield the following solution:

$$U(t, t_0) = e^{-iH(t-t_0)/\hbar}. \tag{C.4}$$

However, in many physical situations, the system under consideration is driven by external time dependent forces such as time dependent electromagnetic fields. In such cases, the dynamics of the system is formulated in terms of a time dependent Hamiltonian $H(t)$, and the solution of Eq. (C.3) is represented by a time-ordered exponential,

$$U(t, t_0) = T_{\leftarrow} e^{-\frac{i}{\hbar}\int_{t_0}^{t} ds H(s)} \tag{C.5}$$

More generally, for a mixed state, state of the system is characterized by a density matrix ρ. Suppose at some inititial time t_0, the state of the system is represented by the density matrix

$$\rho(t_0) = \sum_k P_k \left|\psi_k(t_0)\right\rangle \left\langle\psi_k(t_0)\right|, \tag{C.6}$$

where P_k are positive weights and $\left|\psi_k(t_0)\right\rangle$ are state kets, evolving in time according to Schrodinger equation (C.1). Therefore, at time t, the state of the system is given by

$$\rho(t) = \sum_k P_k U(t, t_0) \left|\psi_k(t_0)\right\rangle \left\langle\psi_k(t_0)\right| U(t, t_0)^\dagger, \tag{C.7}$$

which can be written as

$$\rho(t) = U(t, t_0)\rho(t_0)U(t, t_0)^\dagger. \tag{C.8}$$

Differentiating this equation with respect to time and simplifying a bit, we get the following equation of motion for the density matrix,

$$\frac{d\rho(t)}{dt} = -i\hbar[H(t), \rho(t)]. \tag{C.9}$$

Eq. (C.9) is known as Liouville-von Neumann equation and often written in a form analogous to classical Liouville equation

$$\frac{d\rho(t)}{dt} = \mathcal{L}(t)\rho(t), \tag{C.10}$$

where $\mathcal{L}$ is the Liouville super-operator, defined through the condition

$$\mathcal{L}(t)\rho(t) = -i\hbar[H(t), \rho(t)]. \tag{C.11}$$

In close analogy with Eq. (C.5), the formal solution of Eq. (C.10) is given by

$$\rho(t) = T_{\leftarrow} e^{\int_{t_0}^{t} ds\mathcal{L}(s)} \rho(t_0). \tag{C.12}$$

For a time independent Hamiltonian, $\mathcal{L}(t)$ is also time independent and thus we have

$$\rho(t) = e^{\mathcal{L}(t-t_0)} \rho(t_0). \tag{C.13}$$

C.2 Dynamics of open quantum systems

An open quantum system is a system S coupled to another quantum system B, usually very large as compared to system S, called environment. The total system $S + B$ is assumed to be closed and evolves according to unitary Hamiltonian dynamics. However, the dynamics of subsystem S cannot be represented in terms of unitary Hamiltonian dynamics due to its interaction with the environment.

Denoting Hilbert space of the system S and Hilbert space of the environment B by $\mathcal{H}_S$ and $\mathcal{H}_B$ respectively, the Hilbert space of the total system is given by the tensor product space $\mathcal{H} = \mathcal{H}_S \otimes \mathcal{H}_B$. The total system+environment Hamiltonian $H(t)$ may be written as

$$H(t) = H_S \otimes I_B + I_S \otimes H_B + H_I(t), \tag{C.14}$$

where H_S is self-Hamiltonian of the system S, H_B is the free-Hamiltonian of the environment B. and $H_I(t)$ is the Hamiltonian of system-environment interaction. Often in many physical situations, we need to solve the dynamics of the system S only. This can be done by tracing out the degrees of freedom of the environment by employing various analytical as well as numerical methods. If $\rho(t)$ represents the state of the combined total system, reduced density matrix ρ_S of the open quantum system is given by

$$\rho_S = Tr_B[\rho], \tag{C.15}$$

where Tr_B represents the partial trace over the degrees of freedom of the environment.

At time t, the reduce density matrix $\rho_S(t)$ of the open quantum system is obtained from the density matrix $\rho(t)$ of the total system by partially tracing out the degrees of freedom of the environment. Since $\rho(t)$ evolves unitarily, we have

$$\rho_S(t) = Tr_B[U(t,t_0)\rho(t_0)U(t,t_0)^\dagger], \tag{C.16}$$

where $\rho(t_0)$ is density operator of the total system at some initial time t_0 and $U(t,t_0)$ is the time-evolution operator of the total system. Similarly, by taking the partial trace over the environmental degrees of freedom on both sides of the Liouville-von Neumann equation for the total system, we may obtain equation of motion for the reduced density matrix ρ_S,

$$\frac{d\rho_S(t)}{dt} = -i\hbar[H(t),\rho(t)]. \tag{C.17}$$

C.3 Quantum dynamical semigroups

In general, it is very difficult to solve the dynamics of the reduced system described by Eq. (C.17). However, when environmental correlation times are short-lived, we may apply Markovian approximation to neglect memory effects and formulate the dynamics of reduced system

in terms of a quantum dynamical semigroup [176, 177].

We are interested in the case when the environment is in the equilibrium state. Suppose that at initial time $t = 0$, state of the total system $S + B$ is prepared in an uncorrelated product state $\rho(0) = \rho_S(0) \otimes \rho_B$, where ρ_S and ρ_B represent initial state of the reduced system S and equilibrium state of the bath B, respectively. Then, there exists a quantum dynamical map $\Lambda(t)$, describing the evolution of reduced system S from the initial time $t = 0$ to some other time $t > 0$, such that

$$\rho_S(t) = \Lambda(t)\rho_S(0) \equiv Tr_B \left[U(t,0)(\rho_S(0) \otimes \rho_B)U(t,0)^\dagger\right]. \tag{C.18}$$

It can be shown that $\Lambda(t)$ is a convex-linear, completely positive and trace-preserving quantum operation.

As mentioned earlier, when the reservoir correlation times are much shorter as compared to the characteristic time scale of the system evolution, we may neglect the memory effects (Markovian approximation) in the reduced system dynamics. Under this approximation, the quantum dynamical map $\Lambda(t)$ satisfies the following semigroup property:

$$\Lambda(t_1)\Lambda(t_2) = \Lambda(t_1 + t_2), \qquad t_1, t_2 \geq 0. \tag{C.19}$$

A *quantum dynamic semigroup* is a continuous, one-parameter family $\{\Lambda(t) \,|\, t > 0\}$ of dynamical maps ($\Lambda(0) = I$), satisfying the relation given in Eq. (C.19).

Given a quantum dynamical semigroup, there exists a time independent linear map $\mathcal{L}'$, the generator of the semigroup, which allows us to represent the semigroup in exponential form:

$$\Lambda(t) = e^{\mathcal{L}'t}. \tag{C.20}$$

This representation yields a first-order differential equation [see Eq. (C.18)] for the reduced

density matrix $\rho_S(t)$,

$$\frac{d\rho_S(t)}{dt} = \mathcal{L}'\rho_S(t). \tag{C.21}$$

This equation is known as Markovian quantum master equation. The generator $\mathcal{L}'$ represents a super-operator, and may be considered as the generalization of the Liouville super-operator introduced in section 1.1.

C.4 Lindblad quantum master equation

Lindblad [176] and separately Gorini, Kossakowski and Sudarshan [177] proved that the most general form of the generator $\mathcal{L}'$ of the quantum dynamical semigroup is given by

$$\begin{aligned} \frac{d\rho_S(t)}{dt} = \mathcal{L}'\rho_S &= -i\hbar\left[H, \rho_S\right] + \sum_k \gamma_k \Big(A_k \rho_S A_k^\dagger - \frac{1}{2} A_k^\dagger A_k \rho_S - \frac{1}{2} \rho_S A_k^\dagger A_k \Big), & \text{(C.22)} \\ &\equiv -i\hbar\left[H, \rho_S\right] + \mathcal{L}_\mathcal{D}\rho_S. & \text{(C.23)} \end{aligned}$$

The above quantum master equation is known as the LGKS equation or Lindblad equation. Here γ_k's are positive relaxation constants, A_k are called Lindblad operators, H is effective Hamiltonian of the system. The first term of the generator represents the unitary part of the dynamics generated by the Hamiltonian H. $\mathcal{L}_\mathcal{D}$ is known as the dissipator and represents the effect of the environment on dynamics of the reduced system. Generally, it induces non-unitary, dissipative dynamics.

Appendix D

Three-level laser heat engine

D.1 Steady state solution of density matrix equations

Here, we solve the equations for density matrix in the steady state. Substituting the expressions for H_0, $\bar{H}$, V_0, and using Eqs. (5.2) and (5.3) in Eq. (5.4), the time evolution of the elements of the density matrix are given by following equations:

$$\dot{\rho}_{11} = i\lambda(\rho_{10} - \rho_{01}) - 2\Gamma_h[(n_h + 1)\rho_{11} - n_h\rho_{gg}], \tag{D.1}$$

$$\dot{\rho}_{00} = -i\lambda(\rho_{10} - \rho_{01}) - 2\Gamma_c[(n_c + 1)\rho_{00} - n_c\rho_{gg}], \tag{D.2}$$

$$\dot{\rho}_{10} = -[\Gamma_h(n_h + 1) + \Gamma_c(n_c + 1)]\rho_{10} + i\lambda(\rho_{11} - \rho_{00}), \tag{D.3}$$

$$\rho_{11} = 1 - \rho_{00} - \rho_{gg}, \tag{D.4}$$

$$\dot{\rho}_{01} = \dot{\rho}^*_{10}. \tag{D.5}$$

Solving Eqs. (D.1) - (D.5) in the steady state by setting $\dot{\rho}_{mn} = 0$ $(m, n = 0, 1)$, we obtain

$$\rho_{10} = \frac{i\lambda(n_h - n_c)\Gamma_c\Gamma_h}{\lambda^2[(1 + 3n_h)\Gamma_h + (1 + 3n_c)\Gamma_c] + \Gamma_c\Gamma_h[1 + 2n_h + n_c(2 + 3n_h)][(1 + n_c)\Gamma_c + (1 + n_h)\Gamma_h]}, \tag{D.6}$$

and

$$\rho_{01} = \rho_{10}^{*}. \tag{D.7}$$

Calculating the trace in Eq. (5.5), the output power is given by

$$P = i\hbar\lambda(\omega_h - \omega_c)(\rho_{10} - \rho_{01}), \tag{D.8}$$

Similarly evaluating the trace in Eq. (5.6), heat flux $\dot{Q}_h$ can be written as

$$\dot{Q}_h = -\hbar\omega_h(2\Gamma_h[(n_h + 1)\rho_{11} - n_h\rho_{gg}]). \tag{D.9}$$

Using the steady state condition $\dot{\rho}_{11} = 0$ (see Eq. (D.1)), Eq. (D.9) becomes

$$\dot{Q}_h = -i\hbar\lambda\omega_h(\rho_{10} - \rho_{01}). \tag{D.10}$$

Now EF is given by

$$E = 2P - (1 - \tau)\dot{Q}_h. \tag{D.11}$$

Using Eqs. (D.8) and (D.9), we recast Eq. (D.11) as follows

$$E = i\hbar\lambda(\rho_{01} - \rho_{10})[2(\omega_h - \omega_c) - (1 - \tau)\omega_h] \tag{D.12}$$

Substituting Eqs. (D.6) and (D.7) in Eqs. (D.8) and (D.12), we have

$$P = \frac{2\hbar\lambda^2\Gamma_c\Gamma_h(n_h - n_c)(\omega_h - \omega_c)}{\lambda^2[(1 + 3n_h)\Gamma_h + (1 + 3n_c)\Gamma_c] + \Gamma_c\Gamma_h[1 + 2n_h + n_c(2 + 3n_h)][(1 + n_c)\Gamma_c + (1 + n_h)\Gamma_h]}, \tag{D.13}$$

$$E = \frac{2\hbar\lambda^2\Gamma_c\Gamma_h(n_h - n_c)[2(\omega_h - \omega_c) - \eta_C\omega_h]}{\lambda^2[(1 + 3n_h)\Gamma_h + (1 + 3n_c)\Gamma_c] + \Gamma_c\Gamma_h[1 + 2n_h + n_c(2 + 3n_h)][(1 + n_c)\Gamma_c + (1 + n_h)\Gamma_h]}. \tag{D.14}$$

D.2 Optimization in high temperature limit

In order to obtain the analytic expressions of interest, we optimize power output and the EF given in Eq. (D.14) in the high temperatures limit, assuming the strong matter-field coupling $\lambda >> \Gamma_h, c$. In the said limit, n_h and n_c can be approximated as

$$n_h = \frac{1}{e^{\hbar\omega_h/k_BT_h}-1} \simeq \frac{k_BT_h}{\hbar\omega_h}, \tag{D.15}$$

$$n_c = \frac{1}{e^{\hbar\omega_c/k_BT_c}-1} \simeq \frac{k_BT_c}{\hbar\omega_c}. \tag{D.16}$$

Using Eqs. (D.15) and (D.16) in Eq. (D.14) and ignoring the terms containing $\Gamma_{h,c}$ in comparison to λ, we can write P and E in terms of $\tau = T_c/T_h$ and $\gamma = \Gamma_h/\Gamma_c$ in the following form

$$P \simeq \frac{2\hbar\Gamma_h(\omega_h-\omega_c)(\omega_c-\tau\omega_h)}{3(\omega_c\gamma+\tau\omega_h)}, \tag{D.17}$$

$$E \simeq \frac{2\hbar\Gamma_h(\omega_c-\tau\omega_h)[2(\omega_h-\omega_c)-(1-\tau)\omega_h]}{3(\omega_c\gamma+\tau\omega_h)}. \tag{D.18}$$

One parameter optimization of ecological function

We optimize E w.r.t to one parameter only while keeping the other fixed. Optimizing Eq. (D.14) wrt ω_c, for a fixed ω_h, and solving for ω_c, we obtain

$$\omega_c^* = \frac{\omega_h}{2\gamma}\Big(\sqrt{2\tau(1+\gamma)[\gamma+(2+\gamma)\tau]}-2\tau\Big). \tag{D.19}$$

Using Eq. (D.19) in Eq. (5.10), EMEF is evaluated as given in Eq. (15).

Optimizing Eq. (D.18) wrt ω_h, we have

$$\omega_h^* = \omega_c\frac{\sqrt{(1+\gamma)(1+\tau)[\gamma+2(1+\gamma)\tau]}-\gamma(1+\tau)}{\tau(1+\tau)}. \tag{D.20}$$

Again using Eqs. (D.20) and (5.10), EMEF is derived as given in Eq. (16).

D.3 Ratio E/P for two different target functions

Here, we derive the expressions for the ratios of EF (E) and power (P) for the following four cases.

Optimal E for a fixed ω_h

The optimal value of the EF, $E_{\rm eco}^{*(\omega_h)}$, can be evaluated by substituting Eq. (D.19) into Eq. (D.18). Similarly, substituting Eq. (D.19) into Eq. (D.17), we obtain the expression for power at maximum EF, $P_{\rm eco}^{*(\omega_h)}$. Therefore, we have

$$E_{\rm eco}^{*(\omega_h)} = \frac{2\hbar\omega_h\Gamma_h}{3\gamma^2}\big(\gamma+4\tau+3\gamma\tau-2A\big), \tag{D.21}$$

$$P_{\rm eco}^{*(\omega_h)} = \frac{\hbar\omega_h\Gamma_h}{3\gamma^2 A}(A-2(\gamma+\tau))(A-2(1+\gamma)\tau), \tag{D.22}$$

where $A=\sqrt{2(1+\gamma)\tau[\gamma+(2+\tau)\gamma]}$. The ratio of $E_{\rm eco}^{*(\omega_h)}$ and $P_{\rm eco}^{*(\omega_h)}$ is evaluated to be

$$R_{\rm eco}^{\omega_h} = \frac{\sqrt{2(1+\gamma)\tau[\gamma+(2+\tau)\gamma]}}{(1+\gamma)\tau+\sqrt{2(1+\gamma)\tau[\gamma+(2+\tau)\gamma]}}. \tag{D.23}$$

Now, consider $\gamma\to 0$ and $\gamma\to\infty$. For these limiting cases, the above equation reduces to:

$$R_{\rm eco(0)}^{\omega_h}=\frac{2}{3}, \quad R_{\rm eco(\infty)}^{\omega_h}=\frac{\sqrt{2(1+\tau)}}{\sqrt{\tau}+\sqrt{2(1+\tau)}}. \tag{D.24}$$

Optimal E for a fixed ω_c

In this case, the expression for optimal EF and corresponding power output can be obtained by using Eqs. (D.20) and (D.18), and Eqs. (D.20) and (D.17), respectively.

$$E_{\rm eco}^{*(\omega_c)} = \frac{2\hbar\omega_c\Gamma_h\big(1+3\tau+2\gamma(1+\tau)-2B\big)}{3\tau}, \tag{D.25}$$

$$P_{\rm eco}^{*(\omega_c)} = \frac{2\hbar\omega_c\Gamma_h\big((1+\gamma)(1+\tau)+B\big)\big((\tau+\gamma)(1+\tau)+B\big)}{3\tau(1+\tau)B}, \tag{D.26}$$

where $B = \sqrt{(1+\gamma)(1+\tau)[\gamma+(2+\tau)\gamma]}$. We evaluate the ratio of $E_{\rm eco}^{*(\omega_c)}$ and $P_{\rm eco}^{*(\omega_c)}$ as follows

$$R_{\rm eco}^{\omega_c} = \frac{\sqrt{(1+\gamma)(1+\tau)[\gamma+(2+\tau)\gamma]}}{(1+\gamma)\tau+\sqrt{(1+\gamma)(1+\tau)[\gamma+(2+\tau)\gamma]}}. \tag{D.27}$$

Again the limiting cases $\gamma \to 0$ and $\gamma \to \infty$ yield the following two equations

$$R_{\rm eco(0)}^{\omega_c} = \frac{\sqrt{2(1+\tau)}}{\sqrt{\tau}+\sqrt{2(1+\tau)}}, \quad R_{\rm eco(\infty)}^{\omega_c} = \frac{1+\tau}{1+2\tau}. \tag{D.28}$$

Optimal power with a fixed ω_h

The optimization of power wrt ω_c (ω_h fixed) or ω_h (ω_c fixed) is perfomed in the Ref. [22]. For the former case, the expressions for ω_c^{P*} is given by

$$\omega_c^{P*} = \gamma^{-1}[\tau+\sqrt{\tau(1+\gamma)(\tau+\gamma)}]\omega_h. \tag{D.29}$$

Again, the expressions for optimal power and for the EF at optimal power can be evaluated, and are given by.

$$P_{\rm pow}^{*(\omega_h)} = \frac{2\hbar\omega_h\Gamma_h(\gamma+2\tau+\gamma\tau-2C)}{3\gamma^2}, \tag{D.30}$$

$$E_{\rm pow}^{*(\omega_h)} = \frac{2\hbar\omega_h\Gamma_h(C-(1+\gamma)\tau)(C-2\tau-(1+\tau)\gamma)}{\gamma^2 C}, \tag{D.31}$$

where $C = \sqrt{\tau(1+\gamma)(\tau+\gamma)}$. The required ratio is calculated to be

$$R_{\rm pow}^{\omega_h} = 1 - \frac{\sqrt{\tau(1+\gamma)(\tau+\gamma)}}{\tau+\gamma}. \tag{D.32}$$

The cases of our interest are $\gamma \to 0$ and $\gamma \to \infty$. By evaluating $R_{\rm pow}^{\omega_h}$ for the extreme values of γ, we get

$$R_{\rm pow(0)}^{\omega_h} = 0, \quad R_{\rm pow(\infty)}^{\omega_h} = 1-\sqrt{\tau}. \tag{D.33}$$

Optimal power with a fixed ω_c

For this case, the expressions for ω_h^{P*} is given by [22]

$$\omega_h^{P*} = \tau^{-1}[-\gamma + \sqrt{(1+\gamma)(\tau+\gamma)}]\omega_c. \tag{D.34}$$

In this case, $P_{\rm pow}^{*(\omega_c)}$ and $E_{\rm pow}^{*(\omega_c)}$ are given by, respectively,

$$P_{\rm pow}^{*(\omega_c)} = \frac{2\hbar\omega_c\Gamma_h\big(1+\tau+2\gamma-2D\big)}{3\tau}, \tag{D.35}$$

$$E_{\rm pow}^{*(\omega_c)} = \frac{\big(D-(1+\gamma)\big)\big((1+\tau)D-2\tau-\gamma(1+\tau)\big)}{(2\hbar\omega_c\Gamma_h)^{-1}3\tau\sqrt{(1+\gamma)(\tau+\gamma)}}, \tag{D.36}$$

where $D=\sqrt{(1+\tau)(\tau+\gamma)}$. The ratio of $E_{\rm pow}^{*(\omega_c)}$ and $P_{\rm pow}^{*(\omega_c)}$ is given by

$$R_{\rm pow}^{\omega_c} = 1 - \frac{(1+\gamma)\tau}{\sqrt{(1+\gamma)(\tau+\gamma)}}. \tag{D.37}$$

Evaluating the limit of $R_{\rm pow}^{\omega_c}$ at $\gamma\to 0$ and $\gamma\to\infty$, we obtain, respectively

$$R_{{\rm pow}(0)}^{\omega_c} = 1-\sqrt{\tau}, \quad R_{{\rm pow}(\infty)}^{\omega_c} = 1-\tau. \tag{D.38}$$

Bibliography

[1] M. Esposito, R. Kawai, K. Lindenberg, and C. Van den Broeck, Phys. Rev. Lett. **105**, 150603 (2010).

[2] V. Holubec and A. Ryabov, Phys. Rev. E **92**, 052125 (2015).

[3] R. S. Johal, Eur. Phys. J. Spec. Top. **226**, 489 (2017).

[4] S. Carnot, "Réflexions sur la puissance motrice du feu et sur les machines propres à développer cette puissance," (1824).

[5] R. Clausius, *Mechanical theory of heat* (J. van Voorst, 1867).

[6] H. B. Reitlinger, *Sur l'Utilisation de la chaleur dans les machines à feu* (Vaillant-Carmanne;[Paris, Liége: Béranger], 1929).

[7] J. Yvon, *Saclay Reactor: Acquired knowledge by two years experience in heat transfer using compressed gas*, Tech. Rep. (CEA Saclay, 1955).

[8] P. Chambadal, *Les Centrales Nuclearis* (Armand Colin, Paris, France, 1957).

[9] I. I. Novikov, J. Nucl. Energy II **7**, 125 (1958).

[10] F. L. Curzon and B. Ahlborn, Am. J. Phys. **43**, 22 (1975).

[11] M. H. Rubin, Phys. Rev. A **19**, 1272 (1979).

[12] A. de Vos, *Endoreversible Thermodynamics of Solar Energy Conversion* (Oxford University Press, Oxford, UK, 1992).

[13] B. Andresen, Angew. Chem. **50**, 2690 (2011).

[14] P. Salamon, J. Nulton, G. Siragusa, T. Andersen, and A. Limon, Energy **26**, 307 (2001).

[15] E. Geva and R. Kosloff, Phys. Rev. E **49**, 3903 (1994).

[16] E. Geva and R. Kosloff, J. Chem. Phys. **104**, 7681 (1996).

[17] S. Velasco, J. M. M. Roco, A. Medina, and A. C. Hernndez, J. Phys. D: Appl. Phys. **34**, 1000 (2001).

[18] R. Kosloff and A. Levy, Annu. Rev. Phys. Chem. **65**, 365 (2014).

[19] Z. C. Tu, J. Phys. A **41**, 312003 (2008).

[20] G. Thomas and R. S. Johal, J. Phys. A **48**, 335002 (2015).

[21] S. Sheng, P. Yang, and Z. C. Tu, Commun. Theor. Phys. **62**, 589 (2014).

[22] K. E. Dorfman, D. Xu, and J. Cao, Phys. Rev. E **97**, 042120 (2018).

[23] B. Andresen, R. S. Berry, A. Nitzan, and P. Salamon, Phys. Rev. A **15**, 2086 (1977).

[24] P. Salamon, B. Andresen, and R. S. Berry, Phys. Rev. A **15**, 2094 (1977).

[25] B. Andresen, P. Salamon, and R. S. Berry, J. Chem. Phys. **66**, 1571 (1977).

[26] A. de Vos, Am. J. Phys. **53**, 57 (1985).

[27] V. N. Orlov, Sov. Phys. Dokl. **30**, 506 (1985).

[28] L. Chen and Z. Yan, J. Chem. Phys. **90**, 3740 (1989).

[29] Z. Yan and J. Chen, J. Phys. D: Appl. Phys. **23**, 136 (1990).

[30] D. C. Agrawal and V. J. Menon, J. Phys. A **23**, 5319 (1990).

[31] J. M. Gordon, Am. J. Phys. **58**, 370 (1990).

[32] J. M. Gordon and M. Huleihil, J. Appl. Phys. **69**, 1 (1991).

[33] E. Geva and R. Kosloff, J. Chem. Phys. **96**, 3054 (1992).

[34] E. Geva and R. Kosloff, J. Chem. Phys. **97**, 4398 (1992).

[35] T. Feldmann and R. Kosloff, Phys. Rev. E **61**, 4774 (2000).

[36] R. Kosloff and T. Feldmann, Phys. Rev. E **65**, 055102 (2002).

[37] T. Feldmann and R. Kosloff, Phys. Rev. E **70**, 046110 (2004).

[38] Y. Rezek and R. Kosloff, New J. Phys. **8**, 83 (2006).

[39] M. Esposito, K. Lindenberg, and C. V. den Broeck, Europhys. Lett. **85**, 60010 (2009).

[40] M. Esposito, R. Kawai, K. Lindenberg, and C. Van den Broeck, Phys. Rev. E **81**, 041106 (2010).

[41] T. Schmiedl and U. Seifert, Europhys. Lett. **81**, 20003 (2008).

[42] C. Van den Broeck, Phys. Rev. Lett. **95**, 190602 (2005).

[43] J. Chen, Z. Yan, G. Lin, and B. Andresen, Energy Convers. and Manage. **42**, 173 (2001).

[44] F. Angulo-Brown, J. Appl. Phys. **69**, 7465 (1991).

[45] V. Singh and R. S. Johal, Entropy **19**, 576 (2017).

[46] A. C. Hernández, A. Medina, J. M. M. Roco, J. A. White, and S. Velasco, Phys. Rev. E **63**, 037102 (2001).

[47] J. W. Stucki, Eur. J. Biochem. **109**, 269 (1980).

[48] T. Yilmaz, J. Energy Inst. **79**, 38 (2006).

[49] L. A. Arias-Hernandez, M. A. Barranco-Jimnez, and F. Angulo-Brown, J. Energy Inst. **82**, 223 (2009).

[50] Z. Yan, J. Appl. Phys. **73**, 3583 (1993).

[51] N. Sánchez-Salas, L. López-Palacios, S. Velasco, and A. Calvo Hernández, Phys. Rev. E **82**, 051101 (2010).

[52] C. de Tomás, J. M. M. Roco, A. C. Hernández, Y. Wang, and Z. C. Tu, Phys. Rev. E **87**, 012105 (2013).

[53] Z. Yan and L. Chen, J. Phys. D: Appl. Phys. **29**, 3017 (1996).

[54] Y. Zhang, C. Huang, G. Lin, and J. Chen, Phys. Rev. E **93**, 032152 (2016).

[55] Z. Yan and J. Chen, Phys. Lett. A **217**, 137 (1996).

[56] G. Valencia-Ortega and L. A. Arias-Hernandez, J.Non-Equilib. Thermodyn. **42**, 187 (2016).

[57] L. Chen, Z. Ding, J. Zhou, W. Wang, and F. Sun, Eur. Phys. J. Plus **132**, 293 (2017).

[58] L. A. Arias-Hernandez, F. Angulo-Brown, and R. T. Paez-Hernandez, Phys. Rev. E **77**, 011123 (2008).

[59] J. C. Chimal, N. Sánchez, and P. Ramírez, J. Phys. Conf. Ser. **792**, 012082 (2017).

[60] V. Singh and R. S. Johal, Phys. Rev. E **98**, 062132 (2018).

[61] M. Esposito, K. Lindenberg, and C. Van den Broeck, Phys. Rev. Lett. **102**, 130602 (2009).

[62] B. Cleuren, B. Rutten, and C. Van den Broeck, Eur. Phys. J. Spec. Top. **224**, 879 (2015).

[63] Y. Zhang, J. Guo, G. Lin, and J. Chen, J. Non-Equilib. Thermodyn. **42**, 253 (2017).

[64] Izumida, Y. and Okuda, K., Europhys. Lett. **97**, 10004 (2012).

[65] H. Yan and H. Guo, Phys. Rev. E **85**, 011146 (2012).

[66] R. Uzdin and R. Kosloff, Europhys. Lett. **108**, 40001 (2014).

[67] R. S. Johal and R. Rai, Europhys. Lett. **113**, 10006 (2016).

[68] S. Sheng and Z. C. Tu, Phys. Rev. E **91**, 022136 (2015).

[69] R. Long, Z. Liu, and W. Liu, Phys. Rev. E **89**, 062119 (2014).

[70] R. Long and W. Liu, Phys. Rev. E **91**, 042127 (2015).

[71] V. Holubec and A. Ryabov, J. Stat. Mech. **2016**, 073204 (2016).

[72] H. S. Leff and A. F. Rex, eds., *Maxwell's Demon 2: Entropy, Classical and Quantum Information, Computing* (Institute of Physics, Bristol, 2003).

[73] R. Landauer, IBM J. Res. Dev. **5**, 183 (1961).

[74] C. H. Bennett, Int. J. Theor. Phys. **21**, 905 (1982).

[75] V. Dose, Rep. Prog. Phys. **66**, 1421 (2003).

[76] D. E. Raeside, Am. J. Phys. **40**, 688 (1972).

[77] T. L. Griffiths and J. B. Tenenbaum, Psychol. Sci. **17**, 767 (2006).

[78] J. C. Harsanyi, Am. Econ. Rev. **85**, 291 (1995).

[79] R. Trotta, Contemp. Phys. **49**, 71 (2008).

[80] C. M. Caves, C. A. Fuchs, and R. Schack, Phys. Rev. A **65**, 022305 (2002).

[81] M. S. Leifer and R. W. Spekkens, Phys. Rev. A **88**, 052130 (2013).

[82] R. S. Johal, Phys. Rev. E **82**, 061113 (2010).

[83] G. Thomas and R. S. Johal, Phys. Rev. E **85**, 041146 (2012).

[84] E. T. Jaynes, IEEE Trans. Syst. Sci. Cybernet. **4**, 227 (1968).

[85] T. Bayes, Philos. Trans. Royal Soc. B **53**, 370 (1763).

[86] E. T. Jaynes, Phys. Rev. **106**, 620 (1957).

[87] E. T. Jaynes, Phys. Rev. **108**, 171 (1957).

[88] E. T. Jaynes, *Probability theory: The logic of science* (Cambridge university press, 2003).

[89] P. Aneja and R. S. Johal, J. Phys. A **46**, 365002 (2013).

[90] R. Long and W. Liu, Phys. Lett. A **379**, 1979 (2015).

[91] G. Thomas, P. Aneja, and R. S. Johal, Physica Scripta **2012**, 014031 (2012).

[92] R. S. Johal, Europhys. Lett. **121**, 50009 (2018).

[93] R. P. Feynman, R. B. Leighton, and M. Sands, *The Feynman Lectures on Physics* (Narosa Publishing House, New Delhi, India, 2008).

[94] J. M. R. Parrondo and P. Espanol, Am. J. Phys. **64**, 1125 (1996).

[95] Y. Apertet, H. Ouerdane, C. Goupil, and P. Lecoeur, Phys. Rev. E **90**, 012113 (2014).

[96] J. S. Lee and H. Park, Sc. Rep. **7**, 10725 (2017).

[97] R. Wang, J. Wang, J. He, and Y. Ma, Phys. Rev. E **87**, 042119 (2013).

[98] C. Van den Broeck and K. Lindenberg, Phys. Rev. E **86**, 041144 (2012).

[99] L. Chen and Z. Yan, J. Chem. Phys. **90**, 3740 (1989).

[100] Y. Wang and Z. C. Tu, Phys. Rev. E **85**, 011127 (2012).

[101] R. S. Johal, Phys. Rev. E **96**, 012151 (2017).

[102] R. S. Johal, Phys. Rev. E **94**, 012123 (2016).

[103] M. H. Rubin and B. Andresen, J. Appl. Phys. **53**, 1 (1982).

[104] G. Lebon and D. Jou, *Understanding non-equilibrium thermodynamics* (Springer, Berlin, 2008).

[105] H. Jeffreys, *The theory of probability* (Oxford university Press, 1998).

[106] S. Sheng, P. Yang, and Z. C. Tu, Commun. Theor. Phys. **62**, 589 (2014).

[107] X. Luo, N. Liu, and J. He, Phys. Rev. E **87**, 022139 (2013).

[108] M. Büttiker, Z. Phys. B **68**, 161 (1987).

[109] R. Landauer, J. Stat. Phys. **53**, 233 (1988).

[110] V. Singh and R. S. Johal, J. Stat. Mech. **2018**, 073205 (2018).

[111] Y. Wang, M. Li, Z. C. Tu, A. C. Hernández, and J. M. M. Roco, Phys. Rev. E **86**, 011127 (2012).

[112] Y. Izumida, K. Okuda, A. C. Hernández, and J. Roco, Europhys. Lett. **101**, 10005 (2013).

[113] Y. Yuan, R. Wang, J. He, Y. Ma, and J. Wang, Phys. Rev. E **90**, 052151 (2014).

[114] S. Velasco, J. M. M. Roco, A. Medina, and A. C. Hernández, Phys. Rev. Lett. **78**, 3241 (1997).

[115] C. Van den Broeck, Europhys. Lett. **101**, 10006 (2013).

[116] C. de Tomás, A. C. Hernández, and J. M. M. Roco, Phys. Rev. E **85**, 010104 (2012).

[117] J. Guo, J. Wang, Y. Wang, and J. Chen, Phys. Rev. E **87**, 012133 (2013).

[118] A. C. Hernández, A. Medina, and J. M. M. Roco, New J. Phys. **17**, 075011 (2015).

[119] J. Wang and J. He, Phys. Rev. E **86**, 051112 (2012).

[120] J. Wang, J. He, and Z. Wu, Phys. Rev. E **85**, 031145 (2012).

[121] J. Guo, J. Wang, Y. Wang, and J. Chen, J. Appl. Phys. **113**, 143510 (2013).

[122] Y. Hu, F. Wu, Y. Ma, J. He, J. Wang, A. C. Hernández, and J. M. M. Roco, Phys. Rev. E **88**, 062115 (2013).

[123] J. Gonzalez-Ayala, A. C. Hernández, and J. M. M. Roco, J. Stat. Mech. **2016**, 073202 (2016).

[124] J. Gonzalez-Ayala, J. M. M. Roco, A. Medina, and A. C. Hernández, Entropy **19**, 182 (2017).

[125] F. R. Tang, R. Zhang, H. Li, C. N. Li, W. Liu, and B. Long, Eur. Phys. J. Plus **133**, 176 (2018).

[126] S. Sheng and Z. C. Tu, Phys. Rev. E **89**, 012129 (2014).

[127] V. Cavina, A. Mari, and V. Giovannetti, Phys. Rev. Lett. **119**, 050601 (2017).

[128] H. E. D. Scovil and E. O. Schulz-DuBois, Phys. Rev. Lett. **2**, 262 (1959).

[129] L. A. Correa, J. P. Palao, D. Alonso, and G. Adesso, Sci. Rep **4**, 3949 (2014).

[130] L. A. Correa, J. P. Palao, G. Adesso, and D. Alonso, Phys. Rev. E **90**, 062124 (2014).

[131] D. Segal, Phys. Rev. E **97**, 052145 (2018).

[132] M. Kilgour and D. Segal, Phys. Rev. E **98**, 012117 (2018).

[133] E. Boukobza and D. J. Tannor, Phys. Rev. A **74**, 063823 (2006).

[134] E. Boukobza and D. J. Tannor, Phys. Rev. A **74**, 063822 (2006).

[135] E. Boukobza and D. J. Tannor, Phys. Rev. Lett. **98**, 240601 (2007).

[136] J. He, J. Chen, and B. Hua, Phys. Rev. E **65**, 036145 (2002).

[137] F. Wu, L. Chen, F. Sun, C. Wu, and Q. Li, Phys. Rev. E **73**, 016103 (2006).

[138] G. Thomas and R. S. Johal, Phys. Rev. E **83**, 031135 (2011).

[139] G. Thomas and R. S. Johal, Eur. Phys. J. B **87**, 166 (2014).

[140] V. Mehta and R. S. Johal, Phys. Rev. E **96**, 032110 (2017).

[141] G. Thomas, N. Siddharth, S. Banerjee, and S. Ghosh, Phys. Rev. E **97**, 062108 (2018).

[142] G. S. Agarwal and S. Chaturvedi, Phys. Rev. E **88**, 012130 (2013).

[143] J. Roßnagel, O. Abah, F. Schmidt-Kaler, K. Singer, and E. Lutz, Phys. Rev. Lett. **112**, 030602 (2014).

[144] A. Insinga, B. Andresen, and P. Salamon, Phys. Rev. E **94**, 012119 (2016).

[145] T. D. Kieu, Phys. Rev. Lett. **93**, 140403 (2004).

[146] T. D. Kieu, Eur. Phys. J. D **39**, 115 (2006).

[147] H. T. Quan, P. Zhang, and C. P. Sun, Phys. Rev. E **72**, 056110 (2005).

[148] H. T. Quan, P. Zhang, and C. P. Sun, Phys. Rev. E **73**, 036122 (2006).

[149] H. T. Quan, Y.-x. Liu, C. P. Sun, and F. Nori, Phys. Rev. E **76**, 031105 (2007).

[150] A. E. Allahverdyan, R. S. Johal, and G. Mahler, Phys. Rev. E **77**, 041118 (2008).

[151] S. Abe and S. Okuyama, Phys. Rev. E **83**, 021121 (2011).

[152] F. Altintas, A. U. C. Hardal, and O. E. Müstecaplıoğlu, Phys. Rev. A **91**, 023816 (2015).

[153] D. Gelbwaser-Klimovsky, R. Alicki, and G. Kurizki, Phys. Rev. E **87**, 012140 (2013).

[154] Gelbwaser-Klimovsky, W. Niedenzu, P. Brumer, and G. Kurizki, Sci. Rep. **5**, 14413 (2015).

[155] O. Abah, J. Roßnagel, G. Jacob, S. Deffner, F. Schmidt-Kaler, K. Singer, and E. Lutz, Phys. Rev. Lett. **109**, 203006 (2012).

[156] S. Chand and A. Biswas, Phys. Rev. E **95**, 032111 (2017).

[157] S. Chand and A. Biswas, Europhys. Lett. **118**, 60003 (2017).

[158] M. O. Scully, Phys. Rev. Lett. **87**, 220601 (2001).

[159] M. O. Scully, Phys. Rev. Lett. **104**, 207701 (2010).

[160] X. L. Huang, T. Wang, and X. X. Yi, Phys. Rev. E **86**, 051105 (2012).

[161] S. Rahav, U. Harbola, and S. Mukamel, Phys. Rev. A **86**, 043843 (2012).

[162] H. P. Goswami and U. Harbola, Phys. Rev. A **88**, 013842 (2013).

[163] K. Zhang, F. Bariani, and P. Meystre, Phys. Rev. Lett. **112**, 150602 (2014).

[164] K. Zhang, F. Bariani, and P. Meystre, Phys. Rev. A **90**, 023819 (2014).

[165] A. Dechant, N. Kiesel, and E. Lutz, Phys. Rev. Lett. **114**, 183602 (2015).

[166] B. K. Agarwalla, J.-H. Jiang, and D. Segal, Phys. Rev. B **96**, 104304 (2017).

[167] R. Wang, J. Wang, J. He, and Y. Ma, Phys. Rev. E **87**, 042119 (2013).

[168] A. U. C. Hardal and O. E. Müstecaplıoğlu, Sci. Rep. **5**, 12953 (2015).

[169] D. Türkpençe and O. E. Müstecaplıoğlu, Phys. Rev. E **93**, 012145 (2016).

[170] M. O. Scully, K. R. Chapin, K. E. Dorfman, M. B. Kim, and A. Svidzinsky, Proc. Natl. Acad. Sci. USA **108**, 15097 (2011).

[171] T. Zhang, W.-T. Liu, P.-X. Chen, and C.-Z. Li, Phys. Rev. A **75**, 062102 (2007).

[172] G. F. Zhang, Phys. Rev. A **49**, 123 (2008).

[173] H. Wang, S. Liu, and J. He, Phys. Rev. E **79**, 041113 (2009).

[174] K. V. Hovhannisyan, M. Perarnau-Llobet, M. Huber, and A. Acín, Phys. Rev. Lett. **111**, 240401 (2013).

[175] R. Alicki and D. Gelbwaser-Klimovsky, New J. Phys. **17**, 115012 (2015).

[176] G. Lindblad, Commun. Math. Phys. **48**, 119 (1976).

[177] V. Gorini, A. Kossakowski, and E. C. G. Sudarshan, J. Math. Phys. **17**, 821 (1976).